Title

Bis(pentamethylcyclopentadienyl)ytterbium: Electron-Transfer Reactions with Organotransition Metal Complexes

Author

Matsunaga, P.T.

Publication Date

1991-12-01

LBL-31491

Lawrence Berkeley Laboratory
UNIVERSITY OF CALIFORNIA

Materials & Chemical
Sciences Division

Bis(pentamethylcyclopentadienyl)ytterbium: Electron-Transfer Reactions with Organotransition Metal Complexes

P.T. Matsunaga
(Ph.D. Thesis)

November 1991

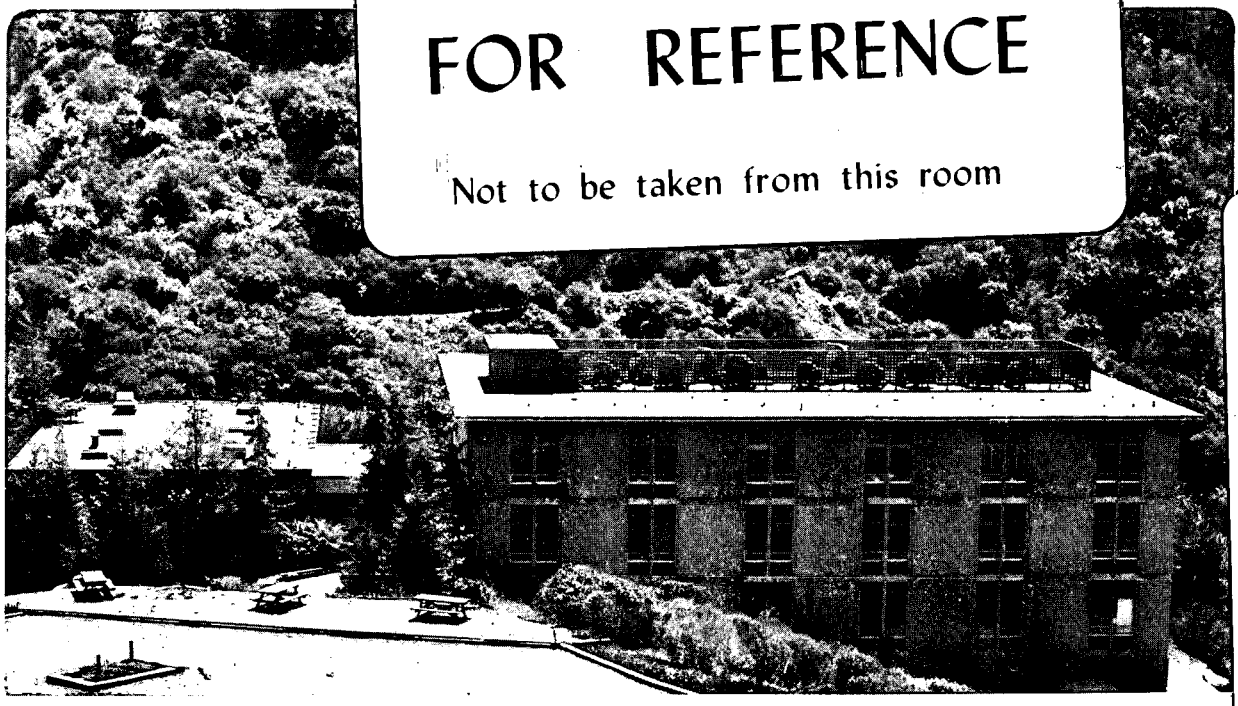

Prepared for the U.S. Department of Energy under Contract Number DE-AC03-76SF00098

DISCLAIMER

DISCLAIMER

LBL-31491

Bis(pentamethylcyclopentadienyl)ytterbium: Electron-Transfer Reactions with Organotransition Metal Complexes

Phillip Thomas Matsunaga

Lawrence Berkeley Laboratory
University of California
Berkeley, California 94720

November 1991

This work was supported by the Director, Office of Energy Research, Office of Basic Energy Sciences, Chemical Sciences Division of the U.S. Department of Energy under contract number DE-AC03-76SF00098

Bis(pentamethylcyclopentadienyl)ytterbium: Electron-Transfer Reactions with Organotransition Metal Complexes

Phillip Thomas Matsunaga

Abstract

The divalent lanthanide complex, $(Me_5C_5)_2Yb$, reacts with methylcopper to produce the base-free, ytterbium-methyl complex, $(Me_5C_5)_2YbMe$. This product forms an asymmetric, methyl-bridged dimer in the solid state. Addition of a second equivalent of $(Me_5C_5)_2Yb$ to $(Me_5C_5)_2YbMe$ affords the mixed-valent, methyl-bridged species, $[(Me_5C_5)_2Yb]_2(\mu\text{-}Me)$. The solid state structure contains a linear methyl bridge with non-equivalent ytterbium-carbon distances. The structure and magnetic behavior are consistent with a trapped-valent complex. Ammonia reacts with $(Me_5C_5)_2YbMe$ to produce the amide complex, $(Me_5C_5)_2YbNH_2(NH_3)$. Attempts to remove the excess ammonia ligand with trimethylaluminum resulted in the formation of the crystallographically characterized diamido-dimethylaluminate complex, $(Me_5C_5)_2Yb(\mu\text{-}NH_2)_2AlMe_2$. The bulky alkyl complex, $(Me_5C_5)_2YbCH(SiMe_3)_2$, displays similar chemistry to $(Me_5C_5)_2YbMe$, but at a reduced reaction rate due to the limited accessibility of the metal in $(Me_5C_5)_2YbCH(SiMe_3)_2$.

Copper and silver halide salts react with $(Me_5C_5)_2V$ to produce the trivalent halide derivatives, $(Me_5C_5)_2VX$ (X = F, Cl, Br, I). The chloride complex, $(Me_5C_5)_2VCl$, reacts with lithium reagents to form

the phenyl and borohydride species. Nitrous oxide transfers an oxygen atom to $(Me_5C_5)_2V$ producing the vanadium-oxo complex, $(Me_5C_5)_2VO$. The trivalent vanadium species, $(Me_5C_5)_2VX$ (X = F, Cl, Br, I, Me, BH_4, N_3), undergo electron-transfer/ligand-exchange reactions with $(Me_5C_5)_2Yb$ to afford the base-free ytterbium complexes, $(Me_5C_5)_2YbX$. Addition of two equivalents of $(Me_5C_5)_2Yb$ to the vanadium ligand donors produces the mixed-valent species, $[(Me_5C_5)_2Yb]_2(\mu\text{-}X)$ (X = F, Cl, Br, Me, BH_4). The variable temperature magnetic susceptibility of these complexes suggests that they are all examples of trapped-valent complexes.

The trivalent titanium species, $(Me_5C_5)_2TiX$ (X = Cl, Br, Me, BH_4), form bimetallic coordination complexes with $(Me_5C_5)_2Yb$. The magnetic behavior of the products indicates that electron transfer has not occurred. The solid state structures of the chloride and bromide complexes show unusual bend angles for the halide bridges between ytterbium and titanium. A model based on frontier orbital theory has been proposed to account for the bending behavior in these species. The bimetallic methyl complex contains a linear methyl bridge between ytterbium and titanium. The hydrogen atoms on the bridging methyl group have been located and refined. The pseudotetrahedral geometry around the carbon atom is retained upon coordination. The bimetallic species act as models for the transition state of the ytterbium-vanadium ligand-exchange process.

Acknowledgements

Having survived a massive earthquake and a devastating fire-storm, it is now time for me to move on (before the next disaster hits!). However, before I depart from the "center of the universe," I would like to acknowledge those who have contributed to my memorable Berkeley experience. Naturally, I would first like to thank Professor Dick Andersen for giving me the opportunity to work on a project that was always scientifically rewarding and for generously sharing his vast chemical knowledge (although some might say that I learned too much in certain special areas.) Our discussions on chemistry, baseball, and random targets in the chemical community were sometimes brutal, usually entertaining, and always enlightening.

I would also like to thank Professor Robert J. Doedens. His continued friendship and support have been invaluable. During my lengthy stay in Berkeley, many group members have left while others have arrived. I would like to thank the old crew: Dave Berg, Carol Burns, Joanne Stewart, Nicki Rutherford, Steve Stults, and Rob Rosen for all of their help in my early graduate career. I would also like to thank the second generation: Marc Weydert, Wayne Lukens, Mike Smith, Sharon Beshouri, Mitch Smith, Chad Sofield, and Brian Campion for their help and friendship. As long as there are machines, there will always be machine hits.

In addition to my fellow group members, there have been many people outside of the group who have helped maintain my sanity (or insanity depending on your perspective): Mike Chan, Randy Myrabo, Dave Sable, Phil Carter, Bill Casteel, Byron Shen, Bob

Simpson, Rick Michelman, and Wing Kot. Thanks to all of the members of the legendary DUX and the champion Latvians softball teams for several great seasons of softball. Thanks also to the members of the Armstrong and Raymond groups for answering all of my crystallography questions and to the rest of the fifth floor gang for tolerating my high-decibel, late-night music assault. Thanks to everyone who knowingly or unknowingly contributed to the infamous Truths list. I wish all of the friends I've made at Berkeley good fortune in their future careers. As you get on with your lives, remember: It's a strange world.

I would like to thank LBL scientists Norm Edelstein, George Shalimoff and Jerry Bucher for assistance with all things Hilloid. Although some fifth floor residents might find fault with this, I would like to thank Fred Hollander for valuable assistance with my more problematic crystal structures.

Lastly, but very importantly, I would like to thank my family for all of their support during my long and continuing education: Mom, Dad, Leslie, Brad, Steve, Sabrina, and John. This work would not be as meaningful without you.

This work was supported by the Director, Office of Energy Research, Office of Basic Energy Sciences, Chemical Sciences Division of the U.S. Department of Energy under contract number DE-AC03-76SF00098.

To

My Family

Table of Contents

Introduction

Since the earliest reports of organolanthanide complexes, much of the fundamental chemistry in this field has been examined. Most of the early studies have focussed on the metals in the trivalent oxidation state owing to its greater stability relative to other oxidation states.[1] However, recently more attention has been directed toward the chemistry of elements which can easily access alternative oxidation states.[2]

The lanthanides are much more restricted in their available oxidation states relative to the transition metals or the actinides.[3] In organolanthanide chemistry, only samarium, europium, and ytterbium have demonstrated the ability to form stable divalent species. The availability of the divalent state has been rationalized in terms of the differences in the third ionization potentials for these metals.[4] This ability to form divalent complexes is attractive because it greatly broadens the scope of the chemistry which can be explored.

Of the lanthanides mentioned above, ytterbium possesses the most attractive features for studying a wide variety of chemistry. The reduction potential of trivalent samarium is large and negative which makes its divalent complexes powerful reducing agents (Table 1).[1b] This limits the ability of samarium to form stable divalent species since many simple ligands often become involved in reductive processes. In contrast, the reduction potential of trivalent europium is much smaller. Therefore, its divalent complexes are more stable and a wider variety of these species can be observed. However, the

smaller potential results in a greatly diminished electron-transfer chemistry for divalent europium. Being intermediate between the two, ytterbium can be used to explore the chemistry of divalent complexes as well as participate in electron-transfer reactions.

Table 1. Physical Properties of Divalent and Trivalent Lanthanides.

	ξ° (V)[a]	Ionic Radius (Å)[b]	
	$M^{3+}(aq) + e^- \rightarrow M^{2+}(aq)$	+2	+3
Sm	-1.55	1.27	1.08
Eu	-0.43	1.25	1.06
Yb	-1.15	1.14	0.98

(a) relative to the standard hydrogen electrode, listed in Reference 1b. (b) listed in Reference 5.

The bonding in lanthanide complexes is considered to be primarily ionic. This is a consequence of the contracted nature of the 4f orbitals. The shielding of these orbitals by the 5s and 5p shells prevents them from effectively interacting with ligand based orbitals.[3] As a result, steric factors play a principal role in determining the ligand environment around the metal. Therefore, the degree of saturation in the coordination sphere of the metal affects the reactivity of the complexes and the ability to isolate monomeric species. Because ytterbium has the smallest ionic radius of the three metals (Table 1),[5] its coordination sphere is more easily saturated

and, therefore, undesirable processes, such as the formation of coordination polymers, can be better controlled.

Lastly, divalent ytterbium has a $4f^{14}$ electronic configuration which is diamagnetic whereas trivalent ytterbium has a $4f^{13}$ electronic configuration which is paramagnetic.[6] This characteristic is particularly advantageous since the two oxidation states can be unambiguously differentiated through NMR spectroscopy or magnetic susceptibility studies. In contrast, both oxidation states for either samarium or europium give paramagnetic complexes.

The bent metallocene, $(Me_5C_5)_2Yb$, has displayed a wide range of chemistry. The versatility of this complex can be attributed to several important features. The electron donating character of the Me_5C_5 ligands results in a more negative reduction potential for the molecule relative to the free ion (Table 2).[7] This enhancement has allowed $(Me_5C_5)_2Yb$ to reduce an assortment of nitrogenous bases[8] and organic dichalcogenides possessing quite unfavorable reduction potentials.[9]

Table 2. Reduction Potentials of $(Me_5C_5)_2M$ Complexes.

	ξ° (V)[a]
M	$(Me_5C_5)_2Yb^+ + e^- \rightarrow (Me_5C_5)_2Yb$
Sm	- 2.0
Eu	- 0.8
Yb	- 1.4

(a) Measured in acetonitrile relative to the standard hydrogen electrode. Reported in Reference 7.

In addition, organometallic complexes such as dimethylzinc have been reduced by $(Me_5C_5)_2Yb$ to produce zincate species (Eqn. 1).[10] The Me_5C_5 ligands also provide the molecule with favorable solubility and crystallinity properties in comparison to unsubstituted cyclopentadienyl analogues.[2] This assists the purification of the products as well as the isolation of crystals suitable for X-ray diffraction studies. Furthermore, the bulky ligands occupy a large portion of the coordination sphere of the metal which minimizes the presence of excess coordinating ligands.

$$(Me_5C_5)_2Yb + 3/2\ Me_2Zn \longrightarrow (Me_5C_5)_2Yb(\mu\text{-}Me)_2ZnMe + 1/2\ Zn \qquad (1)$$

In contrast to its redox behavior, $(Me_5C_5)_2Yb$ is also capable of creating very subtle interactions with weakly coordinating ligands. The strengths of these interactions can be on the order of solvation energies. The solid state structure of $(Me_5C_5)_2Yb$ shows a ring centroid-Yb-ring centroid angle of 145° (Figure 1).[10] Although weak intermolecular interactions in the crystal lattice account for some of the bending in the molecule, gas phase electron diffraction studies verify that the isolated molecules maintain their bent configuration. This geometry enhances the accessibility of the ytterbium atom to incoming ligands by opening an area of the coordination sphere. In addition, the reorganization energy required to bend the rings back from the metallocene sandwich geometry does not contribute to the reaction barrier for ligand binding.[11] This permits ligands that are poor electron donors to interact effectively with the metal.

Figure 1. Structure of $(Me_5C_5)_2Yb$.

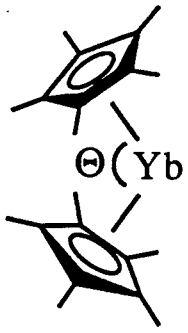

Θ = 145° (solid state)
158° (gas phase)

The strong electropositive character of ytterbium induces the metal to attract any available source of electron density. Therefore, polarizable molecules or species containing a permanent dipole are able to interact with the metal without addressing orbital symmetry considerations. This property has allowed the isolation of stable complexes containing weakly bound ligands such as 2-butyne.[12] Also, a bimetallic complex has been observed in which an ethylene ligand bridges two metal centers (Figure 2).[13] This behavior has also resulted in the observation of an unusual linear methyl bridge bond in the ytterbium-beryllium bimetallic complex (Figure 3).[14]

Figure 2. Structure of $(Me_5C_5)_2Yb(\mu\text{-}C_2H_4)Pt(PPh_3)_2$.

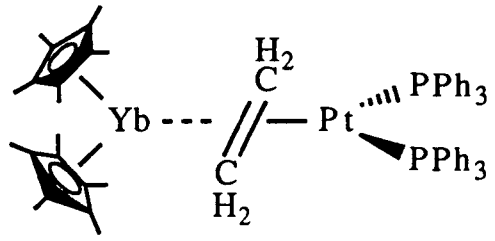

Figure 3. Structure of $(Me_5C_5)_2Yb(\mu\text{-}Me)Be(Me_5C_5)$.

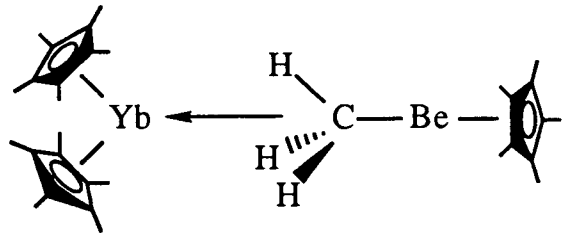

Although many novel reactions have been observed for $(Me_5C_5)_2Yb$, there is a large class of important compounds that has remained elusive. These species are the base-free, trivalent metallocene adducts of fundamental ligands such as halides, alkyls, borohydrides, etc. Although complexes with these ligands have been reported from metathetical routes, they generally contain excess coordinated Lewis bases.[10,15] The tenacity with which ytterbium retains these ligands prevents the isolation of the simple base-free complexes. Since the base adducts have been shown to be less reactive than their base-free analogues,[16] the base-free species would be preferred for chemical studies. The unusual asymmetric structure observed for the dimer of $(Me_5C_5)_2LuMe$[17] suggests that the structure and chemistry of the base-free ytterbium complexes might reveal novel behavior. Therefore, alternative routes must be developed which are compatible with the isolation of base-free products.

The solubility properties of $(Me_5C_5)_2Yb$ allow reactions to be performed conveniently in non-coordinating solvents.[10] Therefore, the electron-transfer capabilities of $(Me_5C_5)_2Yb$ might be employed to obtain base-free complexes provided that suitable ligand donors

could be developed. Thus, the impetus for the work described in this thesis has been to study the electron-transfer properties of $(Me_5C_5)_2Yb$ in an effort to isolate previously inaccessible base-free complexes so that their structure and reactivity could be evaluated. This work has focussed on the development of organotransition metal systems as ligand sources and the study of the subtle details of the interactions between the two metal fragments involved in the electron-transfer/ligand exchange processes.

References

1. (a) Gysling, H.; Tsutsui, M, *Adv. Organomet. Chem.*, **1970**, *9*, 361. (b) Marks, T. J., *Prog. Inorg. Chem.*, **1978**, *24*, 51. (c) Evans, W. J. in "The Chemistry of the Metal-Carbon Bond," Hartley, F. R.; Patai, S., eds., Wiley: New York, **1982**. (d) Marks, T. J.; Ernst, R. D. in "Comprehensive Organometallic Chemistry," Wilkinson, G.; Stone, F. G. A.; Abel, E. W., eds., Pergamon: Oxford, **1982**, Ch. 21.

2. Evans, W. J., *Adv. Organomet. Chem.*, **1985**, *24*, 131.

3. Cotton, F. A.; Wilkinson, G., "Advanced Inorganic Chemistry," 4th Ed., Wiley Interscience: New York, **1980**.

4. Johnson, D. A., "Some Thermodynamic Aspects of Inorganic Chemistry," 2nd Ed., Cambridge University Press: Cambridge, **1982**.

5. Shannon, R. D., *Acta. Cryst.*, **1976**, *A32*, 751.

6. Casey, A. T.; Mitra, S., "Theory and Applications of Molecular Paramagnetism," Boudreaux, E. A.; Mulay, L. N., eds., Wiley-Interscience: New York, **1976**.

7. Finke, R. G.; Keenan, S. R.; Schiraldi, D. A.; Watson, P. L., *Organometallics*, **1986**, *5*, 598.

8. Berg, D. J., Ph.D. Thesis, University of California, Berkeley, **1987**.

9. Berg, D. J.; Andersen, R. A.; Zalkin, A., *Organometallics*, **1988**, *7*, 1858.

10. Burns, C. J., Ph.D. Thesis, University of California, Berkeley, **1987**.

11. (a) Coates, G. E.; Green, M. L. H.; Powell, P.; Wade, K., "Principles of Organometallic Chemistry," Chapman and Hall: London, **1968**. (b) Albright, T. A.; Burdett, J. K.; Whangbo, M-H, "Orbital Interactions in Chemistry," Wiley-Interscience: New York, **1985**.

12. Burns, C. J.; Andersen, R. A., *J. Am. Chem. Soc.*, **1987**, *109*, 941.

13. Burns, C. J.; Andersen, R. A., *J. Am. Chem. Soc.*, **1987**, *109*, 915.

14. Burns, C. J.; Andersen, R. A., *J. Am. Chem. Soc.*, **1987**, *109*, 5853.

15. Tilley, T. D., Ph.D. Thesis, University of California, Berkeley, **1982**.

16. Watson, P. L.; Herskovitz, T., "Initiation of Polymerization," *ACS Symposium Series*, Bailey, F. E., ed. **1983**, *212*, 460.

17. Watson, P. L.; Parshall, G. W., *Acc. Chem. Res.*, **1985**, *18*, 51.

CHAPTER 1

Reactions of Bis(pentamethylcyclopentadienyl)ytterbium with Organocopper Complexes

Metal alkyls are reactive species due to the ease with which the metal-carbon bond is cleaved. This often results in catalytic activity towards small, unsaturated, organic substrates.[1] Because organolanthanide complexes have been invoked as models for Ziegler-Natta polymerization catalysts, it would be of interest to study the reactivity of alkyl complexes of ytterbium.[2] Watson has studied the chemistry of $(Me_5C_5)_2LuMe$ and found it to react with a variety of substrates.[3] For example, the lutetium methyl complex will react with benzene to form the phenyl complex, and with tetramethylsilane to produce the trimethylsilylmethyl complex. In both reactions, methane is released as the byproduct. In addition, the methyl group undergoes exchange with ^{13}C labelled methane in solution.

The lutetium methyl complex can be prepared in a multistep synthesis as outlined in Scheme 1.[4] Although Watson suggests that the analogous ytterbium complex can be obtained from the same route, no synthetic or spectroscopic details have been reported. In an effort to find a more direct route to $(Me_5C_5)_2YbMe$, various methylating agents have been examined. In general, metathesis reactions tend to produce heterobimetallic species in which the entire methylating agent is incorporated into the ytterbium product (Eqn. 1).[5] The unwanted metal fragment can only be removed

Scheme 1

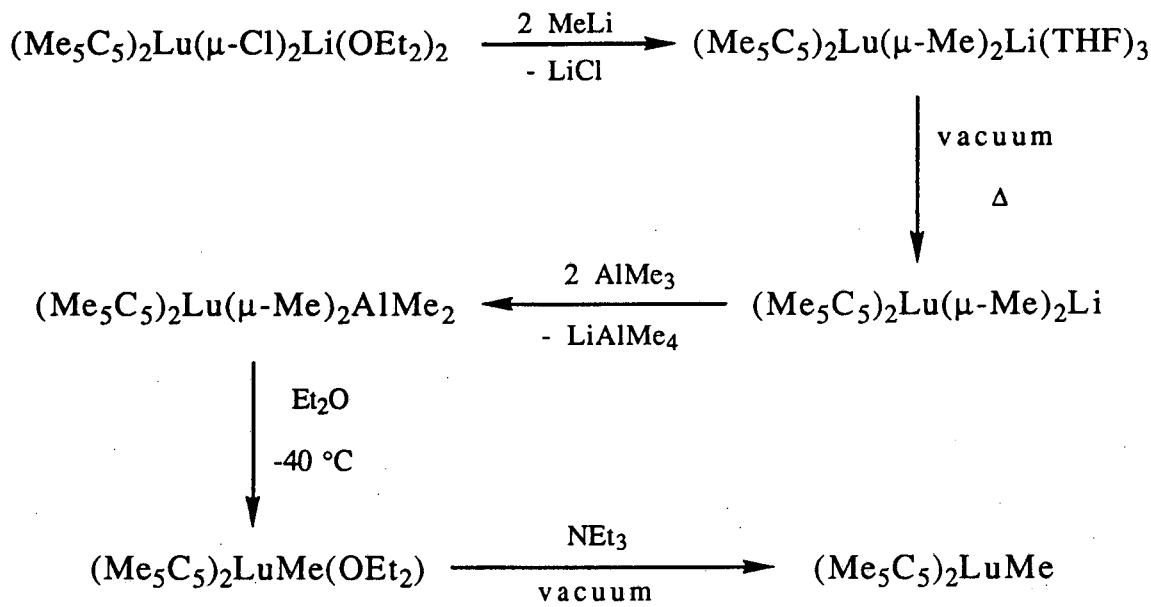

under conditions that leave a Lewis base such as tetrahydrofuran coordinated to ytterbium. Unfortunately, this base cannot be removed from the complex once it coordinates to the metal center. Because incoming substrates often coordinate to the metal prior to reaction, the presence of excess coordinated ligands will interfere with any such processes. Therefore, the base-free species are the desired materials for the studies of chemical behavior.

$$(Me_5C_5)_2Yb(\mu\text{-}Cl)_2Li(OEt_2)_2 \xrightarrow{MeLi} (Me_5C_5)_2Yb(\mu\text{-}Cl)(\mu\text{-}Me)Li(OEt_2)_2 + LiCl \quad (1)$$

In studies of the reactions of ytterbium chalcogenide complexes, $(Me_5C_5)_2YbER(L)$ (E = O, S), with various alkylating agents, Berg found that similar bimetallic adducts are formed (Eqn. 2).[6]

Clearly, an alternate synthetic approach is necessary in order to isolate the simple alkyl complexes from the unwanted metal fragments.

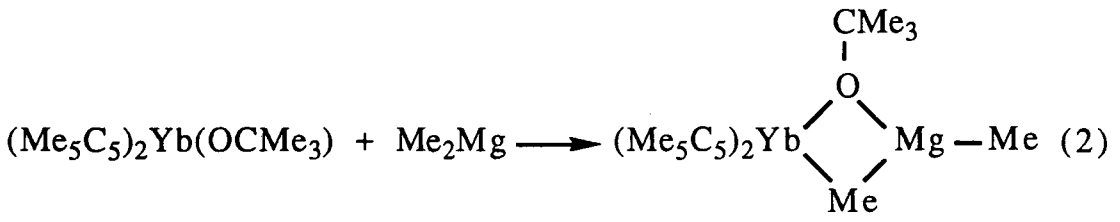

Because ytterbium has multiple oxidation states available to it, electron transfer chemistry can be explored. The high oxidation potential of $(Me_5C_5)_2Yb$ (1.4 V vs. SHE in acetonitrile)[7] has been exploited in the reductions of a variety of organic substrates (eg. aromatic, nitrogenous bases[6] and diorganodichalcogenides[8]). Therefore, an electron-transfer/ligand-exchange process offers a potential route to base-free species, provided suitable donor complexes can be synthesized.

Burns has studied the reactions of $(Me_5C_5)_2Yb$ with the readily available methylating agents dimethylzinc and dimethylmercury.[9] Dimethylmercury does not appear to react cleanly although mercury metal was observed. A subsequent analysis of the spectroscopic data suggests that the product formed is a mixture of two different ytterbium methyl complexes. The reaction with dimethylzinc produces a trimethylzincate complex (Eqn. 3) which has been structurally characterized by X-ray crystallography. The zincate complex

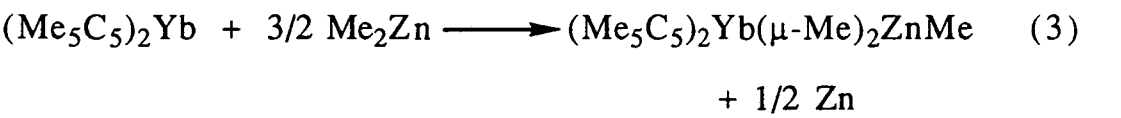

is the only species isolated regardless of the reaction stoichiometry. This suggests that the anionic complex is stable enough to prevent reduction of the coordinated dimethylzinc molecule by free $(Me_5C_5)_2Yb$. Although the simple ytterbium methyl complex is not obtained, these reactions do show that $(Me_5C_5)_2Yb$ is capable of reducing some metal alkyl complexes. Therefore, if a more unstable alkyl transfer reagent could be found, then the electron-transfer reaction would provide a viable synthetic route.

Methylcopper

The favorable reduction potential of aqueous copper(I) ions (0.52 V vs. SHE)[10] suggests that they might be suitable for electron transfer reactions with $(Me_5C_5)_2Yb$. Many dialkylcuprate salts have been used as alkylating agents in organic synthesis.[11] Unfortunately, the presence of lithium ions in these species makes them unattractive for use with ytterbium, as the cation would be likely to become incorporated into the product. However, the neutral, thermally unstable methylcopper complex can be synthesized from dimethylaluminumethoxide and bis(acetylacetonato)copper(II)[12] (Scheme 2). The product must be maintained below -5 °C to prevent spontaneous decomposition. In addition, several low temperature washings with a non-coordinating solvent are required to remove the side products.

In the initial investigation of the reaction between $(Me_5C_5)_2Yb$ and methylcopper, the compound reported by Berg[6] to be the ytterbium methyl complex is actually a related mixed-valent bimetallic species. This complex will be described in detail in

another portion of this thesis. The inability to isolate the proper product can be attributed to the instability of methylcopper. Since the complex must be synthesized and used *in situ*, maintaining exact

Scheme 2

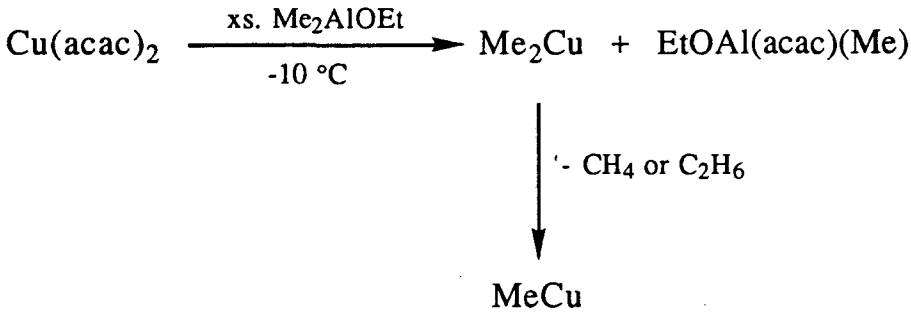

reaction stoichiometry is difficult. The multiple washings and filtrations account for significant manipulative losses. Therefore, it is important to use excess methylcopper. Because the copper(I) species are not capable of oxidizing ytterbium beyond the trivalent state, any unreacted methylcopper will simply decompose once the reaction mixture is allowed to warm to room temperature.

Thus, when a pentane solution of $(Me_5C_5)_2Yb$ is added to a suspension of methylcopper in pentane and allowed to warm from -30 °C to room temperature, the mixture becomes deep red in color and a copper mirror forms on the walls of the flask (Eqn. 4). After stirring for 12 h, $(Me_5C_5)_2YbMe$ can be isolated by filtering the solution away from the insoluble metallic copper. Cooling to -80 °C produces magenta, diamond-shaped crystals which decompose at 219 °C accompanied by gaseous evolution. Although the IR spectrum

provides diagnostic absorptions, the spectrum of the lutetium analogue has not been reported so no comparison can be made.

$$(Me_5C_5)_2Yb + MeCu \xrightarrow{\text{pentane}} (Me_5C_5)_2YbMe + Cu^\circ \quad (4)$$

The mass spectrum shows an ion at 459 amu which corresponds to a simple monomer. Watson reports that the lutetium methyl complex exists as an asymmetric dimer in the solid state[3c] as shown in Figure 1. However, since the strength of the bridging interaction for this lutetium species has been shown to be 12.6 kcal/mol, it is unlikely that the dimer would remain intact in the gas phase.

Figure 1

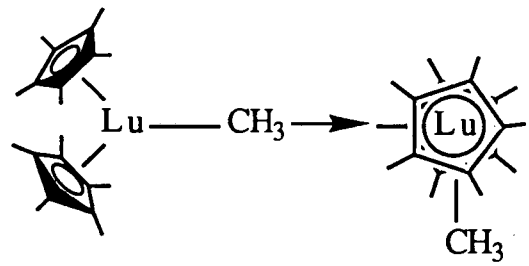

The variable temperature magnetic susceptibility data is consistent with a simple trivalent ytterbium complex. The plot of $1/\chi_M$ vs. T at 5 kG shows the two regions of Curie-Weiss behavior indicative of an Yb(III) ion (Figure 2).[6] The low temperature region (6-30 K) has a μ_{eff} of 3.65 μ_B with Θ = -0.30 K. The high temperature region (50-280 K) has a μ_{eff} of 3.91 μ_B with Θ = -9.31 K. There is no evidence for any magnetic interactions between different metal

centers. A thorough discussion of the magnetic behavior of trivalent ytterbium complexes can be found in Reference 6.

Figure 2. Plot of $1/\chi_M$ vs. T for $(Me_5C_5)_2YbMe$

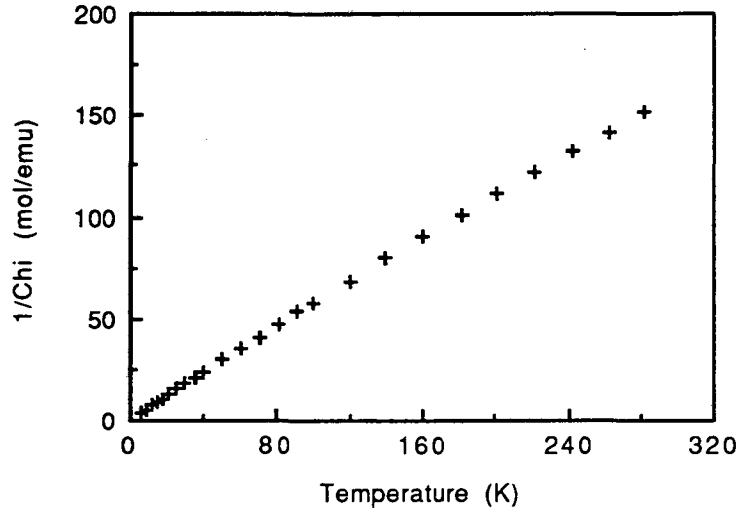

The ^1H NMR spectrum in toluene-d_8 shows a single, broad, resonance at δ 16.7 ($\upsilon_{1/2}$ = 473 Hz) corresponding to the protons on the Me_5C_5 ligands. The resonance due to the protons on the metal bound methyl group is not observed. This is probably due to extreme line broadening resulting from the close interaction with the paramagnetic metal center. Protons on atoms directly bound to trivalent ytterbium are rarely observed.[6] The ^1H NMR spectrum of a hydrolyzed sample contains only resonances due to Me_5C_5H which verifies that no bases such as diethyl ether have been retained in the reaction product.

The variable temperature solution behavior of the lutetium complex[3c] is consistent with the monomer-dimer equilibrium shown in Eqn. 5:

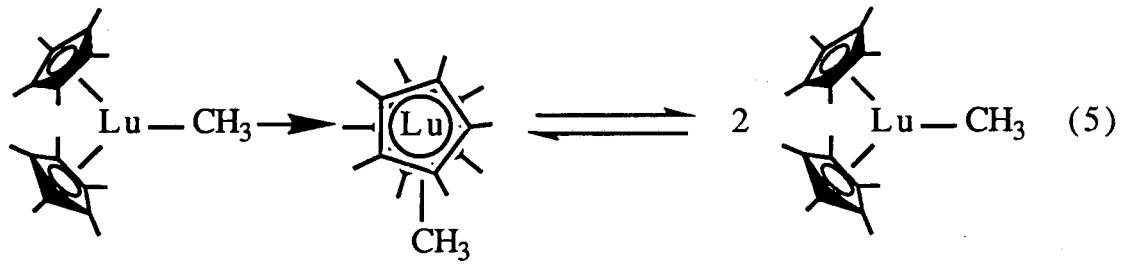

(5)

Above -60 °C, a single resonance is observed, while below -90 °C a 2:1:1 pattern for the Me_5C_5 resonances appears. Unfortunately, the line widths in the spectrum for the paramagnetic ytterbium methyl complex make it much more difficult to study than the diamagnetic lutetium species. The Me_5C_5 resonance shifts with temperature and broadens into the baseline below -30 °C. However, no resonances reappear upon further cooling to -70 °C. Because the ytterbium sample must be concentrated enough to observe a strong signal, the compound may be crystallizing out of solution upon prolonged cooling. Therefore, it may not be possible to reach the temperature at which the dinuclear structure could be spectroscopically observed. However, examination of the available data provides indirect evidence for a monomer-dimer equilibrium. The plot of chemical shift vs. temperature (Figure 3) reveals a slight deviation from Curie-Weiss behavior upon cooling the sample below room temperature. While this is generally indicative of solution equilibria,[13] the exact nature of the process is open to speculation. In addition, since the

solubility of the complex limits the temperature range over which useful data points can be obtained and the line widths of the resonances introduce large errors in their assignments, this analysis cannot be taken as proof that a dimer structure exists. However, it is consistent with the notion that a monomer-dimer equilibrium exists in solution as observed for the lutetium system.

Figure 3. Plot of δ vs. 1/T for $(Me_5C_5)2YbMe$

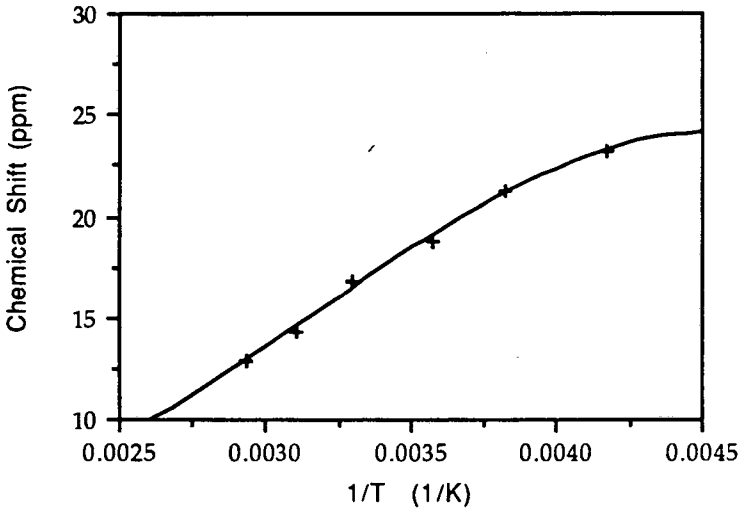

In order to determine the exact nature of the structure in the solid state, an X-ray structural determination has been performed. The structure is almost identical to that of the lutetium methyl complex.[3c] Selected intramolecular bond distances and angles are listed in tables 1 and 2, respectively. An ORTEP diagram is provided in Figure 4.

Table 1. Bond distances for $(Me_5C_5)_2YbMe$ (Å)

Yb1-C1	2.446 (10)	Yb1-Cp3	2.299
Yb2-C1	2.759 (10)	Yb1-Cp4	2.287
Yb2-C2	2.377 (13)	Yb2-Cp1	2.356
		Yb2-Cp2	2.372
Yb1-C31	2.559 (11)	Yb2-C11	2.632 (16)
Yb1-C32	2.599 (14)	Yb2-C12	2.649 (11)
Yb1-C33	2.592 (11)	Yb2-C13	2.648 (18)
Yb1-C34	2.621 (13)	Yb2-C14	2.634 (13)
Yb1-C35	2.576 (11)	Yb2-C15	2.656 (10)
Yb1-C41	2.569 (10)	Yb2-C21	2.673 (13)
Yb1-C42	2.570 (11)	Yb2-C22	2.632 (11)
Yb1-C43	2.616 (11)	Yb2-C23	2.669 (11)
Yb1-C44	2.597 (11)	Yb2-C24	2.642 (13)
Yb1-C45	2.572 (11)	Yb2-C25	2.695 (11)

Cp1, Cp2, Cp3, and Cp4 are the ring centroids of atoms C11-C15, C21-C25, C31-C35, and C41-C45, respectively.

Table 2. Bond Angles for $(Me_5C_5)_2YbMe$ (°)

Yb1-C1-Yb2	170.0 (5)	C1-Yb1-Cp3	112.5
C1-Yb2-C2	91.1 (3)	C1-Yb1-Cp4	109.0
		C1-Yb2-Cp1	105.8
Cp3-Yb1-Cp4	138.4	C1-Yb2-Cp2	104.9
Cp1-Yb2-Cp2	136.4	C2-Yb2-Cp1	104.0
		C2-Yb2-Cp2	105.5

The Yb1-C1 distance of 2.446(10) Å is identical to the Lu1-C1 distance of 2.440(9) Å in the lutetium analogue. In addition, the Yb2-C1 distance of 2.759(10) Å is identical to the lutetium distance of 2.756(9) Å. Lastly, the M1-C1-M2 angle is the same for both molecules at 170°. The very slight differences in the bond distances

can be attributed to the slightly smaller effective ionic radius of trivalent lutetium relative to ytterbium as calculated by Shannon.[14] Unfortunately, further bonding comparisons cannot be made since the full crystallographic details of the lutetium complex have not been reported.

Figure 4. ORTEP diagram for $(Me_5C_5)_2YbMe$

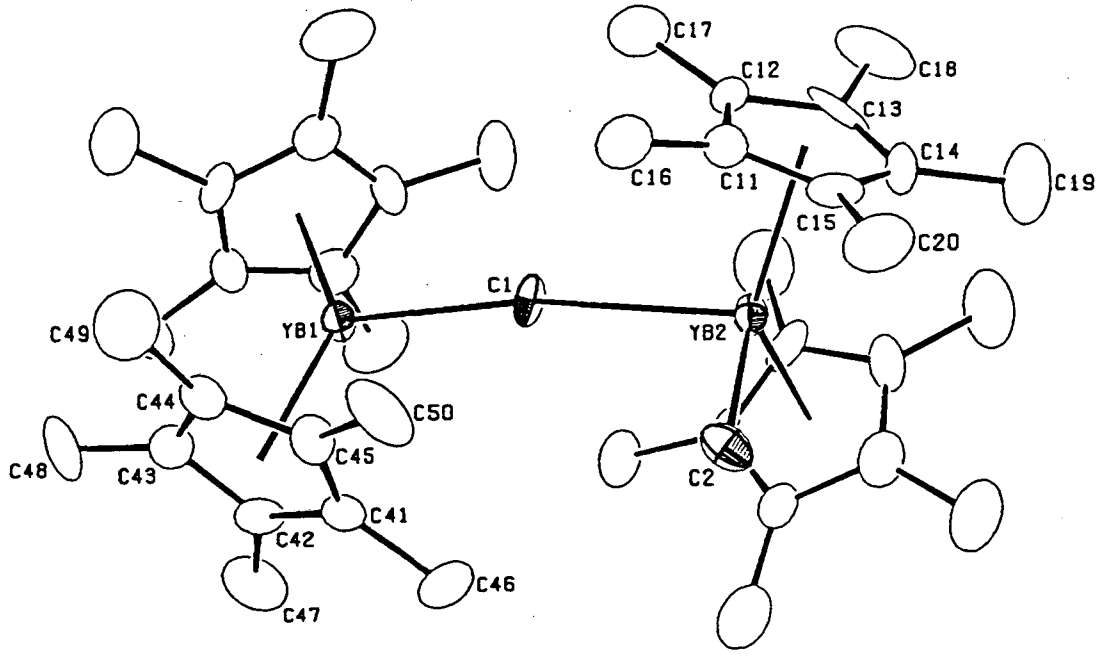

Details of the bonding interactions in the ytterbium methyl complex can be rationalized in the following way. The asymmetric structure is a consequence of the sterically demanding Me_5C_5 ligands. Whereas $[(C_5H_5)_2YbMe]_2$ forms a symmetrically bridged structure[15] (Figure 5), the larger Me_5C_5 ligands occupy too much space in the coordination sphere of ytterbium to allow both methyl groups to bridge in a symmetric fashion. Rotation of one-half of the molecule

Figure 5. Structure of $[(C_5H_5)_2YbMe]_2$

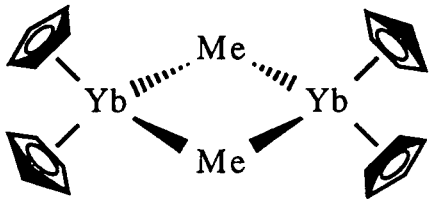

by 90° relieves the steric repulsions created by the bulky Me_5C_5 ligands. However, this rotation prevents the methyl groups from forming symmetrical bridges. This results in a nearly linear methyl bridge bond for which very few examples have been crystallographically characterized. The remaining methyl group is forced to sit in a terminal position.

Many complexes containing methyl bridges between metal atoms have been crystallographically characterized. Figure 6 illustrates examples of the ways methyl groups can bridge two metal centers. Structure 6(a) is the most common orientation observed for methyl bridges with the classic example being the structure of hexamethyl-dialuminum.[1,16] A few examples of type 6(b) have now

Figure 6

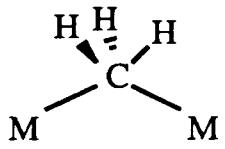

(a)

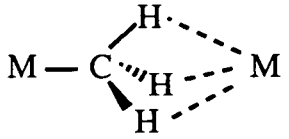

(b)

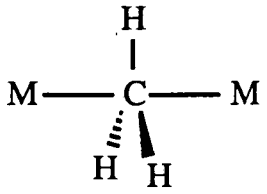

(c)

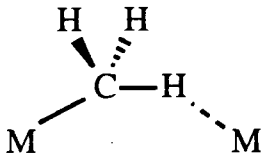

(d)

been observed in which the methyl hydrogen atoms have been located and refined.[17] Other examples have been rationalized as type 6(b) based on bond lengths relative to the position of the methyl group (ie. $(Me_5C_5)_2YbMe$ or $(Me_5C_5)_2LuMe$).[3c,18] Examples of type 6(c) bridges are extremely rare. Recently, two complexes containing a methyl group bridging two zirconium atoms have been crystallographically characterized.[19] The methyl hydrogen atoms have been refined and they form a nearly trigonal bipyramidal geometry around carbon. These are the only confirmed structures with this bonding orientation. There is also a uranium complex which may provide an additional example.[20] Although the methyl hydrogens could not be located, the symmetric positioning of the methyl group between the two uranium atoms suggests that the geometry at carbon is trigonal bipyramidal. Although type 6(d)

bridges have been postulated for species such as hexamethyldialuminum[21] and $[(C_5H_5)_2YbMe]_2$,[15b] these structures have been shown to be type 6(a) when high quality X-ray data were obtained. There are no confirmed complexes with type 6(d) bridges.

Although the methyl group lies between the two ytterbium atoms, it does not interact equally with them. The Yb1-C1 distance is much shorter than the Yb2-C1 distance. The weak coordination of C1 onto Yb2 produces an elongation in the Yb1-C1 bond as shown by comparison of the Yb1-C1 and Yb2-C2 bond lengths (2.446(10) Å vs. 2.377(13) Å). The terminal methyl group bonds at a right angle to C1. Unfortunately, the positions of the hydrogen atoms on the metal bound methyl groups could not be determined from the difference Fourier map. This is a consequence of the large amount of electron density on ytterbium and the influence it has on the electron density of the surrounding atoms. Very small amounts of electron density close to ytterbium will be masked and the accurate determination of their positions would be very difficult, if not impossible. The data may also be affected by the large absorption coefficient resulting from the presence of two heavy ytterbium atoms in the structure which diminishes the intensity of the reflections.

Reactions of $(Me_5C_5)_2YbMe$

The similarities in the structures of the ytterbium and lutetium methyl complexes suggest that the dissociation energies of the dimers should also be similar. The dissociation energy for the lutetium complex was calculated to be 12.6 kcal/mol from NMR

spectroscopic data.[3c] Although the aforementioned difficulty in examining the ytterbium species by NMR spectroscopy prevents the determination of it dissociation energy, the value should not be appreciably different from that of lutetium. Therefore, the bridging interaction should be easily cleaved which would open a coordination site on ytterbium and promote reactivity.

To test this assumption, some simple reactions of the methyl complex have been investigated. Diethyl ether and tetrahydrofuran cleanly produce the previously observed base adducts[2,5] (Eqn. 6). The diethyl ether complex can also be synthesized directly from

$$(Me_5C_5)_2YbMe \xrightarrow{L} (Me_5C_5)_2YbMe(L) \qquad L = Et_2O, THF \quad (6)$$

the reaction of $(Me_5C_5)_2Yb(OEt_2)$ and methylcopper. This can be a useful reagent for reactions in which the ether ligand is easily displaced by the incoming substrate. Trimethylaluminum will also add directly to $(Me_5C_5)_2YbMe$ to form the tetramethylaluminate complex (Eqn. 7), which has been previously synthesized from several different routes.[4,6]

$$(Me_5C_5)_2YbMe + Me_3Al \longrightarrow (Me_5C_5)_2Yb(\mu\text{-}Me)_2AlMe_2 \quad (7)$$

Like many other metal alkyl complexes,[1] $(Me_5C_5)_2YbMe$ acts as a catalyst towards ethylene polymerization. A small quantity of material dissolved in hexane and pressurized with ethylene (7 atm) in a Fischer-Porter high pressure reaction vessel will produce polycrystalline polyethylene instantaneously. The pressure of ethylene

drops rapidly and is completely equilized within a few minutes. The reaction mixture maintains its reddish coloration throughout the polymerization indicating that the system is still active even after the ethylene has been completely consumed. The Cossee mechanism often invoked for Ziegler-Natta catalysts should apply to this system as well.[22] The dimer separates into two monomers which opens a coordination site on ytterbium. Ethylene then coordinates to the metal before inserting into the metal-carbon bond. This process then continues until a β-hydride elimination results in chain termination.

Unfortunately, the methyl complex does not polymerize other alkenes. Propylene forms a yellow oil which may be a mixture of oligomerization products. Tetrafluoroethylene reacts stoichiometrically with the methyl complex to form an insoluble purple powder. Based on Burns' fluoride abstraction studies of $(Me_5C_5)_2Yb$ with fluorocarbons,[23] an ytterbium fluoride complex may have been produced.

If ethylene insertion into the metal-carbon bond is involved in the polymerization mechanism, then it may be possible to insert other small, unsaturated organic substrates into the metal-carbon bond. These products might then provide insight into the role of metallic species in organic transformations. Unfortunately, reactions of $(Me_5C_5)_2YbMe$ with carbon monoxide, 2-butyne, tert-butylnitrile, and tert-butylisocyanide led either to intractable oils or poorly behaved solids. For the solid materials, absorptions in the IR spectra in the region 1500-1700 cm^{-1} suggest that insertion has occurred. However, the species could not be obtained cleanly enough to allow full characterizations.

The methyl complex reacts with hydrogen or deuterium to form the mixed-valent hydride or deuteride, respectively (Eqn. 8). These species are identical to the products of the hydrogenation or deuteration of the bulky alkyl complex, $(Me_5C_5)_2YbCH(SiMe_3)_2$.[9]

$$2\,(Me_5C_5)_2YbMe + 2\,H_2 \longrightarrow [(Me_5C_5)_2Yb]_2(\mu\text{-}H) + 1/2\,H_2 + 2\,MeH \quad (8)$$

As in the case of $(Me_5C_5)_2YbCH(SiMe_3)_2$, the simple ytterbium hydride complex is believed to form initially which is then unstable toward loss of hydrogen and formation of the mixed-valent species (Scheme 3). This process is then driven by the low solubility of the product. Because the simple trivalent ytterbium hydride cannot be isolated, a comparison cannot be made with the chemistry of the highly reactive lutetium hydride complex.

Scheme 3

$$(Me_5C_5)_2YbMe + H_2 \longrightarrow (Me_5C_5)_2YbH + MeH$$

$$2\,(Me_5C_5)_2YbH \longrightarrow 2\,(Me_5C_5)_2Yb + H_2$$

$$(Me_5C_5)_2YbH + (Me_5C_5)_2Yb \longrightarrow [(Me_5C_5)_2Yb]_2(\mu\text{-}H)$$

The synthesis of the mixed-valent hydride complex invokes the question of whether a methyl derivative, $[(Me_5C_5)_2Yb]_2(\mu\text{-}Me)$, could be isolated. The structure of the asymmetric methyl dimer shows that a methyl group can bridge two ytterbium atoms due to the high

Lewis acidity of ytterbium. Thus, when $(Me_5C_5)_2Yb$ is added to $(Me_5C_5)_2YbMe$ in pentane, a dark red precipitate immediately forms. The powder can be recrystallized from toluene to give brick red crystals. This same product can be obtained directly from methylcopper by using two equivalents of $(Me_5C_5)_2Yb$. In this case, a slight excess of $(Me_5C_5)_2Yb$ is used to ensure complete conversion to the mixed-valent species. The lower solubility of the product relative to $(Me_5C_5)_2Yb$ allows it to be separated by fractional crystallization.

Although a parent ion is not observed in the mass spectrum, an ion is observed at 768 amu which corresponds to the loss of one Me_5C_5 ring from $[(Me_5C_5)_2Yb]_2(\mu\text{-Me})$. This suggests that the complex is more tightly bound than the asymmetric dimer since the bridge remains intact in the gas phase. The ^1H NMR spectrum shows a single broad resonance at δ 5.46 ($\upsilon_{1/2}$ = 150 Hz) which is substantially closer than that of the asymmetric dimer to the diamagnetic resonance of $(Me_5C_5)_2Yb$ (δ 1.92). Two explanations can be used to rationalize the presence of only a single resonance: (1) electronic exchange between the two metals is fast on the NMR time scale making all of the Me_5C_5 ligands equivalent by symmetry or (2) there is an equilibrium process occurring such that only an averaged shift for all species involved is observed.

In order to determine whether an equilibrium process is responsible for the observed behavior, a variable temperature NMR study was performed. The plot of δ vs. 1/T (Figure 7) displays a distinct non-linearity in the data points which suggests that an equilibrium is in fact occurring.[13] This behavior can be explained by a fluxional process in which the complex breaks into separate

paramagnetic and diamagnetic fragments (Eqn. 9). Because the observed resonance would be an average of the resonances for all

Figure 7. Plot of δ vs. 1/T for $[(Me_5C_5)_2Yb]_2(\mu\text{-Me})$

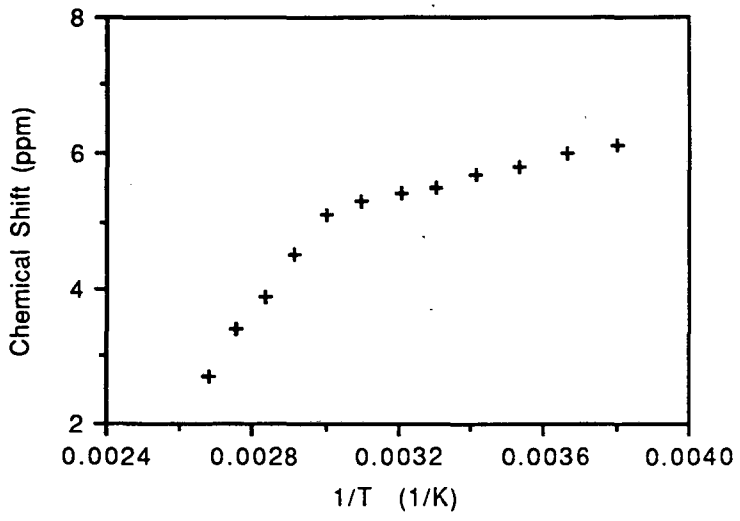

species involved in the equilibrium, addition of an excess of one component should influence the chemical shift in favor of that component. Thus, when excess $(Me_5C_5)_2Yb$ is added to a sample of $[(Me_5C_5)_2Yb]_2(\mu\text{-Me})$, a single resonance is still observed, but it is shifted upfield to 3.27 ppm which is closer to the diamagnetic value for $(Me_5C_5)_2Yb$. Therefore, it can be concluded that an equilibrium process is occurring in solution which involves dissociation of $(Me_5C_5)_2Yb$ from the parent compound.

$$[(Me_5C_5)_2Yb]_2(\mu\text{-Me}) \rightleftharpoons (Me_5C_5)_2YbMe + (Me_5C_5)_2Yb \quad (9)$$

The variable temperature magnetic susceptibility (Figure 8) of $[(Me_5C_5)_2Yb]_2(\mu\text{-Me})$ is consistent with a simple trivalent ytterbium complex with one unpaired electron. The magnetic moment measured at 5 kG in the low temperature region (6-30 K) is 4.56 μ_B with Θ = -0.45 K, while in the high temperature region (50-280 K) the moment is 4.75 μ_B with Θ = -5.85 K. These values indicate that the complex contains an isolated Yb(III) paramagnet with an associated diamagnetic diluent. There is no evidence for electronic communication between the two metal centers.

Figure 8. Plot of $1/\chi_M$ vs. T for $[(Me_5C_5)_2Yb]_2(\mu\text{-Me})$

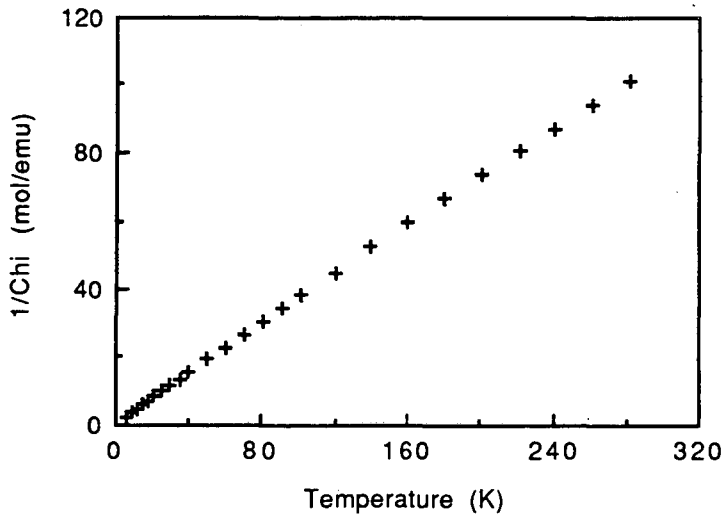

An X-ray crystal structure determination has been undertaken to verify whether the magnetic behavior manifests itself in the solid state structure of the complex. Selected bond lengths and angles are

listed in tables 3 and 4, respectively, and an ORTEP diagram is provided in Figure 9.

Table 3. Bond distances for $[(Me_5C_5)_2Yb]_2(\mu\text{-Me})$ (Å)

Yb1-C1	2.366 (5)	Yb1-Cp1	2.276
Yb2-C1	2.744 (5)	Yb1-Cp2	2.284
		Yb2-Cp3	2.384
		Yb2-Cp4	2.391
Yb1-C11	2.592 (6)	Yb2-C31	2.657 (6)
Yb1-C12	2.580 (6)	Yb2-C32	2.688 (6)
Yb1-C13	2.574 (6)	Yb2-C33	2.698 (6)
Yb1-C14	2.547 (6)	Yb2-C34	2.665 (6)
Yb1-C15	2.576 (6)	Yb2-C35	2.631 (6)
Yb1-C21	2.553 (6)	Yb2-C41	2.671 (6)
Yb1-C22	2.574 (6)	Yb2-C42	2.651 (6)
Yb1-C23	2.595 (6)	Yb2-C43	2.662 (6)
Yb1-C24	2.605 (6)	Yb2-C44	2.707 (6)
Yb1-C25	2.590 (6)	Yb2-C45	2.685 (6)

Cp1, Cp2, Cp3, and Cp4 are the ring centroids of atoms C11-C15, C21-C25, C31-C35, and C41-C45, respectively.

Table 4. Bond Angles for $[(Me_5C_5)_2Yb]_2(\mu\text{-Me})$ (°)

Yb1-C1-Yb2	169.1 (3)	C1-Yb1-Cp1	108.3
		C1-Yb1-Cp2	109.0
Cp1-Yb1-Cp2	142.7	C1-Yb2-Cp3	106.6
Cp3-Yb2-Cp4	144.9	C1-Yb2-Cp4	108.5

The metal-bound methyl group rests between the two ytterbium atoms in a near linear fashion. The Yb1-C1-Yb2 angle of 169.1(3)° is very similar to the bridging angle in the asymmetric methyl dimer. Consistent with the magnetic data, the structure clearly shows that the two ytterbium atoms possess different oxidation states, thus,

making this a static mixed-valent complex. This is demonstrated by the inequivalent bond distances between the methyl group and the

Figure 9. ORTEP diagram of $[(Me_5C_5)_2Yb]_2(\mu\text{-}Me)$

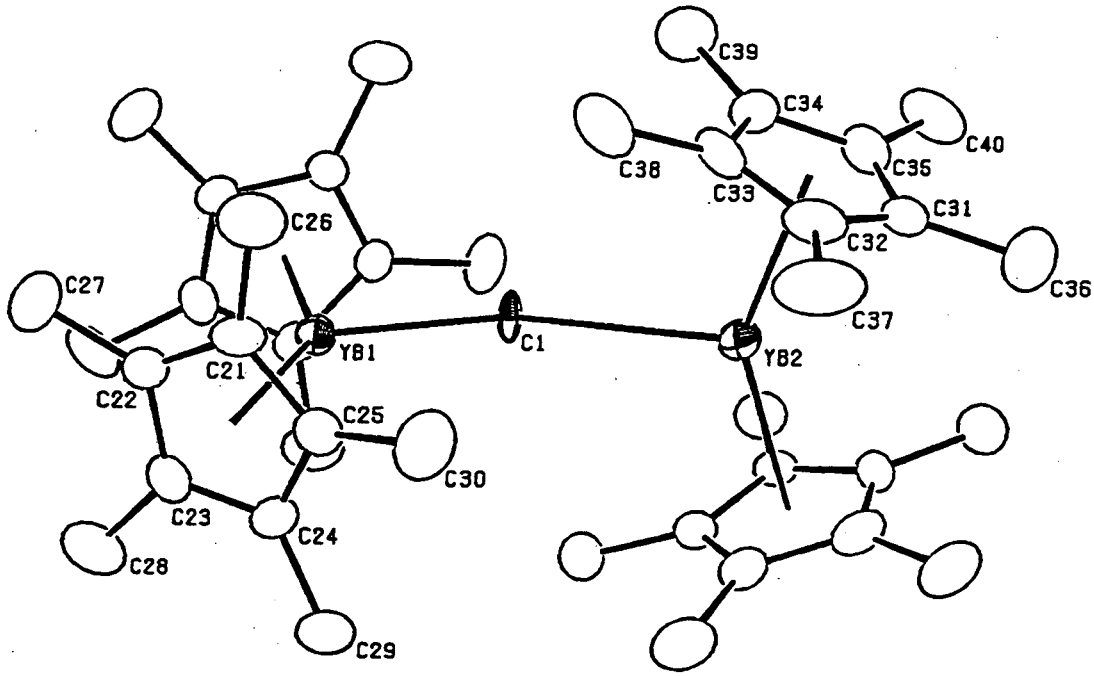

two metal atoms. The Yb1-C1 distance of 2.366(5) Å is much shorter than the Yb2-C1 distance of 2.744(5) Å indicating that the methyl group is directly bound to the trivalent Yb1 while it is coordinated to the divalent Yb2. Thus, the bridging interactions are very similar to those in the asymmetric methyl dimer. Unfortunately, the hydrogen atoms on the metal bound methyl group could not be located in this molecule. However, the position of the methyl group suggests that the geometry around the carbon atom remains tetrahedral with the hydrogen atoms directed toward Yb2.

The two sets of Me_5C_5 ligands are oriented at approximately 90° to each other in order to minimize inter-ligand repulsions between the Me_5C_5 rings. The ring distances also reflect the differences in the oxidation states of the two metals. The Yb1-ring centroid distances of 2.28 Å are substantially shorter than the Yb2-ring centroid distances of 2.39 Å. This reflects the smaller radius of the trivalent Yb1 atom. The increased steric crowding around Yb1 also accounts for the slightly smaller ring centroid-Yb1-ring centroid angle of 143° relative to the ring centroid-Yb2-ring centroid angle of 145°.

Because both ytterbium atoms are formally seven-coordinate, the Me_5C_5 ligands can orient themselves more symmetrically than in the asymmetric dimer observed for $(Me_5C_5)_2YbMe$. This results in a more compact structure and a stronger overall bridging interaction for the mixed-valent complex which is demonstrated by the shorter Yb1-C1 and Yb2-C1 bond lengths relative to those in the asymmetric dimer. This may account for the increased stability towards dissociation in the gas phase as observed in the mass spectrum. This stability is also observed in the mixed-valent fluoride complex, $[(Me_5C_5)_2Yb]_2(\mu\text{-}F)$, which gives a molecular ion in the mass spectrum.[23] This mixed-valent complex has also been structurally characterized and found to be similar to the methyl analogue. Thus, $[(Me_5C_5)_2Yb]_2(\mu\text{-}Me)$ not only represents another example of a complex with an unusual linear methyl bridge, it also displays mixed-valent character which cannot be incorporated into most other lanthanide complexes.

Because of the high reactivity of metal alkyls, $(Me_5C_5)_2YbMe$ should be a useful precursor to other new species through sigma bond metathesis. Because NH_2^- is isoelectronic with CH_3^-, the simple amide complex of ytterbium might display parallel chemistry. The high pK_a of methane suggests that the ytterbium methyl complex may activate the N-H bonds of simple amines.[24] When anhydrous ammonia is condensed onto a frozen solution of $(Me_5C_5)_2YbMe$, a bright yellow-orange product is obtained upon warming to room temperature (Eqn. 10):

$$(Me_5C_5)_2YbMe + \text{xs. } NH_3 \longrightarrow (Me_5C_5)_2YbNH_2(NH_3) + MeH \quad (10)$$

The complex crystallizes as light, feathery needles which precludes an X-ray diffraction study. An elemental analysis reveals that there is excess ammonia in the product which is not surprising given the high affinity of $(Me_5C_5)_2Yb$ for ammonia.[6] There are two broad absorptions in the IR spectrum at 3361 and 3280 cm^{-1} associated with the NH_2^- and NH_3 ligands, respectively. The highest ion in the mass spectrum corresponds to the loss of an ammonia molecule from $(Me_5C_5)_2YbNH_2(NH_3)$ which is consistent with the behavior of other ammonia complexes.[6] The ^1H NMR spectrum displays a single resonance for the Me_5C_5 ligands at δ 2.76. The line width is much narrower ($\upsilon_{1/2}$ = 30 Hz) than for the methyl precursor, perhaps due to lower dissociation in solution. As is common, the nitrogen bound protons are not observed.[6] The deuterated analogue, $(Me_5C_5)_2Yb-ND_2(ND_3)$, can also be synthesized. The N-D stretches in the IR spectrum occur at 2504 and 2380 cm^{-1}.

Because the simple base-free amide is the desired complex for comparative reactivity studies, it would be useful to find a method of removing ammonia from $(Me_5C_5)_2YbNH_2(NH_3)$. Although trimethylaluminum would be unlikely to form a strong enough interaction with ytterbium to displace ammonia, it might be able of abstract ammonia from the complex by forming the acid-base adduct $Me_3Al{\cdot}NH_3$. However, when trimethylaluminum is added to $(Me_5C_5)_2YbNH_2(NH_3)$, the color changes from orange to deep red and a gas is evolved. Rather then removing the ammonia ligand from yttterbium, a methyl group on trimethylaluminum activates an N-H bond and releases methane. The aluminum then bonds to nitrogen to produce a diamidodimethylaluminate complex (Eqn. 11).

$$(Me_5C_5)_2YbNH_2(NH_3) + Me_3Al \longrightarrow (Me_5C_5)_2Yb(\mu\text{-}NH_2)_2AlMe_2 + MeH \quad (11)$$

There are two N-H stretches in the IR spectrum at 3385 and 3331 cm^{-1} consistent with a bridging amide structure[25] and there is an ion in the mass spectrum at 533 amu corresponding to the intact molecule. The ^1H NMR spectrum shows two resonances at δ 4.86 and -22.5 which integrate as the Me_5C_5 protons and the aluminum bound methyl protons, respectively. Unlike the amide protons, the protons on the methyl groups bound to aluminum are far enough from the paramagnetic ytterbium center to allow their observation in the ^1H NMR spectrum. The assignment of the complex as a simple monomer is supported by the similarity of the chemical shift for the aluminum

bound methyl protons to that observed in the monomeric form of the ytterbium tetramethylaluminate complex, $(Me_5C_5)_2Yb(\mu\text{-}Me)_2AlMe_2$ (δ -26.5).[6]

There are many examples of tetramethylaluminate complexes in the literature.[26] For the lanthanide metals, the species $(Me_5C_5)_2M(\mu\text{-}Me)_2AlMe_2$ are known for samarium, ytterbium, and lutetium.[4,6,27] All three species exhibit a monomer-dimer equilibrium in solution (Eqn. 12). In addition, the solid state structure of the samarium complex has been determined and shows the dimer to be

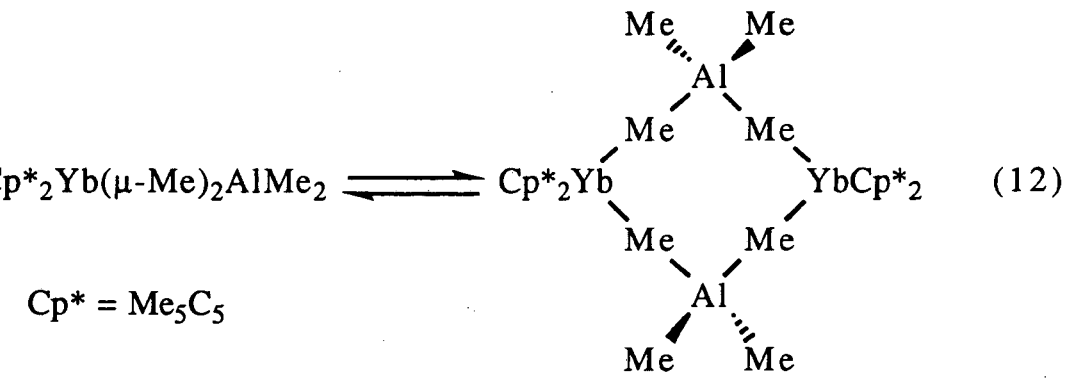

(12)

the more stable form in the solid state. This complex also provides another example of a molecule containing linear methyl bridges. Because of the lone pairs on the amide ligands, the dimeric structure would be expected to be less stable for the diamidodimethylaluminate complex. The amide ligands would be able to direct the lone pairs toward ytterbium much more effectively with bent bridges than with linear bridges.

In order to verify the monomeric nature of the diamidodimethylaluminate complex, an X-ray crystallographic determination has been performed. Selected bond lengths and angles are listed in

Tables 5 and 6, respectively, and an ORTEP diagram is provided in Figure 10.

Table 5. Bond distances for $(Me_5C_5)_2Yb(\mu\text{-}NH_2)_2AlMe_2$ (Å)

Yb-N1	2.346 (8)	Yb-C11	2.630 (9)
Yb-N2	2.338 (9)	Yb-C12	2.609 (10)
Yb-Cp1	2.337	Yb-C13	2.609 (9)
Yb-Cp2	2.332	Yb-C14	2.634 (9)
		Yb-C15	2.658 (9)
Al-N1	1.921 (9)	Yb-C21	2.630 (9)
Al-N2	1.921 (9)	Yb-C22	2.666 (9)
Al-C1	1.957 (12)	Yb-C23	2.639 (9)
Al-C2	1.967 (11)	Yb-C24	2.578 (10)
		Yb-C25	2.604 (10)
N1-HA	0.87 (11)		
N1-HB	0.98 (11)		
N2-HC	0.82 (10)		
N2-HD	0.89 (13)		

Cp1 and Cp2 are the ring centroids of atoms C11-C15 and C21-C25, respectively.

Table 6. Bond Angles for $(Me_5C_5)_2Yb(\mu\text{-}NH_2)_2AlMe_2$ (°)

Yb-N1-Al	96.2 (3)	Cp1-Yb-Cp2	138.4
Yb-N2-Al	96.5 (4)	Cp1-Yb-N1	106.5
N1-Yb-N2	73.6 (3)	Cp1-Yb-N2	106.9
N1-Al-N2	93.8 (4)	Cp2-Yb-N1	106.6
C1-Al-C2	113.0 (5)	Cp2-Yb-N2	106.1
		C1-Al-N1	111.8 (4)
HA-N1-HB	111 (9)	C1-Al-N2	112.8 (5)
HC-N2-HD	110 (10)	C2-Al-N1	112.2 (5)
		C2-Al-N2	111.8 (4)

Figure 10. ORTEP diagram of $(Me_5C_5)_2Yb(\mu\text{-}NH_2)_2AlMe_2$.

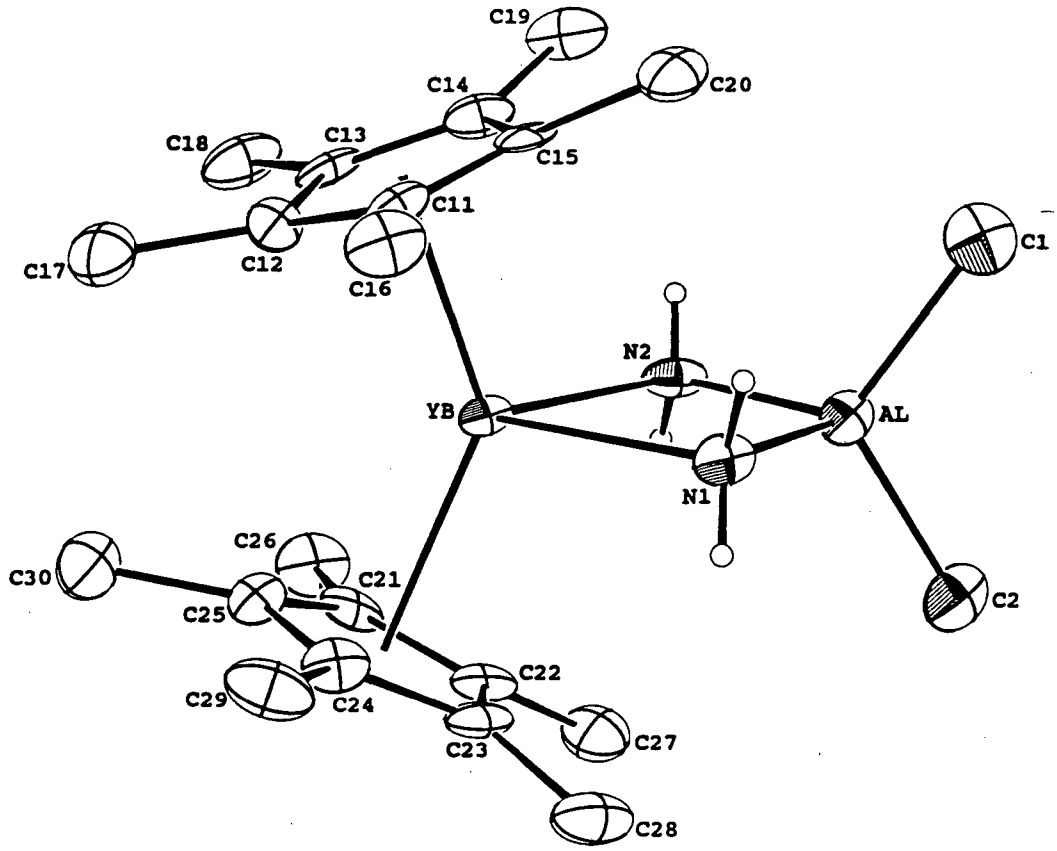

As expected, the complex exists as a monomer in the solid state and substantiates the interpretation of the spectroscopic data. The amide ligands form a four-membered ring with ytterbium and aluminum. The ring is essentially planar with the inner angles close to 90° except for the N1-Yb-N2 angle which is somewhat smaller. This acute angle is a consequence of the longer Yb-N bond lengths and the nature of the metal-ligand bonding interaction. Because both nitrogen atoms are observed equidistant to aluminum and equidistant to

ytterbium, the bonding in the core of the complex can be best described as an average of two resonance forms (Figure 11). The presence of dative interactions betwen the amide ligands and the two metal centers allows the formation of acute bonding angles without creating excessive ring strain. The geometry around aluminum remains pseudotetrahedral with the terminal methyl groups oriented in a plane perpendicular to the four-membered ring.

Figure 11

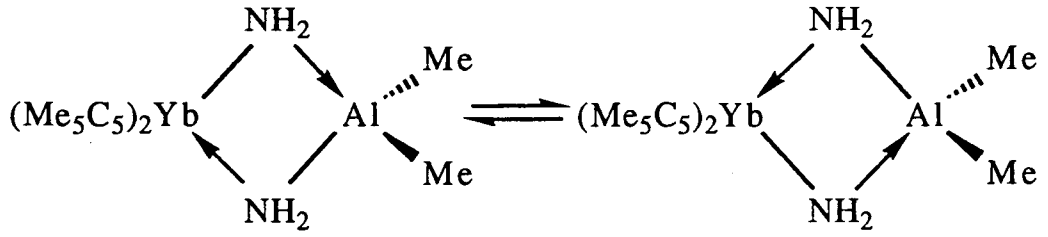

The hydrogen atoms on the amide groups have been located in a difference Fourier map and refined isotropically. Although the hydrogen atom positions are poorly defined, they clearly show that the hydrogen atoms are directed outward away from the four-membered ring. This maintains a pseudotetrahedral geometry around the nitrogen atoms. Although the simple amide complex of ytterbium could not be obtained, this reaction did generate the first example of a diamidodimethylaluminate complex which has been shown to behave differently from the tetramethylaluminate complexes of the lanthanides.

Attempts to observe C-H activation products like those isolated from the reactions of $(Me_5C_5)_2LuMe$ have proven unsuccessful. The

ytterbium phenyl complex could not be isolated by refluxing a benzene solution of $(Me_5C_5)_2YbMe$ for 24 hours. Similarly, using hexane as the solvent and refluxing a mixture of $(Me_5C_5)_2YbMe$ and benzene does not produce the phenyl complex. In addition, $(Me_5C_5)_2YbMe$ does not react with tetramethylsilane to produce the trimethylsilylmethyl complex even in refluxing hexane. There is no simple explanation for the difference in chemistry for ytterbium relative to lutetium. Although experimental details for the lutetium reactions have not been reported, the reactions apparently occur under quite mild conditions.[3a]

Reactions of $(Me_5C_5)_2YbCH(SiMe_3)_2$

Because of the bulkiness of the bis(trimethylsilyl)methyl ligand, the alkyl complex of ytterbium can be synthesized via a metathetical route[9] (Eqn. 13):

$$(Me_5C_5)_2Yb(\mu\text{-}Cl)_2Na(OEt_2)_2 + LiCH(SiMe_3)_2 \longrightarrow (Me_5C_5)_2YbCH(SiMe_3)_2 + NaCl + LiCl \quad (13)$$

Since this complex can be synthesized under much more convenient reaction conditions than $(Me_5C_5)_2YbMe$, it was of interest to compare their relative reactivities. As mentioned earlier, Burns has reported the reaction of $(Me_5C_5)_2YbCH(SiMe_3)_2$ with H_2 which yields the mixed-valent hydride complex, $[(Me_5C_5)_2Yb]_2(\mu\text{-}H)$.[9] Whereas this reaction requires over an hour for completion, the analogous reaction with $(Me_5C_5)_2YbMe$ occurs instantaneously. The difference in rates

can be attributed to the large steric bulk of the bis(trimethylsilyl)-methyl ligand. For the reaction to take place, the hydrogen molecule presumably must first form a weak coordination complex with ytterbium before the H-H bond breaks to produce the hydride complex and the free alkane. Therefore, the bis(trimethylsilyl)methyl ligand makes the metal less accessible to incoming substrates which results in a lower reaction rate.

This behavior has also been observed for the ethylene polymerization reaction as well as the synthesis of the amide complex, $(Me_5C_5)_2YbNH_2(NH_3)$. In the polymerization reaction, the ethylene pressure is not completely consumed for about an hour when the bis(trimethylsilyl)methyl complex is the catalyst. This is in contrast to the results when $(Me_5C_5)_2YbMe$ is the catalyst as the reaction is complete within minutes under similar conditions. In the reaction of $(Me_5C_5)_2YbCH(SiMe_3)_2$ with ammonia, although this reaction is still quite fast, the cooled mixture must warm above 0 °C before the transformation to $(Me_5C_5)_2YbNH_2(NH_3)$ is observed.

It should be noted, however, that despite the slow reaction rates, the bis(trimethylsilyl)methyl complex is capable of activating rather bulky substrates. If allowed to stir for several days with diphenylamine, the dark brown diphenylamide complex can be isolated (Eqn. 14):

$$(Me_5C_5)_2YbCH(SiMe_3)_2 + Ph_2NH \longrightarrow (Me_5C_5)_2YbNPh_2 + (Me_3Si)_2CH_2 \quad (14)$$

This indicates that the bis(trimethylsilyl)methyl ligand does not kinetically prohibit reactions, but merely decreases their reaction rates. Therefore, both $(Me_5C_5)_2YbCH(SiMe_3)_2$ and $(Me_5C_5)_2YbMe$ are useful synthons.

Other Copper Reagents

Other reactive copper complexes are known which could be studied in order to determine the generality of the electron-transfer/ ligand-exchange reactions for the synthesis of trivalent ytterbium species. Berg has found that mesitylcopper does not react with $(Me_5C_5)_2Yb$ even at elevated temperatures.[6] This is presumably a consequence of the bulky mesityl ligands.[28] The more reactive trimethylsilylmethylcopper complex has been reported[29] and is somewhat thermally unstable as well as light sensitive. This complex exists as a tetramer in the solid state and is soluble in nonpolar hydrocarbons from which it can be easily purified by recrystallization.

This copper reagent reacts with $(Me_5C_5)_2Yb$ to produce the trimethylsilylmethyl complex of ytterbium (Eqn. 15). Analysis of the complex is complicated by its extreme solubility which prevents the

$$(Me_5C_5)_2Yb + Me_3SiCH_2Cu \longrightarrow (Me_5C_5)_2YbCH_2SiMe_3 + Cu^\circ \quad (15)$$

isolation of a nicely crystalline material. However, there is spectroscopic evidence that the expected complex has been obtained. The IR spectrum shows absorptions consistent with the presence of a trimethylsilyl group in the product in addition to a low energy absorp-

tion at 313 cm^{-1} which is thought to be diagnostic for a ring tilting mode in trivalent permethylytterbocene species.[6] In addition, there is a molecular ion in the mass spectrum at 531 amu corresponding to the predicted complex with no higher masses being observed.

The ^1H NMR spectrum is unexpectedly complex, however. There are three resonances in approximately a 15:15:9 integrated ratio. This suggests that the protons on the methyl groups bound to silicon are observed and that the Me_5C_5 ligands are inequivalent. The inequivalency of the rings can be rationalized by the construction of a Newman projection shown in Figure 12(a). Looking down the ytterbium-carbon bond axis, the trimethylsilyl group can

Figure 12

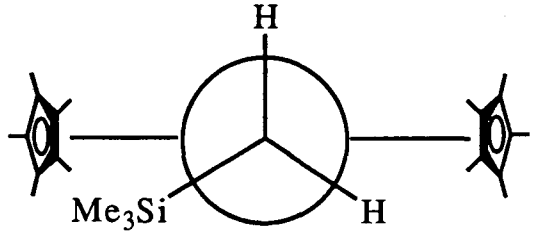

(a)

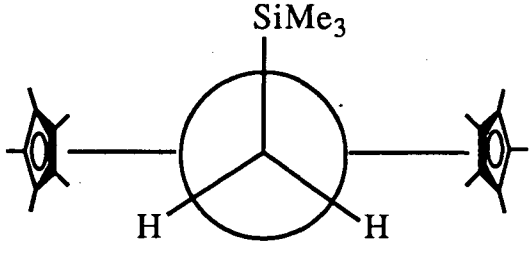

(b)

be oriented such that the two rings exist in different environments. However, this would require rotation about the ytterbium-carbon axis to be slow on the NMR timescale. This might be possible if there are strong agostic M-H interactions with the methylene protons which hold the ligand in a fixed position. Unfortunately, there is no evidence of low energy C-H stretches in the IR spectrum associated with such an interaction. Furthermore, a variable temperature NMR study shows that although the ring resonances appear to broaden at higher temperatures, they are still far from reaching coalescence even at 70 °C. Lastly, steric considerations should favor the orientation shown in Figure 12(b) which places the trimethylsilyl group between the Me_5C_5 rings and makes them equivalent even in the absence of fast rotation. Therefore, a clear understanding of this complex would require a solid state structural determination in order to establish the true bonding interactions. Unfortunately, suitable crystals for an X-ray study have not been obtained.

Several copper(I) amide species have been prepared.[30] These reagents might be used to demonstrate the transfer of inorganic ligands to ytterbium. The reaction of $CuNH_2$ would also eliminate the presence of excess ammonia as found in the reaction of $(Me_5C_5)_2YbMe$ with ammonia. However, despite the appearance of reduced copper metal in the reaction mixture, no ytterbium amide complex could be isolated. This indicates that either the ytterbium amide species is unstable, or that the copper amide decomposes to products such as hydrazine before the ligand can transfer to ytterbium. In order to obtain the simple ytterbium-amide complex,

$(Me_5C_5)_2YbNH_2$, it may be necessary to use high-vacuum techniques to react $(Me_5C_5)_2YbMe$ with one equivalent of ammonia.

The organocopper complexes are useful synthetic reagents for the electron-transfer/ligand-exchange reactions with $(Me_5C_5)_2Yb$. This has allowed base-free $(Me_5C_5)_2YbMe$ to be isolated in one step so that its reaction chemistry could be studied in detail. This complex has also been found to be a useful precursor to other novel ytterbium species. Unfortunately, the use of copper(I) reagents has not led to an abundance of simple base-free complexes. The difficulty in using copper(I) complexes stems from two general characteristics: (1) they are often highly unstable, being sensitive to light, heat and air and (2) they are often polymeric and highly insoluble making purification difficult. For these reasons, some reported species have only minimal characterization and are poorly understood. Therefore, it would be desirable to develop a ligand source which is stable, isolable and easy to purify while also cleanly transferring its ligands to ytterbium and having enough versatility to incorporate different types of ligands.

References

1. Yamamoto, A., "Organotransition Metal Chemistry," Wiley-Interscience: New York, **1986**.

2. Watson, P. L., *J. Am. Chem. Soc.*, **1982**, *104*, 337.

3. (a) Watson, P. L., *J. Chem. Soc., Chem. Commun.*, **1983**, 276.
(b) Watson, P. L., *J. Am. Chem. Soc.*, **1983**, *105*, 6491.
(c) Watson, P. L.; Parshall, G. W., *Acc. Chem. Res.*, **1985**, *18*, 51.

4. Scheme 1 adapted from: Watson, P. L.; Herskovitz, T., "Initiation of Polymerization," *ACS Symposium Series*, Bailey, F. E., ed., **1983**, *212*, 460.

5. Watson, P. L., *J. Chem. Soc., Chem. Commun.*, **1980**, 652.

6. Berg, D. J., Ph.D. Thesis, University of California, Berkeley, **1987**.

7. Finke, R. G.; Keenan, S. R.; Schiraldi, D. A.; Watson, P. L., *Organometallics*, **1986**, *5*, 598.

8. Berg, D. J.; Andersen, R. A.; Zalkin, A., *Organometallics*, **1988**, *7*, 1858.

9. Burns, C. J., Ph.D. Thesis, University of California, Berkeley, **1987**.

10. Johnson, D. A., "Some Thermodynamic Aspects of Inorganic Chemistry," 2nd Ed., Cambridge University Press: Cambridge, **1982**.

11. Posner, G. H., "An Introduction to Synthesis Using Organocopper Reagents," Wiley: New York, **1980**.

12. Ikariya, T.; Yamamoto, A., *J. Organomet. Chem.*, **1974**, *72*, 145.

13. Jahn, W.; Yunlu, K.; Oroschin, W.; Amberger, H. D.; Fischer, R. D., *Inorg. Chim. Acta*, **1984**, *95*, 85.

14. Shannon, R. D., *Acta. Cryst.*, **1976**, *A32*, 751.

15. (a) Holton, J.; Lappert, M. F.; Ballard, D. G. H.; Pearce, R.; Atwood, J. L.; Hunter, W. E., *J. Chem. Soc., Chem. Commun.*, **1976**, 480. (b) Holton, J.; Lappert, M. F.; Ballard, D. G. H.; Pearce, R.; Atwood, J. L.; Hunter, W. E., *J. Chem. Soc., Dalton Trans.*, **1979**, 54.

16. (a) Coates, G. E.; Green, M. L. H.; Powell, P.; Wade, K., "Principles of Organometallic Chemistry," Chapman and Hall: London, **1968**. (b) Lewis, P. H.; Rundle, R. E., *J. Chem. Phys.*, **1953**, *21*, 986. (c) Vranka, R. G.; Amma, E. L., *J. Am. Chem. Soc.*, **1967**, *89*, 3121. (d) Cotton, F. A., *Inorg. Chem.*, **1970**, *9*, 2804. (e) Huffman, J. C.; Streib, W. E., *J. Chem. Soc., Chem. Commun.*, **1971**, 911. (f) Almenningen, A.; Halvorsen, S.; Haaland, A., *Acta Chem. Scand.*, **1971**, *25*, 1937.

17. (a) Burns, C. J.; Andersen, R. A., *J. Am. Chem. Soc.*, **1987**, *109*, 5853. (b) An ytterbium-aluminum complex has also been described in reference 6.

18. (a) Busch, M. A.; Harlow, R.; Watson, P. L., *Inorg. Chim. Acta*, **1987**, *140*, 15. (b) Hitchcock, P. B.; Lappert, M. F.; Smith, R. C., *J. Chem. Soc., Chem. Commun.*, **1989**, 369.

19. (a) Waymouth, R. M.; Santarsiero, B. D.; Coots, R. J.; Brownikowski, M. J.; Grubbs, R. H., *J. Am. Chem. Soc.*, **1986**, *108*, 1427. (b) Waymouth, R. M.; Santarsiero, B. D.; Grubbs, R. H., *J. Am. Chem. Soc.*, **1984**, *106*, 4050. (c) Waymouth, R. M.; Potter, K. S.; Schaeffer, W. P.; Grubbs, R. H., *organometallics*, **1990**, 2843.

20. Stults, S. D.; Andersen, R. A.; Zalkin, A., *J. Am. Chem. Soc.*, **1989**, *111*, 4507.

21. Byram, S. K.; Fawcett, J. K.; Nyburg, S. C.; O'Brien, R. J., *J. Chem. Soc., Chem. Commun.*, **1970**, 16.

22. Cossee, P., *J. Catalysis*, **1964**, *3*, 80.

23. Burns, C. J.; Andersen, R. A., *J. Chem. Soc., Chem. Commun.*, **1989**, 136.

24. Lowry, T. H.; Richardson, K. S., "Mechanism and Theory in Organic Chemistry," 2nd Ed., Harper and Row: New York, **1981**.

25. Nakamoto, K., "Infrared and Raman Spectra of Inorganic and Coordination Compounds," 4th Ed., Wiley-Interscience: New York, **1986**.

26. Schumann, H., *Angew. Chem. Int. Ed. Engl.*, **1984**, *23*, 474.

27. Evans, W. J.; Chamberlain, L. R.; Ulibarri, T. A.; Ziller, J. W., *J. Am. Chem. Soc.*, **1988**, *110*, 6423.

28. Tsuda, T.; Yazawa, T.; Watanabe, K.; Fujii, T.; Saegusa, T., *J. Org. Chem.*, **1981**, *46*, 192.

29. (a) Lappert, M. F.; Pearce, R., *J. Chem. Soc., Chem. Commun.*, **1973**, 24. (b) Jarvis, J. A. J.; Pearce, R.; Lappert, M. F., *J. Chem. Soc., Dalton Trans.*, **1977**, 999.

30. Tsuda, T.; Watanabe, K.; Miyata, K.; Yamamoto, H.; Saegusa, T., *Inorg. Chem.*, **1981**, *20*, 2728.

CHAPTER 2

Reactions of Bis(pentamethylcyclopentadienyl)ytterbium with Organovanadium Complexes

There are innumerable metal complexes which might act as ligand donors toward $(Me_5C_5)_2Yb$. However, the most synthetically useful species would possess a large degree of stability without requiring the presence of excess ligands which might promote unwanted side products. At the same time, the donor system must undergo a clean electron-transfer reaction with $(Me_5C_5)_2Yb$ to produce a single ytterbium product that can be easily separated. Fortunately, the high oxidation potential of $(Me_5C_5)_2Yb$ (1.4 V vs. SHE in acetonitrile) allows even complexes with unfavorable reduction potentials to be considered as possible ligand sources.

Organovanadium Complexes

Vanadium possesses a wide range of accessible oxidation states through which it can interchange.[1] It has been observed that trivalent vanadium halides can be reduced to divalent species via zinc reductions[2] (Eqn. 1):

$$4\ VCl_3(THF)_3 + 2\ Zn \xrightarrow{THF} [V_2Cl_3(THF)_6]_2[Zn_2Cl_6] \qquad (1)$$

These species have been instrumental in the development of low valent vanadium chemistry.[3] The availability of this reduction pathway might be useful for the synthesis of ytterbium complexes through electron-transfer processes with $(Me_5C_5)_2Yb$. Unfortunately,

there are very few examples of neutral, homoleptic vanadium complexes which could act as ligand donors.[4] Therefore, it is necessary to develop a ligand system which would stabilize potential donor complexes while maintaining the accessibility of the ligand to be transferred.

A great deal of organovanadium chemistry involves the use of cyclopentadienyl or substituted cyclopentadienyl ligands.[5] As is observed for the ytterbium complexes, the pentamethylcyclopentadienyl ligand enhances the stability and crystallinity of vanadium complexes relative to the unsubstituted cyclopentadienyl analogues. In addition, by using the same ligands for both donor and acceptor species, ring exchange processes cannot interfere with the isolation of the desired products. Ring exchanges have been observed between $(Me_5C_5)_2Yb$ and kinetically labile first row metallocenes as shown in Eqn. 2.[6]

$$(Me_5C_5)_2Yb + (C_5H_5)_2M \longrightarrow (Me_5C_5)Yb(C_5H_5) + (Me_5C_5)M(C_5H_5) \quad (2)$$

M = Mn, Ni

Trivalent organovanadium halides of the type $(Me_5C_5)_2V\,X$ (X = Cl[7], Br[8], I[7a]) have been reported. Because of their stability and straightforward syntheses, these species would provide a useful starting point for examining reactivity. Unfortunately, only the chloride has been rigorously characterized.[7b] In addition, it would be informative to include the previously unreported fluoride complex and complete the series. Since the known halide complexes have been prepared by various unrelated routes, it would be

beneficial to develop a general synthesis for the entire series and to report their full characterization.

Although cyclic voltammetry studies on $(Me_5C_5)_2V$ do not show reversible one-electron waves,[9] the oxidation potential of $(Me_5C_5)_2V$ can be estimated to be approximately 1.1 V vs. SHE based on cyclic voltammetry studies of $(C_5H_5)_2V$.[10] Studies of other first row decamethylmetallocenes indicate that the electron donating character of the pentamethylcyclopentadienyl ligands imparts an additional 0.5 V to the oxidation potentials relative to the unsubstituted analogues.[9] With this large potential, $(Me_5C_5)_2V$ should be capable of inducing electron transfer processes of its own.

Univalent copper and silver salts are readily available and show favorable reduction potentials[11] (0.52 V and 0.80 V vs. SHE for Cu(I) and Ag(I), respectively) for transferring halides to $(Me_5C_5)_2V$ in electron transfer reactions. Thus, when $(Me_5C_5)_2V$ is mixed with copper or silver halides, the trivalent vanadium species, $(Me_5C_5)_2VX$, can be isolated along with the formation of reduced metals (Eqn. 3). The high solubility of the $(Me_5C_5)_2VX$ complexes in non-polar solvents facilitates their separation from the finely divided metal powder and simplifies their purification.

$$(Me_5C_5)_2V + MX \longrightarrow (Me_5C_5)_2VX + M^\circ \qquad (3)$$

The halide complexes can all be obtained in reasonably good yield. The mass spectra indicate that they are all monomers in the gas phase and the paramagnetic species produce broad resonances in the ^1H NMR spectra. The properties of the halide complexes are

listed in Table 1. The previously unreported vanadium fluoride complex behaves similarly to the known halide species. A variable temperature magnetic susceptibility study (Figure 1) shows that the complex contains a simple trivalent vanadium ion which follows Curie-Weiss behavior from 5-300 K with a magnetic moment of 2.78 μ_B and Θ = -0.48 K.

Table 1. Physical Properties of $(Me_5C_5)_2VX$ Complexes.

X	Color	Yield, %	mp, °C	EIMS[a]	^{1}H NMR[b]
F	blue	65	257	340	18.1 (154)
Cl	blue	91	233	356[c]	7.31 (185)
Br	blue-green	87	249	402	6.07 (229)
I	green	77	266	448	5.23 (211)

a) atomic mass units, highest peak in the isotopic cluster.
b) ppm, measured in C_6D_6 at 30 °C, widths at half-maximum reported in Hz in parentheses. c) measured in Reference 7b.

The halide compounds can also be used as precursors to other complexes. The chloride complex is generally used because it is well behaved and easy to prepare in large quantities. Robbins has used this to synthesize the methyl complex from methyllithium.[7b] Although hydrogenation of the methyl complex produces the vanadium hydride[7b] (Eqn. 4), this reaction is quite slow. In addition,

$$(Me_5C_5)_2VMe + H_2 \longrightarrow (Me_5C_5)_2VH + MeH \qquad (4)$$

neither the methyl nor the hydride complex will react with ammonia to produce the amide complex. This indicates that these complexes are not suitable for generating further products through acid-base chemistry.

Figure 1. Plot of $1/\chi_M$ vs. T for $(Me_5C_5)_2VF$

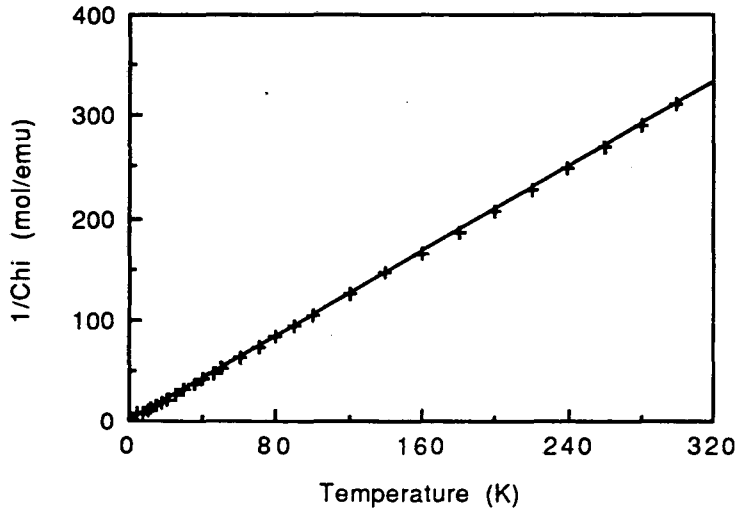

The lack of reactivity for these species may be attributed to the presence of an electron in a valence orbital that prevents incoming substrates from coordinating to the metal. Using the molecular orbital diagram for $(C_5H_5)_2VH$ (Figure 2)[12] as a model for $(Me_5C_5)_2VH$, it is observed that an electron occupies the b_2 nonbonding orbital. Since this orbital lies in the plane through which an incoming molecule must pass in order interact with the metal center, the electron may hinder the formation of the intermediate in the acid-base reaction.

Figure 2. Molecular Orbital Diagram for $(C_5H_5)_2VH$.

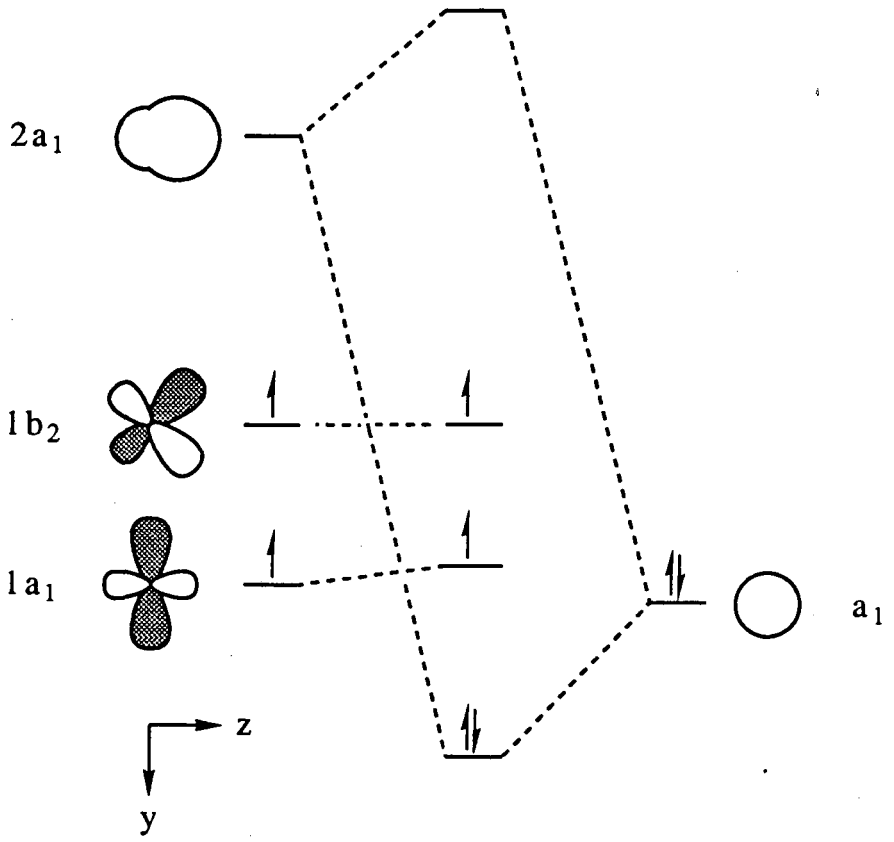

Fortunately, it is possible to generate other vanadium complexes through standard metathetical routes. The phenyl complex can be synthesized from phenyllithium (Eqn. 5). Diphenylmagnesium, however, is ineffective. In addition, attempts to synthesize this complex through electron transfer reactions with $(Me_5C_5)_2V$ have been unsuccessful. No reaction is observed with phenylcopper, phenylsilver, diphenylzinc, or diphenylmercury. Therefore, the phenyl reagents must not be capable of interacting with the vana-

dium center effectively enough to allow an electron transfer to take place.

$$(Me_5C_5)_2VCl + PhLi \longrightarrow (Me_5C_5)_2VPh + LiCl \quad (5)$$

The previously unreported borohydride complex can be synthesized from $(Me_5C_5)_2VCl$ and lithium borohydride as shown in Eqn. 6. The IR spectrum (Figure 3) is similar to that observed by Marks

Figure 3. IR Spectra for $(Me_5C_5)_2VBH_4$ (top) and $(Me_5C_5)_2VBD_4$ (bottom).

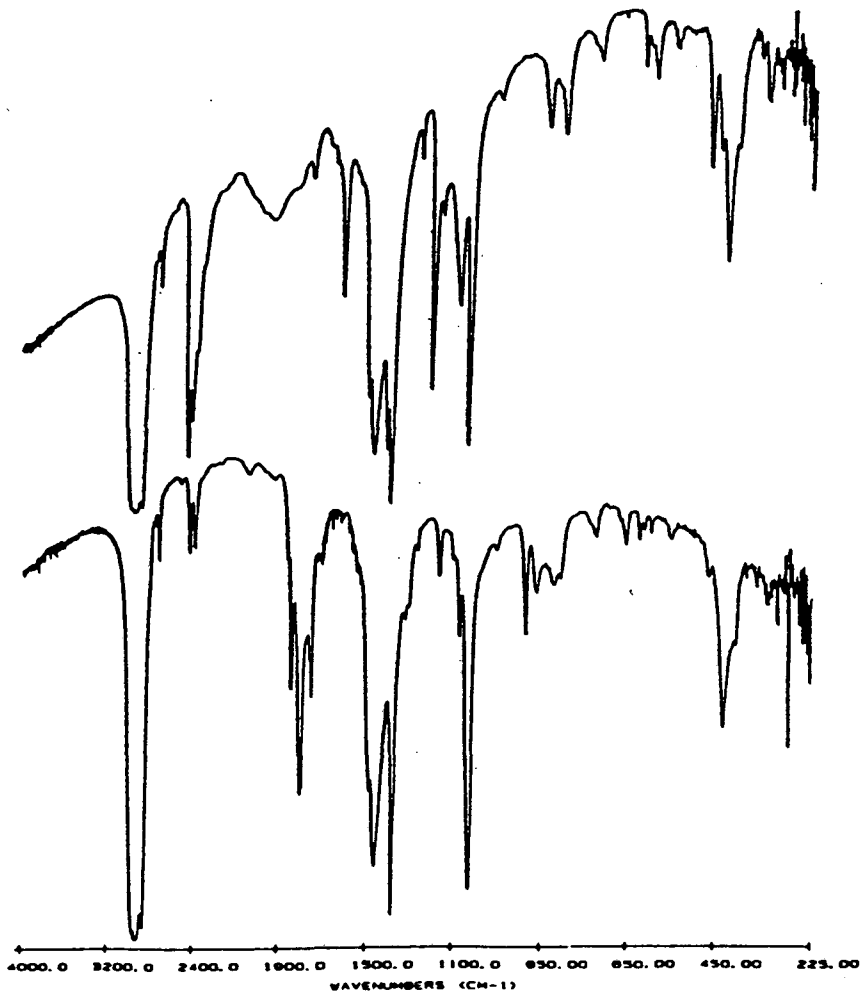

$$(Me_5C_5)_2VCl + LiBH_4 \longrightarrow (Me_5C_5)_2VBH_4 + LiCl \quad (6)$$

for $(C_5H_5)_2VBH_4$.[13a] The terminal B-H stretches are at 2444 and 2407 cm^{-1} which are typical values for metal borohydride complexes.[13b] However, like the spectrum of $(C_5H_5)_2VBH_4$, the bridging B-H stretches at 1759 and 1611 cm^{-1} are much reduced from the typical region of 2100-1960 cm^{-1}. By comparison to the analysis of Marks,[13b] the Me_5C_5 analogue can be considered to behave more like a "covalent" boron hydride than an "ion-pair" complex. More importantly, these data are consistent with a bidentate bridging structure for this complex (Figure 4).

Figure 4

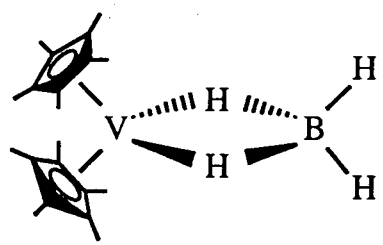

In order to examine the shifts in the stretches upon deuteration, the borodeuteride complex has also been synthesized. The terminal B-D stretches fall between 1740 cm^{-1} (υ_H/υ_D = 1.40) and 1840 cm^{-1} (υ_H/υ_D = 1.31) as expected (Figure 3). However, the shifts in the bridging B-D stretches are somewhat more difficult to assign. There are two weak absorptions at 1318 and 1304 cm^{-1} either of which may correspond to the 1759 cm^{-1} stretch in the borohydride complex. Also, the absorption at 1160 cm^{-1} may be related to the

1611 cm^{-1} stretch in $(Me_5C_5)_2VBH_4$. In general, the spectrum is consistent with what Marks et al. have observed upon deuteration of $(C_5H_5)_2VBH_4$. The IR data are listed in Table 2.

Table 2. IR Data for Vanadium Borohydride Complexes (cm^{-1}).

	$\upsilon_{B\text{-}Ht}$ A_1 and B_1	$\upsilon_{B\text{-}Hb}$ A_1 and B_2	B.E.[a] A_1	$\delta(BH_2)$ B_2
$(Me_5C_5)_2VBH_4$	2444, 2407	1759, 1611	1397	1193
$(C_5H_5)_2VBH_4$[b]	2442, 2418	1745, 1650	1395	1180
$(Me_5C_5)_2VBD_4$	1841, 1801 1745	1318, 1304 1160 (?)	1021 (?)	882
$(C_5H_5)_2VBD_4$[b]	1820, 1760 1720	1290, 1230 1180 (?)	1030	860

a) symmetric bridge expansion. b) measured in Reference 13.

The boron hydride character of $(Me_5C_5)_2VBH_4$ can be further illustrated by its reaction with ammonia (Eqn. 7). When anhydrous

$$(Me_5C_5)_2VBH_4 + NH_3 \longrightarrow (Me_5C_5)_2VH + H_3NBH_3 \quad (7)$$

ammonia is added to the borohydride complex and the product is recrystallized from diethyl ether, the previously reported hydride complex,[7b] $(Me_5C_5)_2VH$, is isolated. This suggests that there is a significant metal hydride interaction and that the BH_3 fragment is somewhat labile in $(Me_5C_5)_2VBH_4$. This interpretation is further supported by the lack of a molecular ion in the mass spectrum. Although the highest isotopic cluster occurs at 321 amu, the excessive

number of peaks may be due to overlap of the cluster representing the hydride complex with the isotopic cluster of $(Me_5C_5)_2V$.

Decamethylvanadocene can also undergo a two-electron oxidation via reaction with nitrous oxide. This versatile oxygen transfer reagent has been shown to cleanly transfer oxygen to metal complexes with the release of dinitrogen.[14] Bottomley has examined the reactions of a number of vanadium complexes with nitrous oxide and other oxygen-transfer reagents.[15] Recently, he has reported that the reaction of $(Me_5C_5)_2V$ with nitrous oxide gives a vanadium oxide cluster complex as the sole product (Eqn. 8).[16] Ring loss appears to

$$4\ (Me_5C_5)_2V\ +\ 6\ N_2O \xrightarrow{72\ h} (Me_5C_5)_4V_4O_6 + 2\ (Me_5C_5)_2\ +\ 6\ N_2 \qquad (8)$$

be a common feature in the majority of these studies. Similar behavior has been observed for complexes of titanium and chromium.[17] However, the surprising lability of the rings in $(Me_5C_5)_2V$ suggests that a more careful examination of the reaction with nitrous oxide might be informative. Because metal oxides are believed to exist as intermediates in the heterogeneous catalytic formation of functionalized organic products,[18] the isolation of a vanadium-oxo complex may provide a useful model for studying the catalytic processes.

In Bottomley's studies, the vanadium complexes are exposed to an atmosphere of nitrous oxide for extended periods.[15,16] Since reactions with nitrous oxide are generally quite fast,[14] this treatment

seemed unnecessary. If simple oxygen-transfer is the first step in the formation of the cluster complex, then using a high pressure of nitrous oxide over a shorter reaction time may allow isolation of a vanadium-oxo complex such as $(Me_5C_5)_2VO$. Thus, when $(Me_5C_5)_2V$ is exposed to a pressure of 4-5 atmospheres of nitrous oxide in a Fischer-Porter high pressure bottle, a dark, green-brown hexane solution is produced. If the volatile materials are removed after 4 hours and the residue is crystallized from pentane, a brown-green product can be isolated.

The major reaction product is not the cluster complex observed by Bottomley. The IR spectrum does not match the absorptions reported for the cluster.[16] In addition, there is a strong absorption at 852 cm^{-1} which may correspond to a V-O stretch.[1] The inability to observe any resonances in the ^1H NMR spectrum suggests that the product is a tetravalent, d^1 vanadium complex. This is supported by a variable temperature magnetic susceptibility study (Figure 5) which is consistent with one unpaired electron in the molecule. The magnetism follows Curie-Weiss behavior from 5-300 K with a magnetic moment of 1.95 μ_B and Θ = -0.49 K. The EPR spectrum of a 10^{-1} M methylcyclohexane solution at room temperature displays an eight line pattern with a g value of 1.9844 and a coupling constant of 25 G. Furthermore, the elemental analysis is consistent with the formulation of $(Me_5C_5)_2VO$ and the highest ion in the mass spectrum occurs at 337 amu which corresponds to $(Me_5C_5)_2VO$. All of this data conflicts with the characterization reported for the cluster complex. Therefore, it can be concluded that the transformation shown in Eqn. 9 occurs for short reaction times.

Figure 5. Plot of $1/\chi_M$ vs. T for $(Me_5C_5)_2VO$.

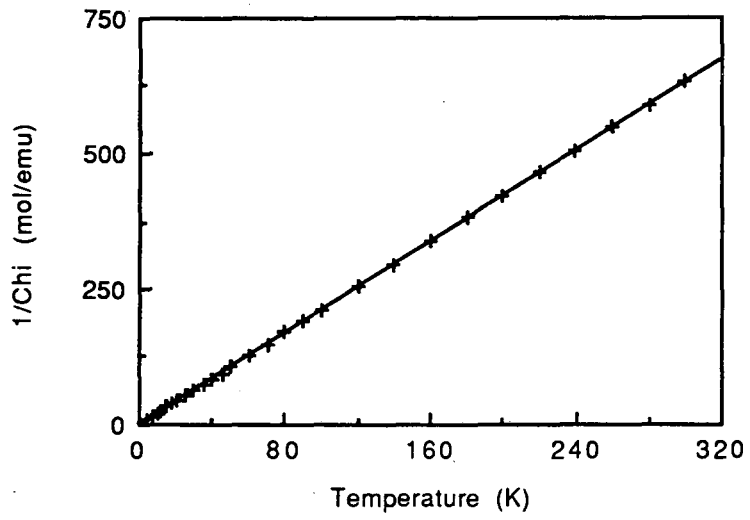

$$(Me_5C_5)_2V + N_2O \xrightarrow{4\ h} (Me_5C_5)_2VO + N_2 \qquad (9)$$

A second product is also observed in the reaction. This insoluble material is left behind when the reaction residue is extracted with pentane. IR and mass spectral data identify this product as the cluster complex, $(Me_5C_5)_4V_4O_6$. This observation provides additional support for the postulate that the vanadium-oxo complex is formed initially and that $(Me_5C_5)_2VO$ rearranges to $(Me_5C_5)_4V_4O_6$ over time. Thus, the extended reaction times used by Bottomley preclude the isolation of the simple oxo complex, as even short durations result in significant quantities of the cluster. It should also be noted that very short reaction times are not suitable either. If the reaction is terminated too soon in order to minimize the amount of the cluster complex, the product will be contaminated with unreacted

$(Me_5C_5)_2V$. Therefore, there is a period during which all three species coexist. In order to obtain a maximum yield of the desired product, the reaction time must be carefully monitored.

A solid state structural determination would be very informative. Unfortunately, X-ray quality crystals cannot be obtained. In addition, the oxo-complex is not stable in solution over long periods of time which prevents the solution molecular weight from being measured by the Signer method.[19] Because the complex has thus far shown no reactivity towards unsaturated species such as ethylene or tert-butylacetylene, further studies need to be undertaken in order to gain useful information on the behavior of this complex.

Ytterbium Halide Complexes

The synthesis of the halide complexes, $(Me_5C_5)_2YbX$, free from coordinated bases has been of interest for some time.[20] These simple species ought to display unusual solution and solid state behavior similar to $(Me_5C_5)_2YbMe$. In addition, these complexes might also simplify the synthesis of other base-free compounds through reactions in non-coordinating solvents. However, all previously reported halide complexes of ytterbium contain excess coordinated ligands. Like $(Me_5C_5)_2YbMe$, the halide complexes often retain alkali metals which can only be removed in the presence of coordinating bases (Eqn. 10).[20] These bases are then impossible to remove from the products.

Because the vanadium halide complexes are soluble in hydrocarbon solvents, their reactions can be performed in the absence of coordinating solvents. Therefore, if the vanadium complexes transfer

$$YbCl_3 + 2\,Na(Me_5C_5) \xrightarrow{THF} (Me_5C_5)_2Yb(\mu\text{-}Cl)_2Na(THF)_2 \quad (10)$$

$$\downarrow \text{ THF/toluene}$$

$$(Me_5C_5)_2YbCl(THF)$$

their halide ligands cleanly to ytterbium, the base-free ytterbium halide products should be obtained. With the oxidation potential of $(Me_5C_5)_2Yb$ measured as +1.4 V vs. SHE and the reduction potentials of the $(Me_5C_5)_2VX$ complexes being estimated as approximately -1.1 V vs. SHE, the electron-transfer process between vanadium and ytterbium should be thermodynamically favorable.[11] If this can compensate for any changes in the metal-ligand bond strengths, then the ligand transfer should occur.

Thus, when the vanadium halide complexes are mixed with $(Me_5C_5)_2Yb$ in hexane or pentane (Eqn. 11), a precipitate immediately forms. Filtering and washing the microcrystalline solid allows isolation of the ytterbium halide species. The $(Me_5C_5)_2V$ that is formed in the reaction can be recovered from the mother liquor and purified by sublimation. This can be converted to $(Me_5C_5)_2VX$ and recycled.

$$(Me_5C_5)_2Yb + (Me_5C_5)_2VX \longrightarrow (Me_5C_5)_2YbX + (Me_5C_5)_2V \quad (11)$$

All of the ytterbium halide complexes behave similarly. Their properties are listed in Table 3. They are slightly soluble in toluene with the solubility decreasing with increasing halide size. This trend

Table 3. Physical Properties of $(Me_5C_5)_2YbX$ Complexes.

X	Color	Yield, %	mp, °C[a]	EIMS[b]	^{1}H NMR[c]
F	purple	77	285	463	d
Cl	blue-purple	91	280	479	19.8 (295)
Br	blue	78	275	523	14.4 (316)
I	blue	78	258	571	e

a) decomposition temperature.
b) atomic mass units, highest peak in the isotopic cluster.
c) ppm, measured in C_7D_8, width at half maximum measured in Hz and reported in parentheses.
d) no resonance observed
e) solubility too low in non-coordinating solvents for solution studies.

suggests that the larger halide ligands promote greater intermolecular interactions which lower the solubility of the complexes. Although the halide complexes can be recrystallized from halogenated solvents such as dichloromethane and chlorobenzene, their elemental analyses remain poor. Fortunately, the identity of the halide complexes can be clearly established through the synthesis of their tetrahydrofuran adducts (Eqn. 12). Tetrahydrofuran complexes are known for the fluoride,[6] chloride,[20b] and iodide[20a] ligands. In each

$$(Me_5C_5)_2YbX \xrightarrow{THF} (Me_5C_5)_2YbX(THF) \qquad (12)$$

case, the base-free complex cleanly dissolves in tetrahydrofuran. Recrystallization from toluene then affords the crystalline tetrahydrofuran products. The identity of the fluoride complex can be

further established through the formation of the previously observed mixed-valent species, $[(Me_5C_5)_2Yb]_2(\mu\text{-}F)$,[21] upon addition of a second equivalent of $(Me_5C_5)_2Yb$ (Eqn. 13). In the initial synthesis of $(Me_5C_5)_2YbF$, there is no evidence for the formation of the mixed-valent fluoride or the tetranuclear fluoride complex, $(Me_5C_5)_6Yb_4(\mu\text{-}F)_4$,[22] as in the reactions of $(Me_5C_5)_2Yb$ with silver fluoride. The base-free halides to decompose without melting when heated. However, they are volatile enough to show monomeric ions in the mass spectra. Attempts to measure their solution molecular weights in dichloromethane by the Signer method[19] produce values that are intermediate between monomer and dimer suggesting that equilibria are occurring in solution.

$$(Me_5C_5)_2YbF + (Me_5C_5)_2Yb \longrightarrow [(Me_5C_5)_2Yb]_2(\mu\text{-}F) \qquad (13)$$

Broad resonances corresponding to the Me_5C_5 protons are observed in the ^1H NMR spectra of the chloride and bromide complexes in toluene-d_8. A variable temperature ^1H NMR experiment on the chloride complex (Figure 6) reveals a deviation from Curie-Weiss behavior suggesting that some type of equilibrium exists in solution,[23] consistent with the results of the solution molecular weight studies.

As in the study of $(Me_5C_5)_2YbMe$, the low solubility of the complex limits the temperature range over which useful data can be obtained. Although a monomer-dimer equilibrium (Figure 7) seems likely, suitable crystals for an X-ray structural determination, which might have proven the existence of a dimeric species, could not be

Figure 6. Plot of δ vs. 1/T for $(Me_5C_5)_2YbCl$.

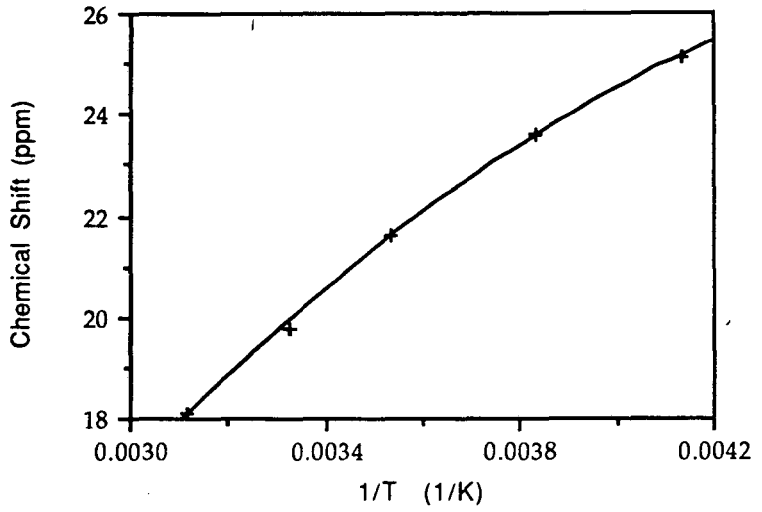

Figure 7

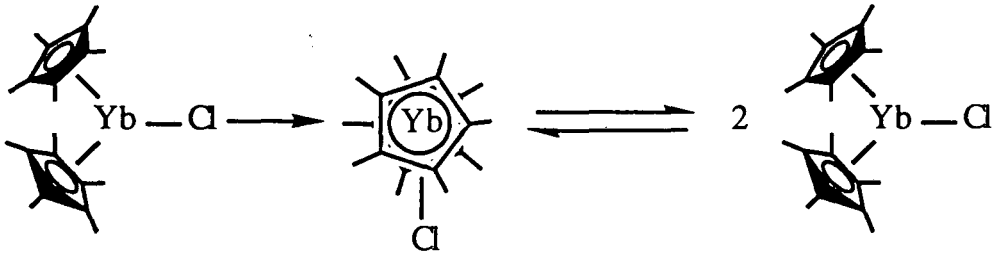

produced. No ^1H NMR line is observed for the fluoride complex, consistent with the behavior of other ytterbium fluoride complexes.[21,22] The solubility of the iodide complex is too low in toluene and solution studies could not be undertaken.

Group Transfer Reactions

The clean transfer of halide ligands from vanadium to ytterbium prompts the question of whether more complex ligands can be

exchanged. When $(Me_5C_5)_2Yb$ is mixed in hexane with $(Me_5C_5)_2VMe$, a red solution is obtained (Eqn. 14). Although $(Me_5C_5)_2YbMe$ can be isolated, its solubility is only slightly less than that of $(Me_5C_5)_2V$.

$$(Me_5C_5)_2Yb + (Me_5C_5)_2VMe \longrightarrow (Me_5C_5)_2YbMe + (Me_5C_5)_2V \quad (14)$$

Therefore, separation is difficult and, consequently, yields are significantly reduced. Although the vanadium methyl complex provides a stable, isolable methyl transfer reagent, the use of methylcopper remains the preferable route to $(Me_5C_5)_2YbMe$.

Unfortunately, not all $(Me_5C_5)_2VX$ complexes undergo ligand exchange with $(Me_5C_5)_2Yb$. The phenyl complex of vanadium, $(Me_5C_5)_2VPh$, does not react with $(Me_5C_5)_2Yb$. This may be due to the inability of the α-carbon of the phenyl ring to approach the ytterbium site due to steric restrictions. The vanadium hydride complex also will not transfer its ligand to ytterbium. In this case, the small ionic radius of trivalent vanadium[24] coupled with a short V-H bond may prevent the hydride ligand from approaching ytterbium closely enough to allow an effective interaction.

It appears that only ligands which can form effective bridging interactions between the two metals can be transferred. The vanadium borohydride complex, $(Me_5C_5)_2VBH_4$, will transfer its borohydride ligand to ytterbium as shown in Eqn. 15:

$$(Me_5C_5)_2Yb + (Me_5C_5)_2VBH_4 \longrightarrow (Me_5C_5)_2YbBH_4 + (Me_5C_5)_2V \quad (15)$$

The borohydride ligand on vanadium should be able to interact with the ytterbium atom through its terminal hydrogen atoms, thus, facilitating the ligand transfer. Unlike the vanadium complex, the ytterbium borohydride shows a molecular ion in the mass spectrum. However, like the other trivalent ytterbium species, the borohydride complex shows a broad, single resonance in the ^1H NMR spectrum. The non-linear behavior observed in the variable temperature ^1H NMR study (Figure 8) suggests that an equilibrium process exists in solution.[23]

Figure 8. Plot of δ vs. 1/T for $(Me_5C_5)_2YbBH_4$

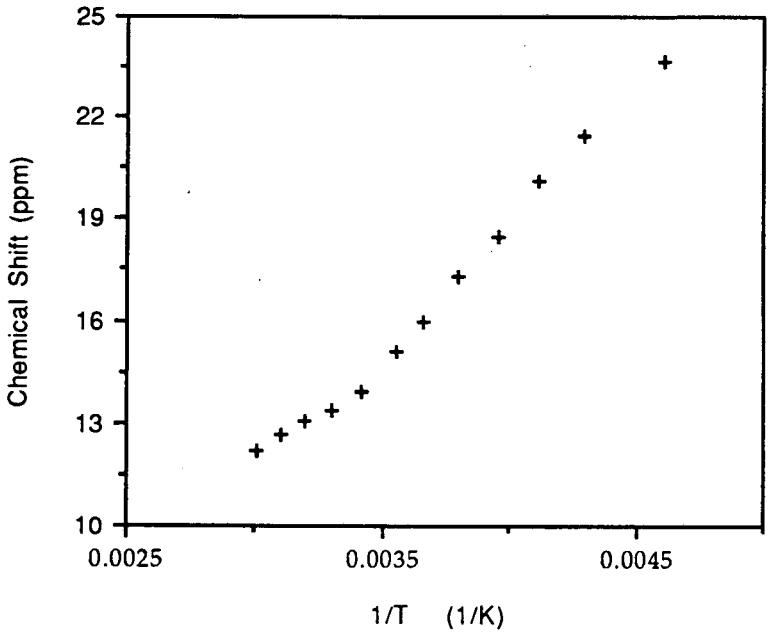

The IR spectrum (Figure 9) reveals two strong, broad absorptions at 2337 and 2198 cm^{-1} that appear in regions typical of terminal and bridging B-H stretches, respectively. The corresponding

borodeuteride complex (Figure 9) shows the expected isotopic shifts for the B-D stretches down to 1727 cm^{-1} (υ_H/υ_D = 1.35) and 1563 cm^{-1} (υ_H/υ_D = 1.41).

Figure 9. IR Spectra for $(Me_5C_5)_2YbBH_4$ (top) and $(Me_5C_5)_2YbBD_4$ (bottom).

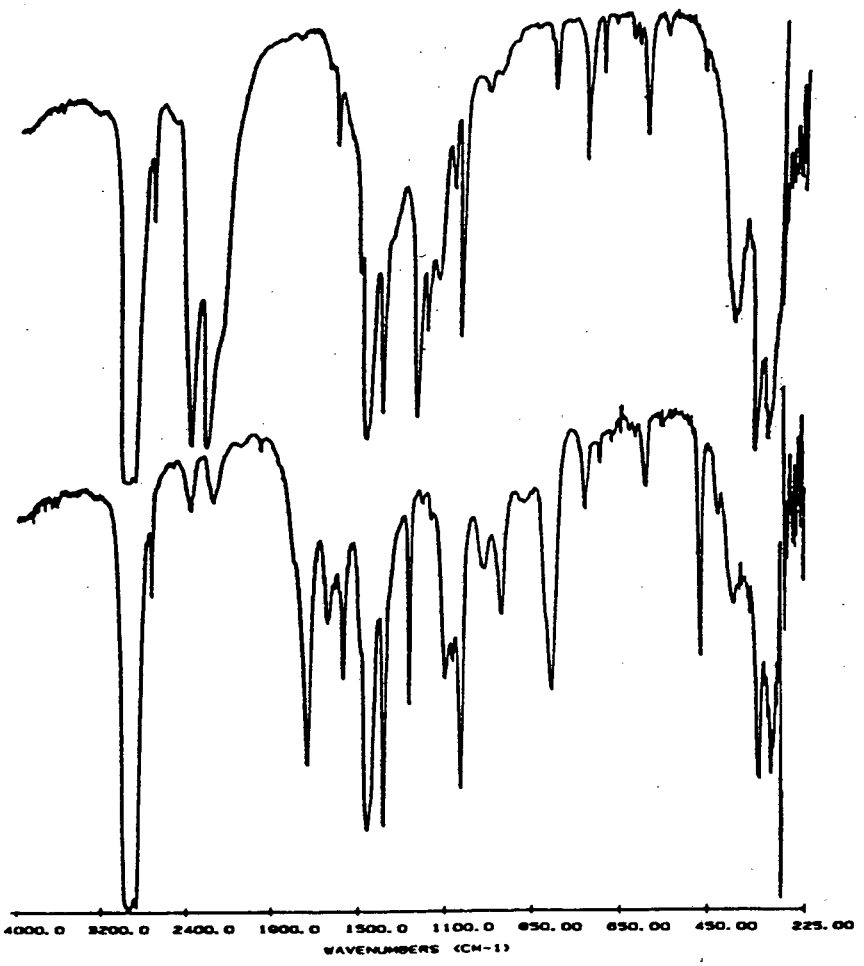

The existence of an asymmetric dimer structure in the solid state (Figure 10), analogous to $(Me_5C_5)_2YbMe$, might account for the broad absorptions in the IR spectrum as well as the solution behavior. The bridging B-H_a stretches should have slightly different energies as compared to the bridging B-H_b stretches due to the inequivalent coordination environments of the two ytterbium atoms.

Figure 10

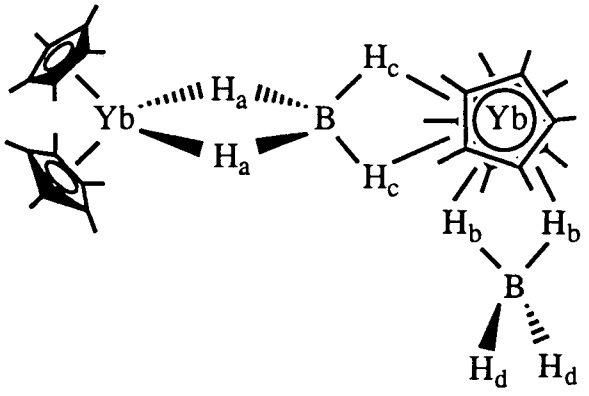

Also, the Yb-H_c interactions should be relatively weak due to the increased crowding at that metal. Therefore, the B-H_c stretches should remain similar in energy to the terminal B-H_d stretches. If the B-H_a and B-H_b stretches are all of similar energy, then the overlapping absorptions may result in the observation of only a single, broad, unresolved absorption in the IR spectrum. This would also be the case for the B-H_c and B-H_d stretches.

Unfortunately, very few complexes have been crystallographically characterized in which a borohydride ligand bridges two metal centers.[25] Therefore, without crystallographic evidence for an asym-

metric dimer, an extended structure, such as that shown in Figure 11, cannot be dismissed. The family of B-H vibrations in a polymer could also account for the broad absorptions in the IR spectrum.

Figure 11

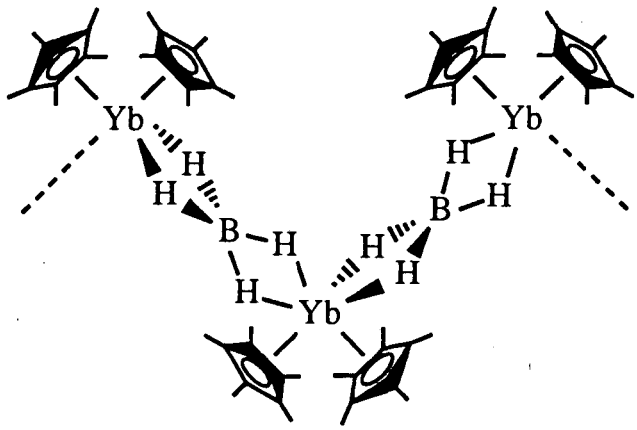

Trogler has reported the synthesis of the azide complex, $(Me_5C_5)_2VN_3$, from $(Me_5C_5)_2V$ and tritylazide.[26] This complex will cleanly transfer its azide ligand to $(Me_5C_5)_2Yb$ as shown in Eqn. 16:

$$(Me_5C_5)_2Yb + (Me_5C_5)_2VN_3 \longrightarrow [(Me_5C_5)_2YbN_3]_x + (Me_5C_5)_2V \quad (16)$$

However, the purple product is virtually insoluble in all common organic solvents. Although the compound will dissolve in pyridine, it does not crystallize from this solvent. In addition, the product does not melt below 330 °C and does not give a molecular ion in the mass spectrum. The presence of a strong azide stretch in the IR spectrum at 2155 cm^{-1}, however, coupled with the observation that the direct reaction of $(Me_5C_5)_2Yb$ with trimethylsilylazide produces the same

product, indicates that an azide species has been produced. The complex probably adopts a polymeric form in the solid state (Figure 12).

Figure 12

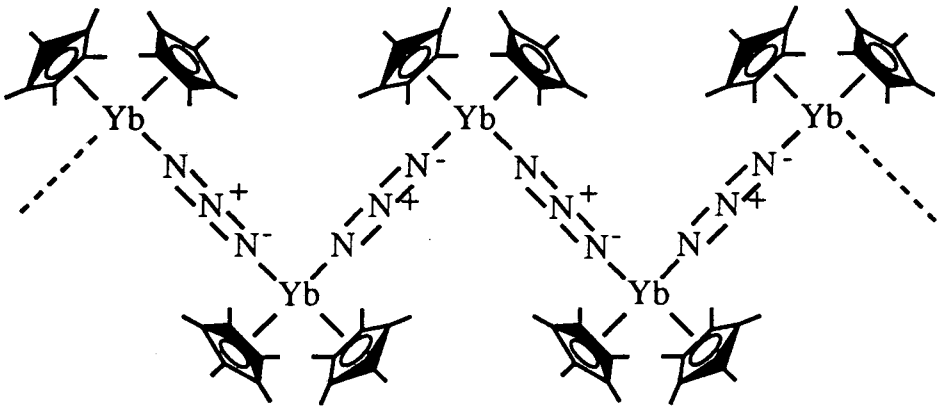

If the complex does in fact form a polymer, the presence of $(Me_5C_5)_2Yb$ in the mass spectrum suggests that the monomeric unit is a simple azide, $(Me_5C_5)_2YbN_3$. This might then polymerize by creating azide bridges between adjacent ytterbium atoms. An azide group which is directly bound to one ytterbium atom coordinates through its terminal lone pair to an open coordination site on an adjacent metal producing a long continuous chain. Similar extended chain interactions have been proposed to account for the physical properties of a 4,4'-bipyridine complex of $(Me_5C_5)_2Yb$.[27] The 4,4'-bipyridine molecule contains nitrogen atoms at its opposite ends which can bridge two metal atoms similarly to the azide ligand. Unfortunately, the low solubility of the azide product prevents a more thorough study of its structure and solution behavior.

Mixed-valent Complexes

The isolation of the mixed-valent methyl complex, $[(Me_5C_5)_2Yb]_2(\mu\text{-Me})$, described in Chapter 1, suggests that other similar complexes should be stable. Burns et al. have reported the isolation of the mixed-valent fluoride complex, $[(Me_5C_5)_2Yb]_2(\mu\text{-F})$.[21] The structural and magnetic behavior is consistent with a trapped-valent complex like that observed for the methyl analogue. Because the trivalent vanadium derivatives transfer their ligands cleanly to ytterbium, these should be effective reagents for synthesizing an entire family of mixed-valent species.

Thus, when a hexane solution of $(Me_5C_5)_2VX$ is added to a solution of $(Me_5C_5)_2Yb$, a precipitate immediately forms (Eqn. 17). Although these products can be also be obtained by adding a second equivalent of $(Me_5C_5)_2Yb$ to the already prepared $(Me_5C_5)_2YbX$ complexes, the low solubilities of the $(Me_5C_5)_2YbX$ species make this route more difficult and time consuming. In addition, if the $(Me_5C_5)_2Yb$ solution is instead added to the concentrated $(Me_5C_5)_2VX$ solution, the reaction is slowed by the initial formation and precipitation of the $(Me_5C_5)_2YbX$ complexes. Therefore, the manner in which the reaction is conducted has a pronounced effect on the ease with which the products are obtained.

$$2\,(Me_5C_5)_2Yb + (Me_5C_5)_2VX \longrightarrow [(Me_5C_5)_2Yb]_2(\mu\text{-X}) + (Me_5C_5)_2V \quad (17)$$

The mixed-valent complexes are generally intensely colored and only slightly soluble in aliphatic hydrocarbons, although they can

be recrystallized from toluene. The properties of the known mixed-valent complexes are summarized in Table 4. Although the fluoride, chloride, and bromide species are readily synthesized, the iodide is apparently too unstable towards formation of the insoluble trivalent complex, $(Me_5C_5)_2YbI$. This product immediately precipitates from the reaction mixture regardless of the stoichiometry or reaction conditions. The lattice energy of $(Me_5C_5)_2YbI$ may be too high to allow the weak bridging interaction in $[(Me_5C_5)_2Yb]_2(\mu\text{-}I)$ to exist since these complexes are likely to be undergoing dissociative processes in solution analogous to $[(Me_5C_5)_2Yb]_2(\mu\text{-}Me)$. This same behavior is also observed for the azide ligand for which the stability of the trivalent complex; $(Me_5C_5)_2YbN_3$, prevents the isolation of the mixed-valent complex.

Table 4. Physical Properties of $[(Me_5C_5)_2Yb]_2(\mu\text{-}X)$ Complexes.

X	Color	Yield, %	mp, °C[a]	^{1}H NMR[b]
F[c]	green-brown	d	290	e
Cl	brown	90	282	11.0 (153)
Br	brown	70	252	13.7 (150)
H[f]	purple	56	196	7.80 (98)[g]
Me	red-brown	71	223	5.46 (150)
BH_4	green-brown	71	294	8.97 (73)

a) decomposition temperature b) ppm, measured in C_7D_8, width at half maximum measured in Hz and reported in parentheses. c) measured in Reference 21. d) not measured e) not observed f) measured in Reference 6. g) measured in C_6D_6.

In contrast to the synthesis of the trivalent methyl complex, $(Me_5C_5)_2YbMe$, the use of $(Me_5C_5)_2VMe$ to obtain the mixed-valent ytterbium methyl complex is quite clean due to the lower solubility of the mixed-valent species. This allows the product to be easily separated from the $(Me_5C_5)_2V$ formed in the reaction. Thus, $(Me_5C_5)_2VMe$ is a more attractive methylating agent than methyl-copper in this case since it can be isolated, stored, and measured out quantitatively.

The physical properties of the mixed-valent borohydride complex are similar to the other analogous species. A molecular structure can be postulated that is similar to the observed structure for $[(Me_5C_5)_2Yb]_2(\mu\text{-}Me)$ (Figure 13). This structure can be rationalized by comparison of the B-H stretches in its IR spectrum (Figure 14) to those observed for $(Me_5C_5)_2TiBH_4$.[28]

Figure 13

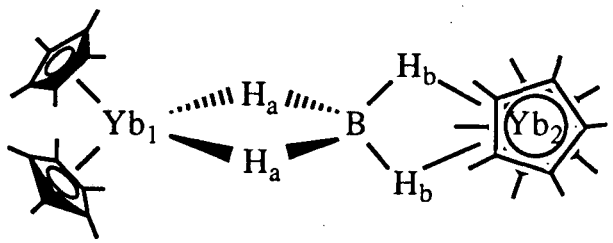

If Yb_1 is considered to be the trivalent metal and Yb_2 the divalent metal, then the Yb_1-H_a-B bridge will be stronger than the Yb_2-H_b-B bridge. This is reflected in the B-H stretching energies. The B-H_b stretches for the ytterbium complex are at 2389 and 2323 cm^{-1} which are close to the terminal B-H stretches of $(Me_5C_5)_2TiBH_4$

Figure 14. IR Spectra for $[(Me_5C_5)_2Yb]_2(\mu\text{-}BH_4)$ (top) and $[(Me_5C_5)_2Yb]_2(\mu\text{-}BD_4)$ (bottom).

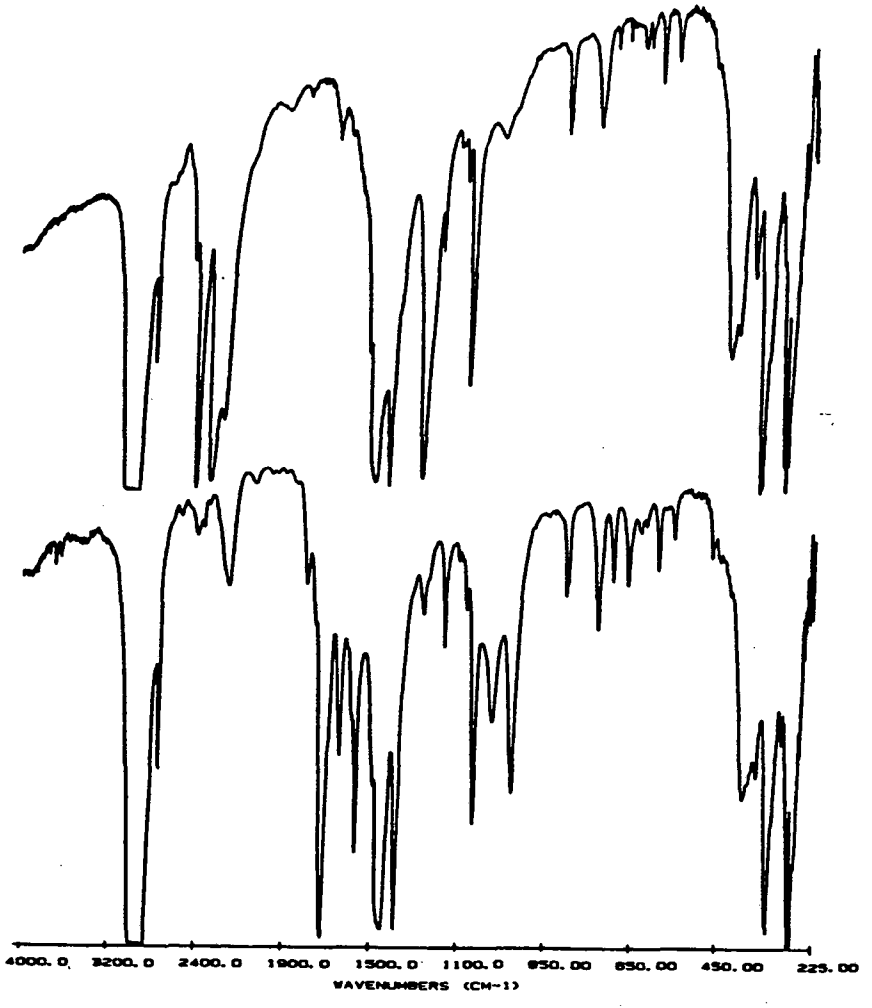

at 2445 and 2410 cm^{-1}. However, the interaction of the borohydride ligand with Yb_2 results in a lowering of the energies of the B-H_b stretches relative to typical terminal B-H stretches. The B-H_a stretches at 2194 and 2142 cm^{-1} are lower in energy than the

bridging B-H_b stretches indicating that the borohydride ligand has a stronger interaction with Yb_1 than with Yb_2. However, the B-H_a stretches are actually higher in energy than typical bridging B-H stretches found in $(Me_5C_5)_2TiBH_4$ at 2070 and 1950 cm^{-1}. This is because the presence of Yb_2 weakens the interaction of the borohydride ligand with Yb_1. As a result, the B-H_a bond is strengthened relative to the corresponding B-H bonds in $(Me_5C_5)_2TiBH_4$. Therefore, shifts in the B-H stretching energies can be used to rationalize bonding interactions in the ytterbium borohydride species. These shifts are further verified by the synthesis of the analogous borodeuteride complex. The B-H_a stretches shift to 1559 cm^{-1} (υ_H/υ_D = 1.41) and 1483 cm^{-1} (υ_H/υ_D = 1.44) while the B-H_b stretches move to 1714 cm^{-1} (υ_H/υ_D = 1.39) and 1633 cm^{-1} (υ_H/υ_D = 1.42) upon deuteration (Figure 14). The behavior of these complexes is consistent with the expected isotopic shifts in relation to the proposed structures.

Figure 15

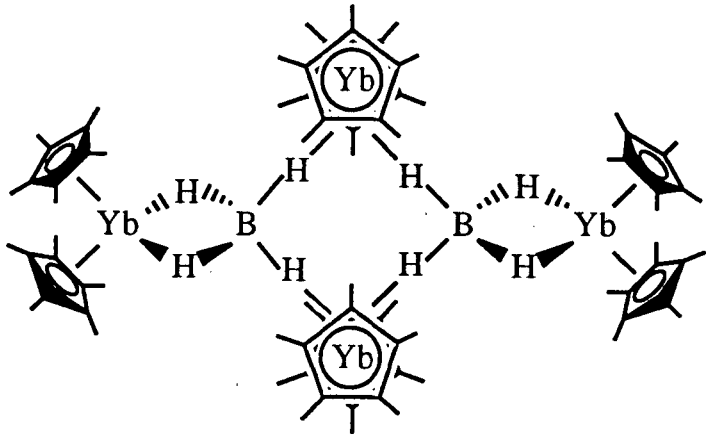

Unfortunately, suitable crystals for an X-ray crystallographic study could not be obtained. Because borohydride ligands are capable of binding in a monodentate, bidentate, or tridentate fashion to a metal center,[13,25] a more complex, extended structure for the 2:1 ytterbium borohydride species, such as that shown in Figure 15, must be considered as a possibility.

The variable temperature ^1H NMR behavior of the ytterbium mixed-valent species is shown in Figures 16-18. The plots of δ vs. 1/T indicate that a single, discreet species does not exist in solution. The molecules are presumably undergoing dissociative processes similar to that proposed for the methyl analogue, as discussed in Chapter 1. All of these complexes should be structurally related and this should be reflected in their solution behavior.

Figure 16. Plot of δ vs. 1/T for $[(Me_5C_5)_2Yb]_2(\mu\text{-}Cl)$.

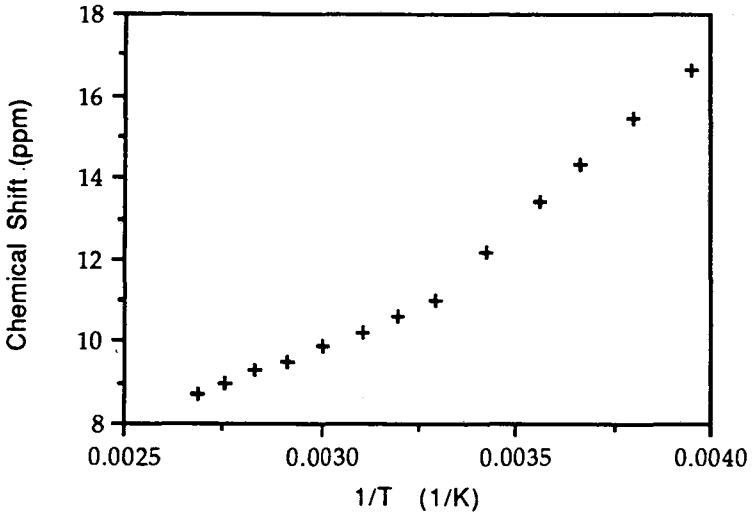

Figure 17. Plot of δ vs. 1/T for $[(Me_5C_5)_2Yb]_2(\mu\text{-}Br)$.

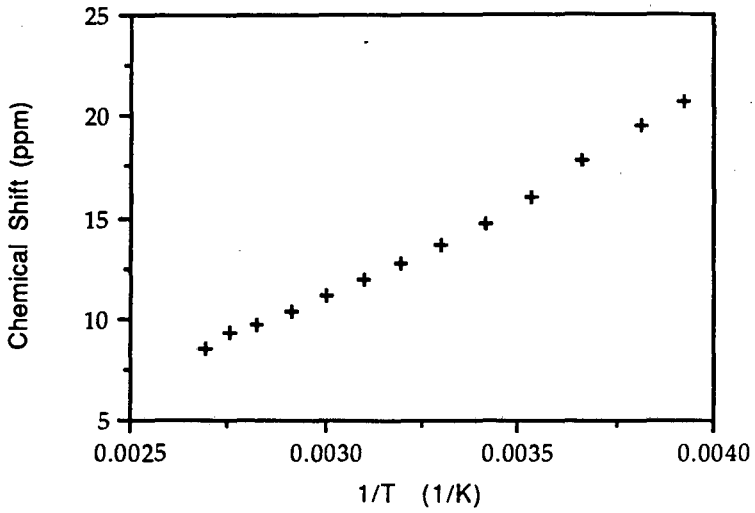

Figure 18. Plot of δ vs. 1/T for $[(Me_5C_5)_2Yb]_2(\mu\text{-}BH_4)$.

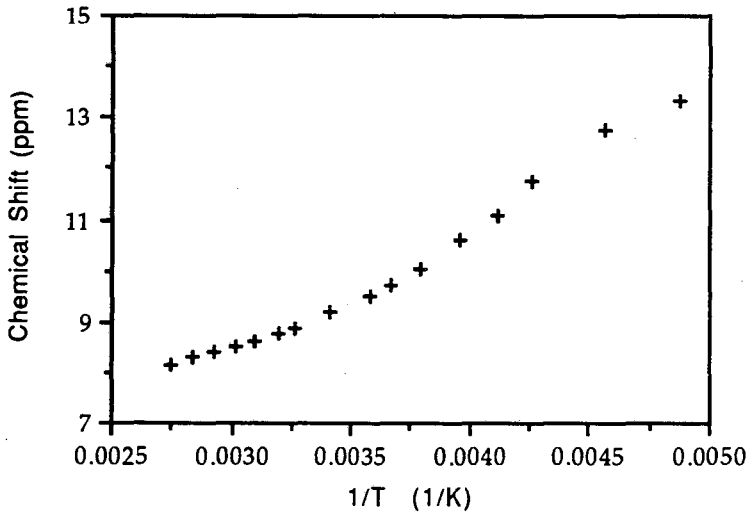

The fluxional process also explains the observation of only a single resonance in the ^1H NMR spectrum. If the bimetallic species remain intact in solution, then there should be separate resonances for the Me_5C_5 protons associated with the two discreet metal atoms

in the absence of any exchange processes. Since this is not observed in the ^1H NMR spectrum, the single resonance is most likely due to an averaged chemical shift resulting from solution equilibria which are fast on the NMR time scale.

The variable temperature magnetic susceptibilities of the mixed-valent complexes support the postulate that there is no electronic communication between the two metal atoms down to 5 K, thus, making these additional examples of trapped-valent species. The magnetic behavior of the ytterbium mixed-valent complexes is consistent with isolated trivalent ytterbium paramagnets with a large diamagnetic diluent (Figures 19-21).[29] This is also consistent

Figure 19. Plot of $1/\chi_M$ vs. T for $[(Me_5C_5)_2Yb]_2(\mu\text{-}Cl)$.

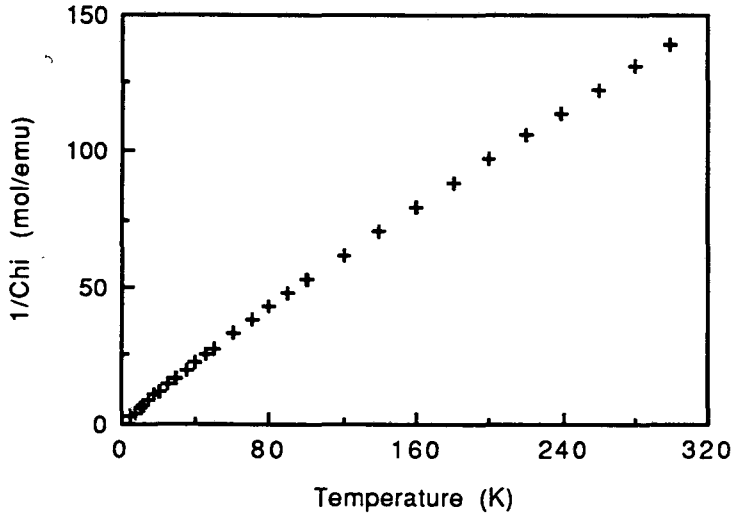

with what has been observed for the structurally characterized methyl analogue obtained from methylcopper. The plots of $1/\chi_M$ vs. T display two linear regions which follow Curie-Weiss behavior typi-

Figure 20. Plot of $1/\chi_M$ vs. T for $[(Me_5C_5)_2Yb]_2(\mu\text{-}Br)$.

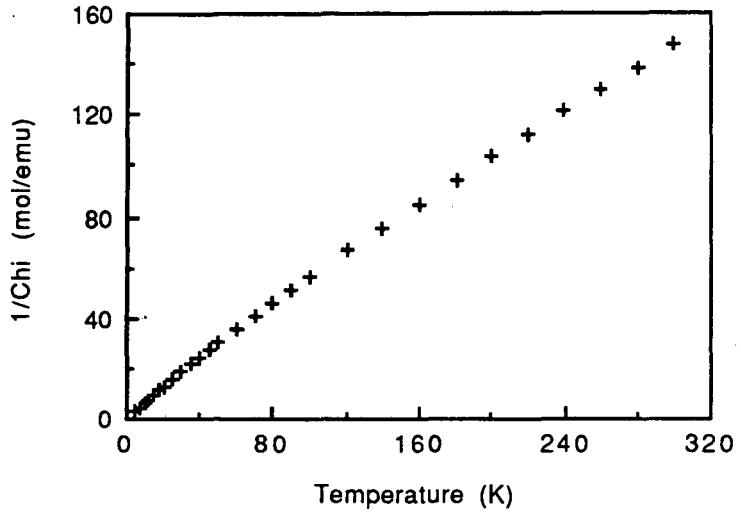

Figure 21. Plot of $1/\chi_M$ vs. T for $[(Me_5C_5)_2Yb]_2(\mu\text{-}BH_4)$.

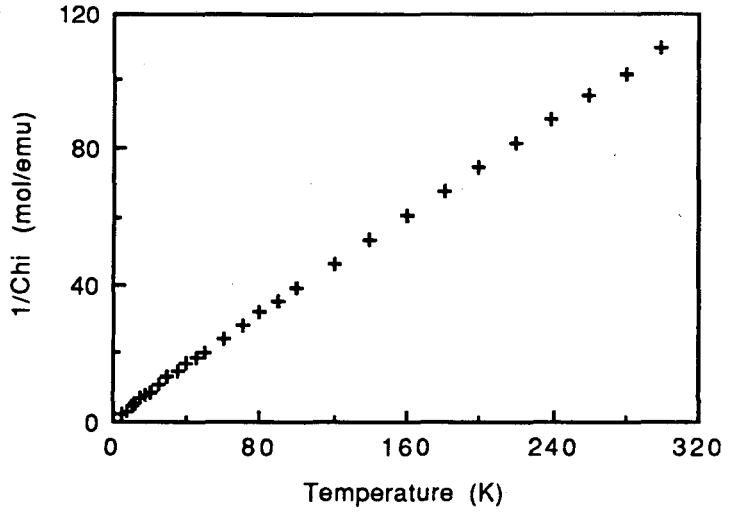

cal of simple trivalent ytterbium complexes.[27] This characteristic, coupled with the magnitudes of the magnetic moments, indicates that the two ytterbium atoms are magnetically distinct, and, therefore, they have the same electronic structure as $[(Me_5C_5)_2Yb]_2(\mu\text{-}Me)$. The

magnetic moments of the mixed-valent species are summarized in Table 5.

Table 5. Magnetic Moments of $[(Me_5C_5)_2Yb]_2(\mu\text{-}X)$ Complexes.

	Low Temp. Region[a]		High Temp. Region[b]	
X	μ (μ_B)[c]	Θ (K)	μ (μ_B)[c]	Θ (K)
F[d]	4.11	0	4.69	-25
Cl	3.83	-0.93	4.32	-26
Br	3.68	-1.1	4.23	-30
H[e]	4.03	-2	4.25	-30
Me	4.56	-0.45	4.75	-5.85
BH_4	4.41	-1.14	4.78	-12

a) typically in the range from 5-60 K. b) typically in the range from 100-300 K. c) the effective magnetic moment per molecule averaged over a temperature range displaying linear behavior in the plot of $1/\chi_M$ vs. T. d) reported in Reference 21. e) reported in Reference 6.

The trivalent organovanadium complexes have proven to be excellent reagents for the synthesis of base-free ytterbium species through electron-transfer/ligand-exchange processes. The vanadium complexes possess several attractive characteristics: (1) the reactions proceed cleanly with no side reactions, (2) the reactions can be performed in aliphatic hydrocarbon solvents to avoid coordinating bases, (3) the ytterbium products can be easily separated from the

vanadium products in most cases, (4) a variety of ligands can be transferred to ytterbium, and (5) decamethylvanadocene can be recovered from the reaction mixture and recycled into more ligand transfer reagents.

Because the ligand transfer reactions are very fast, it is impossible to study how the ligand transfers from one metal fragment to the other. Although steric restrictions would suggest that the transition state has a form like that shown in Figure 22, it would be

Figure 22

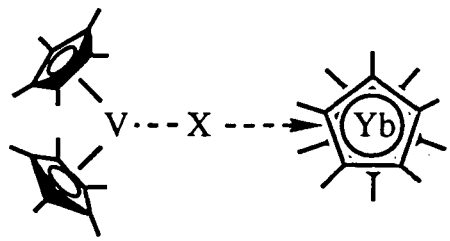

of interest to observe the structural details of the interaction between the two metal complexes. A set of metal complexes isostructural to the vanadium species, yet prohibited from being reduced, might provide models for the transition state in the ligand exchange reactions. Several titanium complexes analogous to the vanadium species have been reported.[28] Because these species should have less favorable reduction potentials relative to those of vanadium,[30] they would make attractive candidates for a modelling study.

References

1. Cotton, F. A.; Wilkinson, G., "Advanced Inorganic Chemistry," 4th Ed., Wiley Interscience: New York, **1980**.

2. (a) Kohler, F. H.; Prossdorf, W., *Z. Naturforsch., B: Anorg. Chem., Org. Chem.*, **1977**, *32B*, 1026. (b) Hall, V. M.; Schmulbach, C. D.; Soby, W. N., *J. Organomet. Chem.*, **1981**, *209*, 69. (c) Bouma, R. J.; Teuben, J. H.; Beukema, W. R.; Bansemer, R. L.; Huffman, J. C.; Caulton, K. G., *Inorg. Chem.*, **1984**, *23*, 2715.

3. (a) Boas, L. V.; Pessoa, J. C., "Comprehensive Coordination Chemistry," Wilkinson, G.; Gillard, R. D.; McClevery, J. A., eds., Pergamon: Oxford, **1987**, Ch. 33. (b) Holloway, C. E.; Melnik, M., *J. Organomet. Chem.*, **1986**, *304*, 41.

4. (a) Mowat, W.; Shortland, A; Yagupsky, G; Hill, N. J.; Yagupsky, M.; Wilkinson, G., *J. Chem. Soc., Dalton Trans.*, **1972**, 533. (b) Barker, G. K.; Lappert, M. F.; Howard, J. A. K., *J. Chem. Soc., Dalton Trans.*, **1978**, 734. (c) Ibekwe, S. D.; Myatt, J., *J. Organomet. Chem.*, **1971**, *31*, C65.

5. Connelly, N. G., "Comprehensive Organometallic Chemistry," Wilkinson, G.; Stone, F. G. A.; Abel, E. W., eds., Pergamon: Oxford, **1982**, Ch. 24.

6. Burns, C. J., Ph.D. Thesis, University of California, Berkeley, **1987**.

7. (a) Gambarotta, S.; Floriani, C.; Chiesi-Villa, A.; Guastini, C.; *Inorg. Chem.*, **1984**, *23*, 1739. (b) Curtis, C. J.; Smart, J. C.; Robbins, J. L., *Organometallics*, **1985**, *4*, 1283.

8. Bottomley, F.; Darkwa, J.; White, P. S., *Organometallics*, **1985**, *4*, 961.

9. Robbins, J. L.; Edelstein, N.; Spencer, B.; Smart, J. C., *J. Am. Chem. Soc.*, **1982**, *104*, 1882.

10. (a) Holloway, J. D. L.; Bowden, W. L.; Geiger, W. E., Jr., *J. Am. Chem. Soc.*, **1977**, *99*, 7089. (b) Holloway, J. D. L.; Geiger, W. E., Jr., *J. Am. Chem. Soc.*, **1979**, *101*, 2038.

11. Johnson, D. A., "Some Thermodynamic Aspects of Inorganic Chemistry," 2nd Ed., Cambridge University Press: Cambridge, **1982**.

12. Lauher, J. W.; Hoffman, R., *J. Am. Chem. Soc.*, **1976**, *98*, 1729.

13. (a)Marks, T. J.; Kennelly, W. J., *J. Am. Chem. Soc.*, **1975**, *97*, 1439. (b) Marks, T. J.; Kennelly, W. J.; Kolb, J. R.; Shimp, L. A., *Inorg. Chem.*, **1972**, *11*, 2540.

14. (a) Berg, D. J.; Burns, C. J.; Andersen, R. A.; Zalkin, A., *Organometallics*, **1989**, *8*, 1865. (b) Vaughn, G. A.; Hillhouse, G. L.; Lum, R. T.; Buchwald, S. L.; Rheingold, A. L., *J. Am. Chem. Soc.*, **1988**, *110*, 7215. (c) Holm, R. H., *Chem. Rev.*, **1987**, *87*, 1401.

15. (a) Bottomley, F.; White, P. S., *J. Chem. Soc., Chem Commun.*, **1981**, 28. (b) Bottomley, F.; Paez, D. E.; White, P. S., *J. Am. Chem. Soc.*, **1982**, *104*, 5651. (c) Bottomley, F.; Drummond, D. F.; Paez, D. E.; White, P. S., *J. Chem. Soc., Chem Commun.*, **1986**, 1752. (d) Bottomley, F.; Paez, D. E.; White, P. S., *J. Am. Chem. Soc.*, **1985**, *107*, 7226. (e) Bottomley, F.; Magill, C. P.; White, P. S., *J. Am. Chem. Soc.*, **1989**, *111*, 3070. (f) Bottomley, F.; Sutin, L., *J. Chem. Soc., Chem Commun.*, **1987**, 1112.

16. (a) Bottomley, F.; Magill, C. P.; Zhao, B, *Organometallics*, **1990**, *9*, 1700. (b) Bottomley, F.; Magill, C. P.; Zhao, B., *Organometallics*, **1991**, *10*, 1946.

17. (a) Bottomley, F.; Lin, I. J. B.; White, P. S., *J. Am. Chem. Soc.*, **1981**, *103*, 703. (b) Bottomley, F.; Egharevba, G. O.; Lin, I. J. B.; White, P. S., *Organometallics*, **1985**, *4*, 550. (c) Bottomley, F.; Paez, D. E.; White, P. S., *J. Am. Chem. Soc.*, **1981**, *103*, 5581. (d) Bottomley, F.; Paez, D. E.; White, P. S., *J. Am. Chem. Soc.*, **1982**, *104*, 5651. (e) Bottomley, F.; Paez, D. E.; Sutin, L.; White, P. S.; Kohler, F. H.; Thompson, R. C.; Westwood, N. P. C., *Organometallics*, **1990**, *9*, 2443.

18. (a) Ozin, G. A., *Acc. Chem. Res.*, **1977**, *10*, 21. (b) Mason, R.; Roberts, M. W., *Inorg. Chim. Acta.*, **1981**, *50*, 53.

19. (a) Signer, R., *Annalen*, **1930**, *478*, 246. (b) Clark, E. P., *Ind. Eng. Chem., Anal. Ed.*, **1941**, *13*, 820.

20. (a) Tilley, T. D., Ph.D. Thesis, University of California, Berkeley, **1982**. (b) Watson, P. L., *J. Chem. Soc., Chem Commun.*, **1980**, 652.

21. Burns, C. J.; Andersen, R. A., *J. Chem. Soc., Chem. Commun.*, **1989**, 136.

22. Burns, C. J.; Berg, D. J.; Andersen, R. A., *J. Chem. Soc., Chem. Commun.*, **1987**, 272.

23. Jahn, W.; Yunlu, K.; Oroschin, W.; Amberger, H. D.; Fischer, R. D., *Inorg. Chim. Acta*, **1984**, *95*, 85.

24. Shannon, R. D., *Acta. Cryst.*, **1976**, *A32*, 751.

25. (a) Rhodes, L. F.; Venanzi, L. M.; Sorato, C; Albinati, A., *Inorg. Chem.*, **1986**, *25*, 3335. (b) Holah, D. G.; Hughes, A. N.; Maciaszek, S.; Magnuson, V. R., *J. Chem. Soc., Chem. Commun.*, **1983**, 1308. (c) Green, B. E.; Kennard, C. H. L.; Smith, G.; James, B. D.; Healy, P. C.; White, A. H., *Inorg. Chim. Acta.*, **1984**, *81*, 147. (d) Zalkin, A.; Rietz, R. R.; Templeton, D. H.; Edelstein, N. M., *Inorg. Chem.*, **1978**, *17*, 661. (e) Vites, J. C.; Eigenbrot, C.; Felhner, T. P., *J. Am. Chem. Soc.*, **1984**, *106*, 4633.

26. Osborne, J. H.; Rheingold, A. L.; Trogler, W. C., *J. Am Chem. Soc.*, **1985**, *107*, 7945.

27. Berg, D. J., Ph.D. Thesis, University of California, Berkeley, **1987.**

28. Pattiasina, J. W.; Heeres, H. J.; van Bolhuis, F.; Meetsma, A.; Teuben, J. H.; Spek, A. L., *Organometallics*, **1987**, *6*, 1004.

29. Casey, A. T.; Mitra, S., "Theory and Applications of Molecular Paramagnetism," Boudreaux, E. A.; Mulay, L. N., eds., Wiley-Interscience: New York, **1976**.

30. (a) Bercaw, J. E.; Marvich, R. H.; Bell, L. G.; Brintzinger, H. H., *J. Am. Chem. Soc.*, **1972**, *94*, 1219. (b) Dessy, R. E.; King, R. B.; Waldrop, M., *ibid.*, **1966**, *88*, 5112. (c) Doisneau, R. G.; Marchon, J. C., *J. Electroanal. Chem.*, **1971**, *30*, 487. (d) Gubin, S. P.; Smirnova, S. A., *J. Organomet. Chem.*, **1969**, *229*, 241.

CHAPTER 3

Reactions of Bis(pentamethylcyclopentadienyl)ytterbium with Organotitanium Complexes

Titanium analogues of the organovanadium ligand donor complexes may provide structural models for the ligand exchange processes between vanadium and ytterbium species. Because titanium lies adjacent to vanadium in the periodic table, its complexes containing bulky pentamethylcyclopentadienyl ligands should be isostructural with the vanadium analogues, distinguished only by the slightly shorter bonds resulting from the smaller ionic radius of vanadium.[1] However, the trivalent titanium complexes are likely to be much more resistant to reduction by ytterbium than the vanadium species. Electrochemical studies on titanocene derivatives[2] suggest that the reduction potentials of trivalent permethyltitanocene species may be in excess of -2 V. Since this would make an electron transfer process between ytterbium and titanium thermodynamically unfavorable, the titanium complex may simply coordinate to ytterbium in a manner similar to that observed for the trivalent ytterbium fragment in $[(Me_5C_5)_2Yb]_2(\mu\text{-Me})$. These coordination complexes would then reveal details of the subtle interactions involved in the ligand transfer from vanadium to ytterbium.

Organotitanium Complexes

Teuben has reported the synthesis of the halide complexes, $(Me_5C_5)_2TiX$ (X = Cl, Br, I).[3] Unlike the vanadium halide analogues, the titanium complexes are synthesized from metathetical routes in-

volving only trivalent species. The chloride complex is obtained directly from the reaction of $TiCl_3(THF)_3$ with two equivalents of sodium pentamethylcyclopentadienide while the bromide and iodide are isolated <u>via</u> halide exchange reactions with the chloride (Eqn. 1). Electron transfer routes are less attractive for the titanium complexes due to the difficulty in synthesizing divalent permethyltitan-

$$(Me_5C_5)_2TiCl + MX \longrightarrow (Me_5C_5)_2TiX + MCl \quad (1)$$

$(M = Li, BBr_2, Me_3Si; X = Br)$

$(M = Li, Me_3Si; X = I)$

ocene.[4] Unfortunately, attempts to isolate the unreported fluoride complex through halide exchanges have proven unsuccessful. The reaction of borontrifluoride diethyletherate with alkyl and amido complexes of uranium has led to the isolation of uranium fluoride species (Eqn. 2).[5] However, analogous reactions with the titanium system do not yield the desired fluoride complexes. Therefore, it may be necessary to synthesize permethyltitanocene if the fluoride is to be obtained.

$$(R_2C_5H_3)_2UR'_2 + BF_3{\cdot}OEt_2 \longrightarrow (R_2C_5H_3)_2UF_2 + R'_2BF{\cdot}OEt_2 \quad (2)$$

$(R = Me_3C, Me_3Si; R' = Me, NMe_2)$

The borohydride complex can also be synthesized from the chloride by reaction with lithium borohydride.[3] Unlike the vanadium analogue, this complex shows typical terminal and bridging B-H stretches in the IR spectrum.[6] Teuben has recently reported the full

synthetic details for the methyl complex, $(Me_5C_5)_2TiMe$,[7] although it has been mentioned in previous publications.[3,8] Although Teuben implies that methyllithium can be used as the methylating agent in this preparation, an orange, lithium containing product is isolated rather than the desired methyl complex. However, our studies have found that dimethylmagnesium will cleanly transfer a methyl group to titanium in diethyl ether to produce the green methyl complex (Eqn. 3).

$$(Me_5C_5)_2TiCl + 1/2\ Me_2Mg \longrightarrow (Me_5C_5)_2TiMe + 1/2\ MgCl_2 \quad (3)$$

When exposed to hydrogen, the methyl complex reacts to form a dark red product (Eqn. 4). There is no distinct absorption in the IR spectrum which can be clearly assigned to the Ti-H stretch. The V-H

$$(Me_5C_5)_2TiMe + H_2 \longrightarrow (Me_5C_5)_2TiH + MeH \quad (4)$$

stretch in the vanadium analogue, $(Me_5C_5)_2VH$,[9] appears at 1625 cm^{-1} while the Sc-H stretch in the scandium complex, $(Me_5C_5)_2ScH$-(THF),[10] is found at 1390 cm^{-1}. Therefore, the Ti-H stretch in $(Me_5C_5)_2TiH$ should fall in between these two values. Unfortunately, this is the region where the strong absorptions associated with Nujol appear. However, an additional resolved absorption is observed at 1489 cm^{-1} which could be attributed to the Ti-H stretch. The ^1H NMR spectrum (toluene-d_8, 30 °C) shows a broad singlet at 22.6 ppm ($\upsilon_{1/2}$ = 128 Hz) that is similar to the reson-ance Bercaw observed at

22.2 ppm (toluene-d_8, 30 °C) for the product of the removal of 0.5 equivalent of hydrogen from $(Me_5C_5)_2TiH_2$ (Eqn. 5).[4]

$$(Me_5C_5)_2TiH_2 \xrightarrow{\text{vacuum}} (Me_5C_5)_2TiH + 1/2\ H_2 \qquad (5)$$

Furthermore, the variable temperature magnetic susceptibility is consistent with a trivalent titanium complex (Figure 1). From 5-100 K, the complex obeys Curie-Weiss behavior and has a magnetic moment of 1.72 μ_B with Θ = -2.12 K. This is consistent with the expected spin-only value for a simple trivalent titanium ion with one

Figure 1. Plot of $1/\chi_M$ vs. T for $(Me_5C_5)_2TiH$.

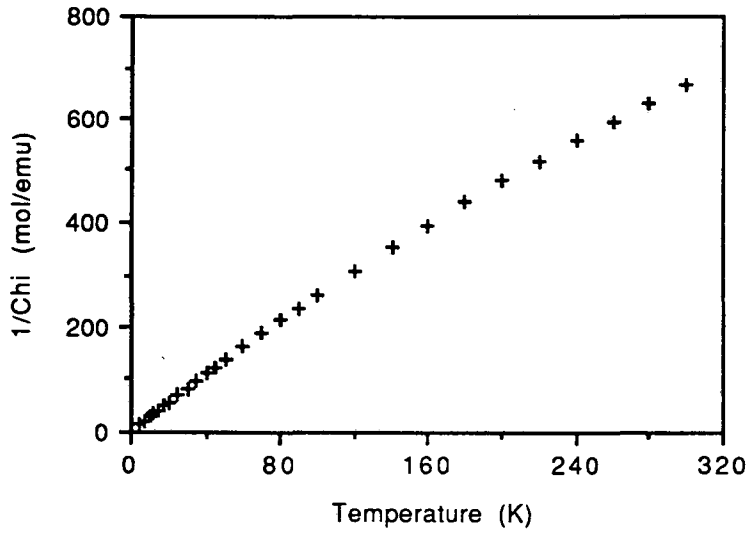

unpaired spin.[11] From 180-300 K, the average moment increases slightly to 1.97 μ_B with Θ = -42.32 K. It is unlikely that sample impurities could be responsible for this deviation. The change might be attributable to larger errors in the data at high temperature due

to the decrease in the magnitude of the magnetic signal. However, the magnitude of the magnetic moment still supports a trivalent titanium product.[12] In addition, the room temperature EPR spectrum shows a single resonance with a g value of 1.993 which is typical of other simple trivalent titanium species.[3] Unfortunately, because the mass of $(Me_5C_5)_2TiH$ is so close to that of $(Me_5C_5)_2Ti$, elemental analysis and mass spectrometry cannot provide conclusive evidence for the existence of the hydride. The highest mass peak observed in the mass spectrum can be attributed to $(Me_5C_5)_2Ti^+$.

With the hope of providing additional support through comparison with the analogous deuteride complex, the reaction of $(Me_5C_5)_2TiMe$ with deuterium has also been studied. However, the reaction is complicated by the incorporation of deuterium into the methyl groups of the Me_5C_5 ligands. Upon exposure to high pressures of deuterium for prolonged periods, approximately 85 % incorporation can be achieved as determined by IR spectroscopy (Eqn. 6).

$$(Me_5C_5)_2TiMe + D_2 \xrightarrow[5\ d]{6\ atm} (d_{15}\text{-}Me_5C_5)_2TiD + MeD + H_2 \quad (6)$$

This result is not entirely surprising given the tendency of titanium complexes to activate methyl groups of Me_5C_5 ligands. Bercaw has observed the activation of ring methyl groups as well as deuteration of the Me_5C_5 ligands in reactivity studies of $(Me_5C_5)_2Ti$.[4] Thermolysis of $(Me_5C_5)_2TiMe$ has also been shown to result in ring activated products.[8a] In addition, other decamethylmetallocene complexes have also demonstrated this behavior. The scandium

complex, $(Me_5C_5)_2ScH$, has been found to catalyze the deuteration of free Me_5C_5H.[13] However, the reaction conditions required are much more robust than what is used in the titanium reactions. The similarity in appearance and behavior of this product relative to the hydride complex suggests that the final isolated product may remain a deuteride species. If this is correct, then the absorption at 1048 cm^{-1} in the IR spectrum could be assigned to the Ti-D stretch. This absorption does not appear in the spectrum for $(Me_5C_5)_2TiH$ and is in excellent agreement with the expected H/D isotopic shift based on the assignment of the 1489 cm^{-1} absorption as the Ti-H stretch.

Based on the observed behavior of simple trivalent titanium species,[2a,4] a process such as that outlined in Scheme 1 might account for the deuterium incorporation into the Me_5C_5 ligands. The deuteride complex would form initially in the first step with elimination of MeD. The deuteride could then activate a ring methyl proton to release HD and leave the methylene complex which Bercaw has observed as a product from the decomposition of $(Me_5C_5)_2Ti$. This complex could then react with additional D_2 to reform the deuteride with the incorporation of deuterium in the Me_5C_5 ligand. The last two steps could then repeat until deuterium has been completely exchanged. Steps (b) and (c) constitute an equilibrium process wherein D_2 replaces HD due to the much higher concentration of D_2 in the reaction mixture.

Incorporation of perdeuterated ligands into other metallocene species could also provide valuable information on ring exchange processes. Unfortunately, attempts to isolate the free deuterated

Scheme 1

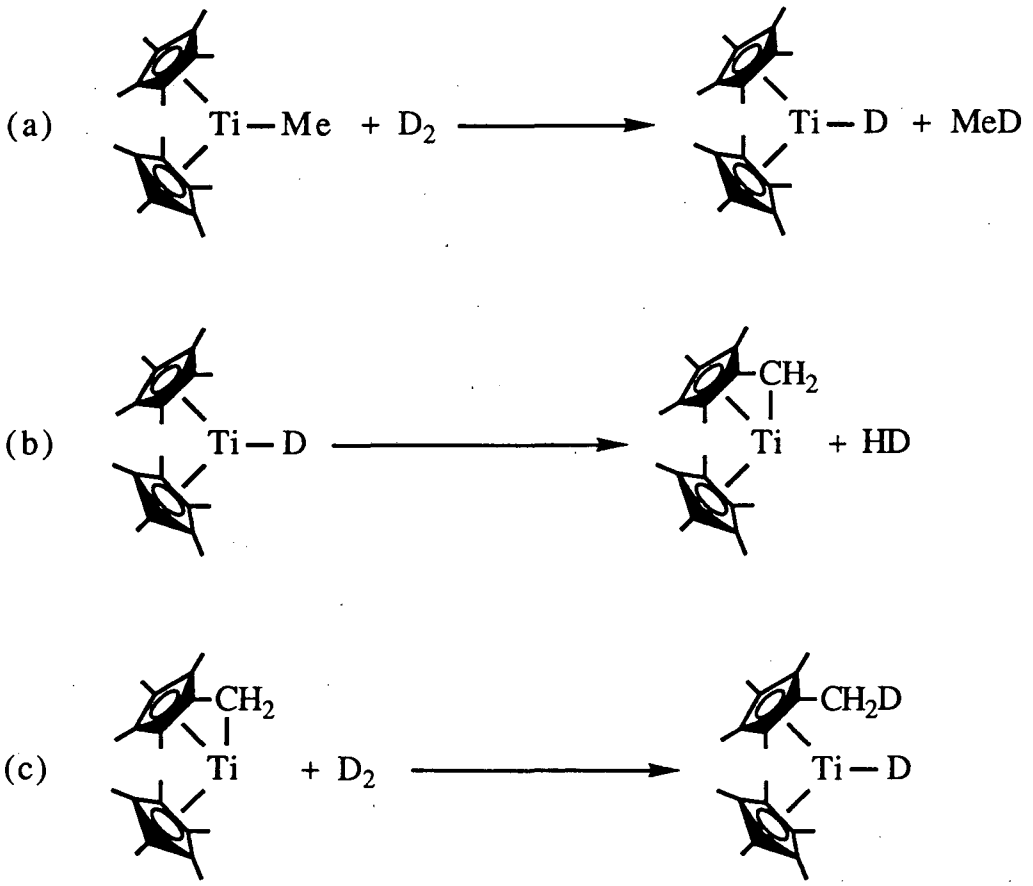

ligand through hydrolysis of the titanium complex have been unsuccessful. Therefore, further studies will have to be undertaken in order to examine the possibility of accessing the perdeuterated ligands for use in other applications.

Bimetallic Complexes

When the titanium complexes, $(Me_5C_5)_2TiX$ (X = Cl, Br, I, H, Me, BH_4), are mixed with $(Me_5C_5)_2Yb$ in pentane, dark-colored precipitates are generated. The faint coloration of the mother liquor suggests that the yellow-orange $(Me_5C_5)_2Ti$ is not produced. There-

fore, the bimetallic, ligand-bridged complexes must be formed as shown in Eqn. 7. These species are similar to the mixed-valent complexes, $[(Me_5C_5)_2Yb]_2(\mu\text{-}X)$, in that they are sparingly soluble in aliphatic hydrocarbon solvents but can be recrystallized from toluene. The apparent formation of the bridging hydride complex provides further support for the existence of the parent titanium hydride since a related species such as $(Me_5C_5)(Me_4C_5CH_2)Ti$ would be unlikely to coordinate to ytterbium. The physical properties of the bimetallic complexes are summarized in Table 1.

$$(Me_5C_5)_2Yb + (Me_5C_5)_2TiX \longrightarrow (Me_5C_5)_2Yb(\mu\text{-}X)Ti(Me_5C_5)_2 \quad (7)$$

Table 1. Physical Properties of $(Me_5C_5)_2Yb(\mu\text{-}X)Ti(Me_5C_5)_2$ Complexes.

X	Color	Yield, %	mp, °C
Cl	green-brown	91	244
Br	green-brown	82	238
H	red-brown	56	196
Me	brown	71	176
BH_4	green-brown	86	302

The IR spectra appear to consist of the superimposed spectra of the individual metal complexes. The key feature in each spectrum is the low energy, metal-ring symmetric tilting vibration at approximately 275 cm^{-1} which is generally diagnostic for divalent ytterbium species.[14] Therefore, no electron transfer has occurred between the two metal centers and the titanium complexes are acting as large

coordinating ligands toward ytterbium. The IR spectrum for the bridging borohydride complex provides information on the nature of the interaction between the borohydride ligand and the two metal centers. The similarity between the two sets of absorptions in the bridging complex and the free titanium complex indicates that the ligand has a bidentate interaction to each metal (Figure 2).[3] The coordination of the ligand to ytterbium is evidenced by the decrease in the B-H_a stretching energies at 2385 and 2324 cm^{-1} relative to the terminal B-H stretches in the parent titanium complex at 2445 and 2410 cm^{-1}.

Figure 2

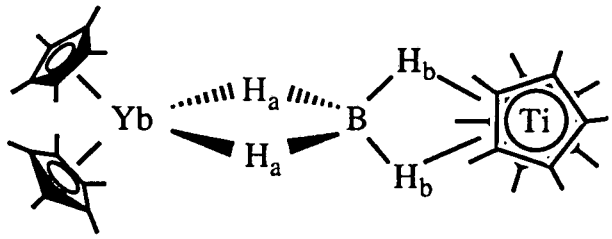

In addition, the B-H_b stretches increase in energy from 2070 and 1950 cm^{-1} in the parent complex to 2156 and 2075 cm^{-1} in the bimetallic product. The stronger B-H_b stretches in the bimetallic complex result from a weakening of the bonding between the borohydride ligand and the titanium atom as the ligand is drawn toward ytterbium. This behavior should be manifested in a lengthening of the Ti-H distances in the solid state structure.

The ^1H NMR spectra of the free titanium complexes are extremely broad with peak widths at half maximum in the range

from 600-1000 Hz.[3,7] Because the bimetallic complexes are substantially less soluble than the parent titanium complexes, it is virtually impossible to observe distinct resonances for the Me_5C_5 protons on titanium. Therefore, ^1H NMR spectroscopy is uninformative for these species. In addition, the extremely weak bridging interactions in the bimetallic complexes preclude the observation of molecular ions in the mass spectra. Consequently, the identities of the products can only be inferred by the observation of the separate metal fragments in the gas phase.

Magnetic Behavior

Although the IR spectra suggest that the two metal atoms in the bimetallic complexes do not change oxidation state upon coordination, examination of the magnetic behavior can clearly establish the presence of trivalent ytterbium. There are two distinct forms that can result upon coordination (Figure 3).

Figure 3

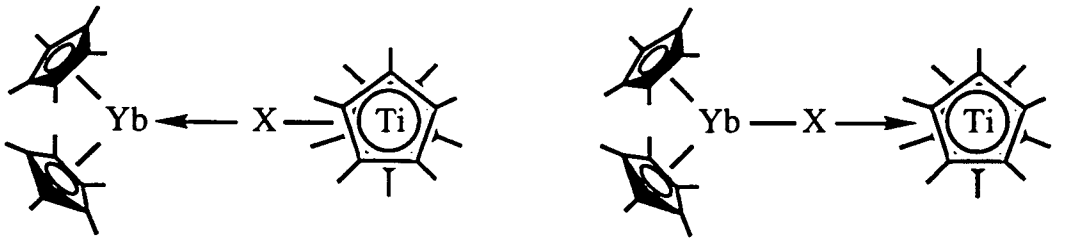

II III III II

(a) (b)

In Figure 3(a), the titanium complex merely coordinates to the ytterbium center without any electron exchange. Because the ytterbium fragment remains diamagnetic, it should have little effect on the magnetic behavior of the titanium fragment. Therefore, the variable temperature magnetic susceptibility should be consistent with the behavior expected for a simple trivalent titanium complex.

In Figure 3(b), electron transfer occurs and the ytterbium fragment is oxidized to the trivalent state while the titanium fragment is reduced to the divalent state. If there is no electronic communication between the two metal centers, then the magnetic moment should combine the contributions of each separate fragment according to Eqn. 8:[12]

$$\mu(\text{complex}) = [\mu^2(\text{Yb}) + \mu^2(\text{Ti})]^{1/2} \qquad (8)$$

The plot of $1/\chi_M$ vs. T should display two regions of linear behavior due to the influence of the paramagnetic ytterbium center. If there is communication between the unpaired electrons on the two metal atoms, then the variable temperature behavior would be more complex and the data would not be consistent with either of the extreme cases in Figure 3.

It is clear from the variable temperature magnetic susceptibility measurements (Figures 4-8) that electron transfer does not occur and that the titanium fragment simply coordinates to the ytterbium center in agreement with the IR data. Small deviations from linearity at high temperatures in the plots of $1/\chi_M$ vs T are again observed. Because of the high molecular weights and low mag-

netic moments of these complexes , the high temperature data may contain significant errors. Therefore, it would be difficult to speculate on any physical causes for the observed deviations from spin-only magnetic moments. One simple explanation for the increase in

Figure 4. Plot of $1/\chi_M$ vs. T for $(Me_5C_5)_2Yb(\mu\text{-}Cl)Ti(Me_5C_5)_2$.

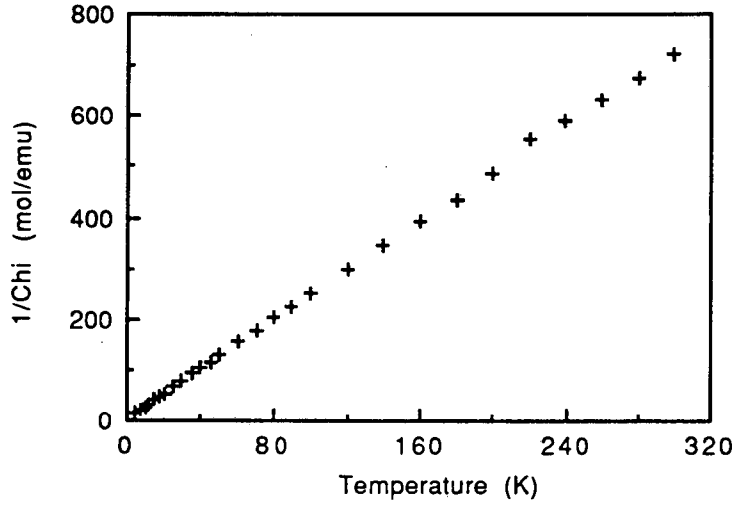

Figure 5. Plot of $1/\chi_M$ vs. T for $(Me_5C_5)_2Yb(\mu\text{-}Br)Ti(Me_5C_5)_2$.

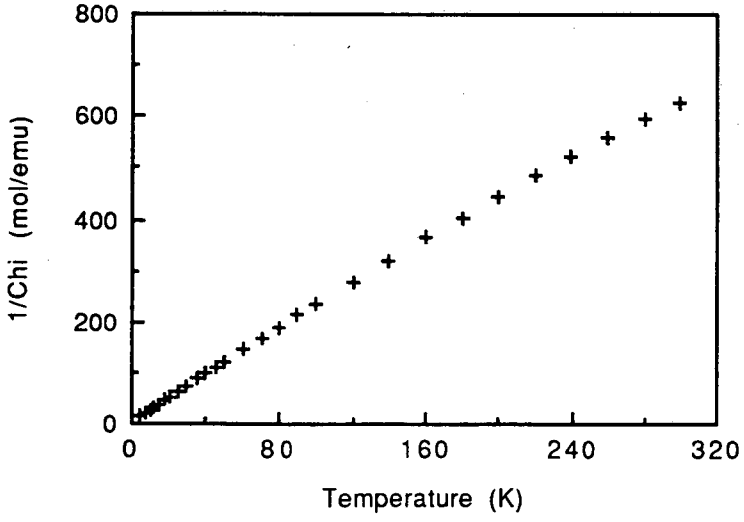

Figure 6. Plot of $1/\chi_M$ vs. T for $(Me_5C_5)_2Yb(\mu\text{-}H)Ti(Me_5C_5)_2$.

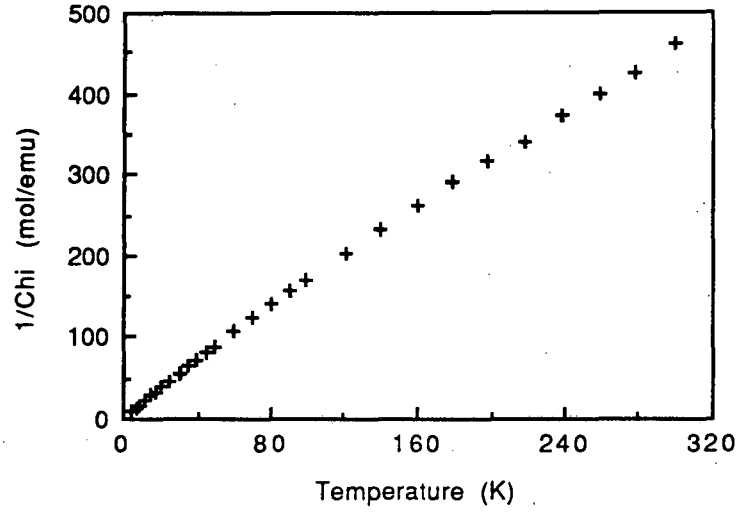

Figure 7. Plot of $1/\chi_M$ vs. T for $(Me_5C_5)_2Yb(\mu\text{-}Me)Ti(Me_5C_5)_2$.

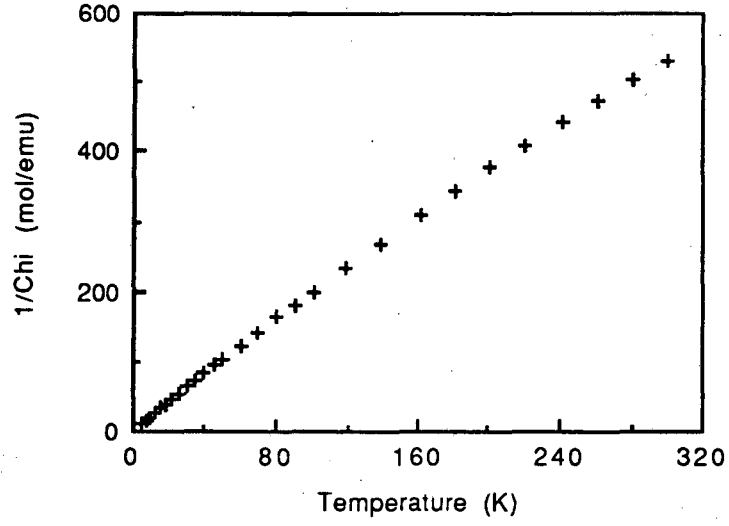

Figure 8. Plot of $1/\chi_M$ vs. T for $(Me_5C_5)_2Yb(\mu\text{-}BH_4)Ti(Me_5C_5)_2$.

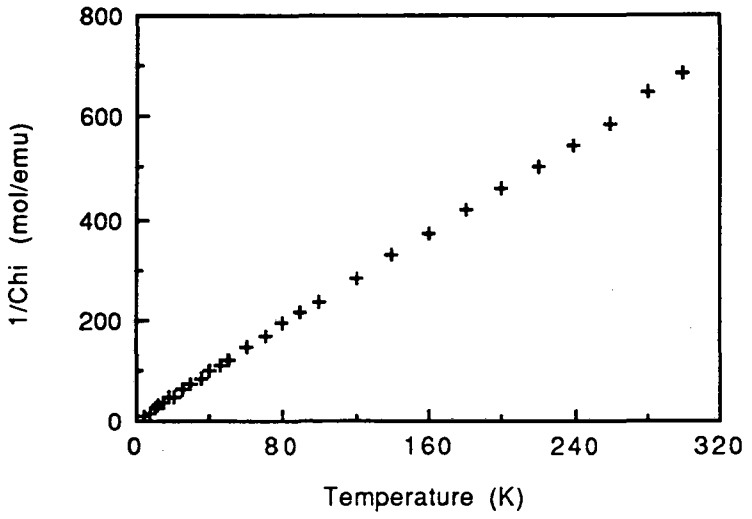

the moment relative to the spin-only value, would be the presence of a small amount of the electron transfer products. Even a minute amount of a Ti(II)/Yb(III) product would result in a noticeable rise in the magnetic moment for the bulk sample. This condition would be expected to show an enhancement as the temperature is elevated and might account for the slightly high magnetic moments even at low temperatures. Regardless of the cause for the change in the observed magnetic moments, the magnitudes of the changes indicate that the effect is relatively small in comparison to the properties of the bulk material and, therefore, it can be concluded that titanium remains primarily in the trivalent state. The magnetic moments for the bimetallic species are listed in Table 2.

Table 2. Magnetic Moments of $(Me_5C_5)_2Yb(\mu\text{-}X)Ti(Me_5C_5)_2$ Complexes.

	5-100 K		180-300 K	
X	μ (μ_B)[a]	Θ (K)	μ (μ_B)[a]	Θ (K)
Cl	1.79	-1.24	1.85	-10.57
Br	1.85	-1.59	2.07	-39.66
H	2.18	-2.36	2.40	-28.97
Me	2.02	-2.12	2.25	-38.51
BH_4	1.84	-0.76	1.89	-4.60

a) the effective magnetic moment per molecule averaged over the temperature range specified.

The room temperature EPR data are also consistent with titanium remaining in the trivalent state. The EPR data for the parent titanium complexes[3,7] as well as the bimetallic species are summarized in Table 3. The complexes all produce sharp, single line spectra without any additional coupling observed. Examination of the data reveals that the measured g values change only slightly upon coordination of the titanium complex to ytterbium. This indicates that although the presence of ytterbium does have an effect on the titanium fragment, the influence is quite small. Therefore, solid state structural studies should provide more meaningful information on the interaction between the two metal fragments.

Table 3. EPR Data for $(Me_5C_5)_2Yb(\mu\text{-}X)Ti(Me_5C_5)_2$ Complexes.[a]

	g
$(Me_5C_5)_2TiCl$[b]	1.956
$(Me_5C_5)_2TiBr$[b]	1.953
$(Me_5C_5)_2TiH$[c]	1.993
$(Me_5C_5)_2TiMe$[d]	1.957
$(Me_5C_5)_2TiBH_4$[b]	1.978
$(Me_5C_5)_2Yb(\mu\text{-}Cl)Ti(Me_5C_5)_2$	1.968
$(Me_5C_5)_2Yb(\mu Br)Ti(Me_5C_5)_2$	1.966
$(Me_5C_5)_2Yb(\mu\text{-}H)Ti(Me_5C_5)_2$[c]	1.987
$(Me_5C_5)_2Yb(\mu\text{-}Me)Ti(Me_5C_5)_2$	1.956
$(Me_5C_5)_2Yb(\mu\text{-}BH_4)Ti(Me_5C_5)_2$	1.994

(a) methylcyclohexane solutions, 10^{-2}-10^{-3} M at 298 K.
(b) measured in Reference 3. (c) toluene solution, ca. 10^{-2} M.
(d) measured in Reference 7.

Crystallographic Studies

With the properties of the bimetallic complexes well established, the details of the bridging ligand interactions can be examined through the use of X-ray crystallography. The simplest interactions should involve the halide bridges. Whereas typical halide bridges between two metal atoms form very sharp angles (Figure 9),[15] the bulky Me_5C_5 ligands in these species should force the halide atom into a more linear orientation. This assertion is verified by the crystal structure determination of the chloride complex which reveals an Yb-Cl-Ti angle of 154.00(4)° (Figure 10). Selected

bond distances and angles are provided in Tables 4 and 5, respectively.

Figure 9

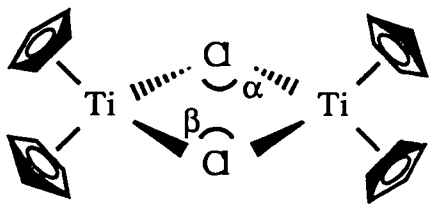

Figure 10. ORTEP Diagram of $(Me_5C_5)_2Yb(\mu\text{-}Cl)Ti(Me_5C_5)_2$.

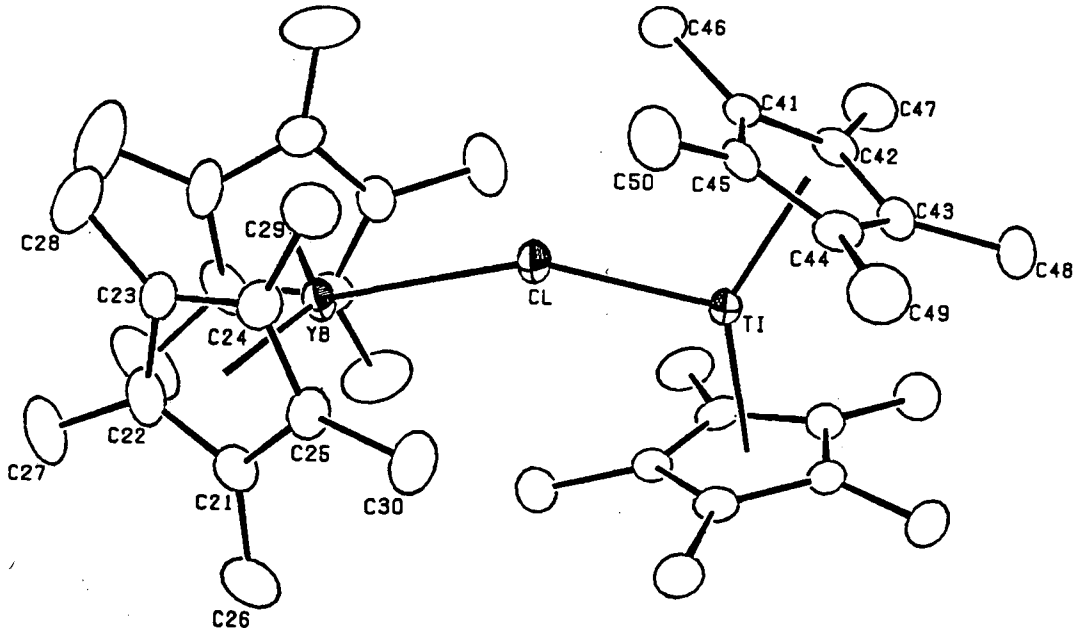

Table 4. Bond distances for $(Me_5C_5)_2Yb(\mu\text{-}Cl)Ti(Me_5C_5)_2$ (Å)

Yb-Cl	2.778 (2)	Ti-Cl	2.418 (2)
Yb-Cp1	2.397	Ti-Cp3	2.059
Yb-Cp2	2.393	Ti-Cp4	2.050
Yb-C11	2.698 (7)	Ti-C31	2.412 (7)
Yb-C12	2.690 (7)	Ti-C32	2.373 (7)
Yb-C13	2.659 (7)	Ti-C33	2.357 (5)
Yb-C14	2.644 (7)	Ti-C34	2.375 (7)
Yb-C15	2.717 (7)	Ti-C35	2.413 (7)
Yb-C21	2.651 (7)	Ti-C41	2.394 (7)
Yb-C22	2.675 (7)	Ti-C42	2.361 (7)
Yb-C23	2.695 (7)	Ti-C43	2.371 (5)
Yb-C24	2.686 (7)	Ti-C44	2.373 (7)
Yb-C25	2.691 (7)	Ti-C45	2.391 (7)

Cp1, Cp2, Cp3, and Cp4 are the ring centroids of atoms C11-C15, C21-C25, C31-C35, and C41-C45, respectively.

Table 5. Bond Angles for $(Me_5C_5)_2Yb(\mu\text{-}Cl)Ti(Me_5C_5)_2$ (°)

Yb-Cl-Ti	154.00 (7)	Cp1-Yb-Cl	110.0
		Cp2-Yb-Cl	108.0
Cp1-Yb-Cp2	140.8	Cp3-Ti-Cl	110.9
Cp3-Ti-Cp4	142.6	Cp4-Ti-Cl	106.5

As expected, the two sets of Me_5C_5 ligands are twisted relative to each other in order to maximize the ligand-metal interactions while minimizing steric repulsions between the methyl groups on the rings. The bond distances and angles in the $(Me_5C_5)_2Yb$ portion of the molecule are consistent with a divalent oxidation state for ytterbium. The Yb-Cl distance of 2.778(1) Å is significantly longer than would be expected for an ytterbium-chloride bond, based on ionic radii.[1] The $(Me_5C_5)_2TiCl$ fragment can be compared to the

structure of the free complex studied by Teuben.[3] The ring centroid-Ti-ring centroid angle of 143.6° in the free molecule is slightly larger than the angle of 142.6° in the bimetallic complex which reflects the greater steric crowding introduced by $(Me_5C_5)_2Yb$. The most striking difference between the two structures is the lengthening of the Ti-Cl bond from 2.363(1) Å to 2.418(2) Å upon coordination to ytterbium. This reflects a weakening of the Ti-Cl bond as electron density is drawn from the chloride ligand toward the electropositive ytterbium center. The structurally observed effect on the strength of the Ti-Cl interaction provides physical evidence for the interpretation of the EPR data of the bimetallic complexes discussed earlier. The slight change in the measured g values for the bimetallic species relative to the parent titanium complexes may be a consequence of the perturbation of the Ti-Cl bond resulting from the influence of $(Me_5C_5)_2Yb$.

Although the angle of the chloride bridge is substantially greater than what is typically observed for metal halide complexes, the orientation is far from linear. If steric crowding is maximized, a linear bridge configuration, such as that observed for $[(Me_5C_5)_2Yb]_2(\mu\text{-}F)$, can be enforced.[16] Therefore, the significant bend in the chloride bridge suggests that there is still room for the separate metal fragments to move around and that the halide is attempting to optimize its interaction with ytterbium.

A simple model based on frontier orbital theory can be invoked to rationalize the preference for a bent interaction in the bridge.[17] For a simple three-atom molecule, H_2X, a linear geometry will produce the two bonding molecular orbitals $1\sigma_g$ and $1\sigma_u$ and a pair

of degenerate nonbonding orbitals of π symmetry (Figure 11). As the molecule bends, the symmetry changes from $D_{\infty h}$ to C_{2v}. The $1\sigma_g$ molecular orbital is stabilized to lower energy forming the $1a_1$ orbital

Figure 11. Walsh Diagram for an H_2X Molecule.

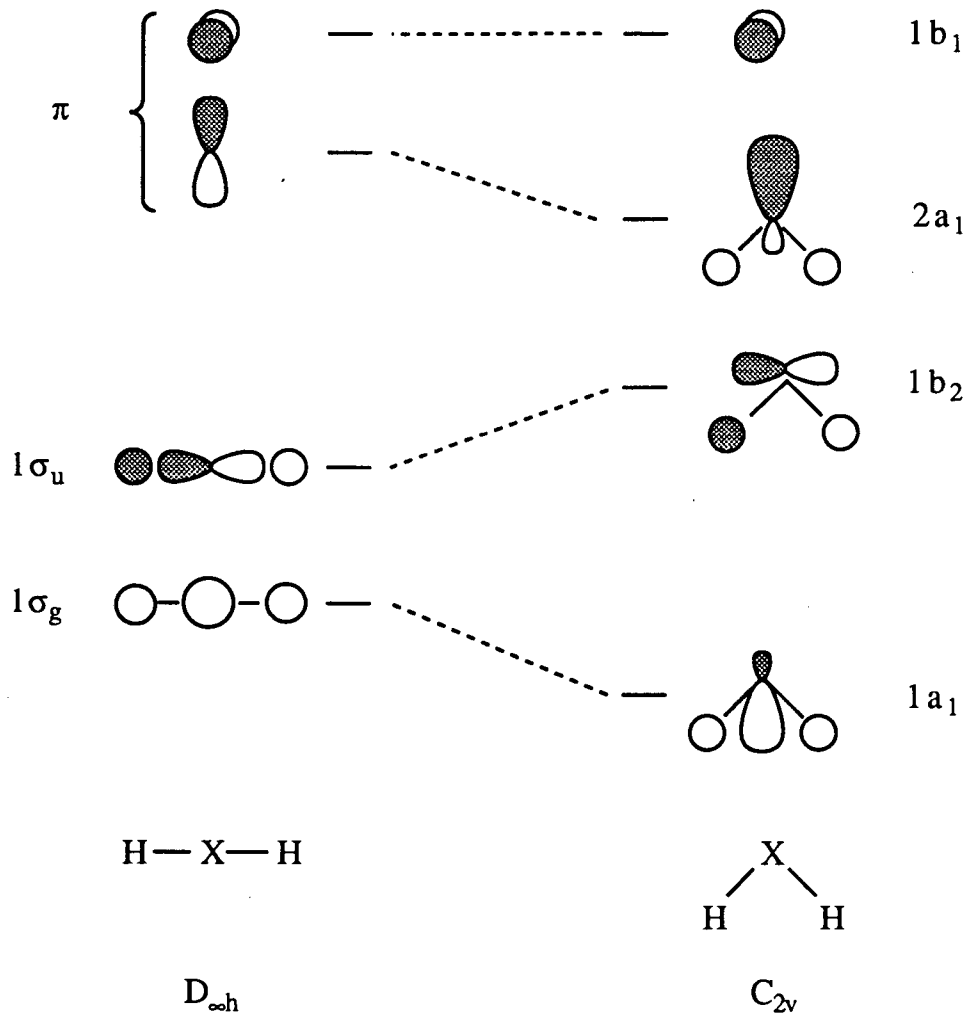

as the increase in the overlap of the two s orbitals contributed from the H atoms enhances the overall bonding interaction. In addition, the $1\sigma_u$ orbital is destabilized to the $1b_2$ orbital due to a decrease in

the effective overlap of the s orbitals with the p_z orbital and an increase in the s-s antibonding interaction. One of the degenerate π orbitals also experiences a positive overlap upon bending to form the $2a_1$ molecular orbital.

According to Walsh's rule,[17] the molecule will adopt the geometry which best stabilizes the highest occupied molecular orbital (HOMO). Therefore, examination of the molecular orbital diagram indicates that an H_2X molecule containing two electrons will prefer a bent geometry with the $1a_1$ orbital being filled. However, a molecule with three or four electrons will be linear due to filling of the more stable $1\sigma_u$ orbital. With five or six electrons, the bent geometry will again be more favorable because of the lower energy $2a_1$ orbital. When the structural perturbation does not affect the energy level of the HOMO, Walsh's rule states that the geometry will be determined by the more stable second highest occupied molecular orbital (SHOMO). Thus, for a molecule containing seven or eight electrons, the bent geometry must still be favored due to the lower energy of the $2a_1$ orbital.

The bent geometry of $(Me_5C_5)_2Yb(\mu\text{-}Cl)Ti(Me_5C_5)_2$ can be related to the structure of the H_2X molecule because the tendency toward nonlinearity is governed by the Yb-Cl-Ti interaction. Thus, assigning $(Me_5C_5)_2Yb$ to H^+ and $(Me_5C_5)_2TiCl$ to HX creates an H_2X^+ molecule which contains eight electrons. According to the Walsh diagram, the complex should prefer a bent geometry, and this is what is observed in the solid state structure. The tendency toward bending is inherent in the bridging interaction while the actual

degree of bending in the structure is regulated by the bulkiness of the Me_5C_5 ligands.

Examination of the molecular orbitals of $(Me_5C_5)_2TiCl$ reveals the likely source of electron density that is donated to ytterbium. The orientation of these orbitals account for the bending behavior observed in the crystal structure of the ytterbium-titanium bimetallic complex. A molecular orbital diagram for $(Me_5C_5)_2TiCl$ can be constructed by analogy to the $(C_5H_5)_2MX$ species analyzed by Hoffman[18] and Green[19] (Figure 12). For $(Me_5C_5)_2TiCl$, the HOMO has

Figure 12. Molecular Orbital Diagram for $(Me_5C_5)_2TiX$, C_{2v} symmetry.

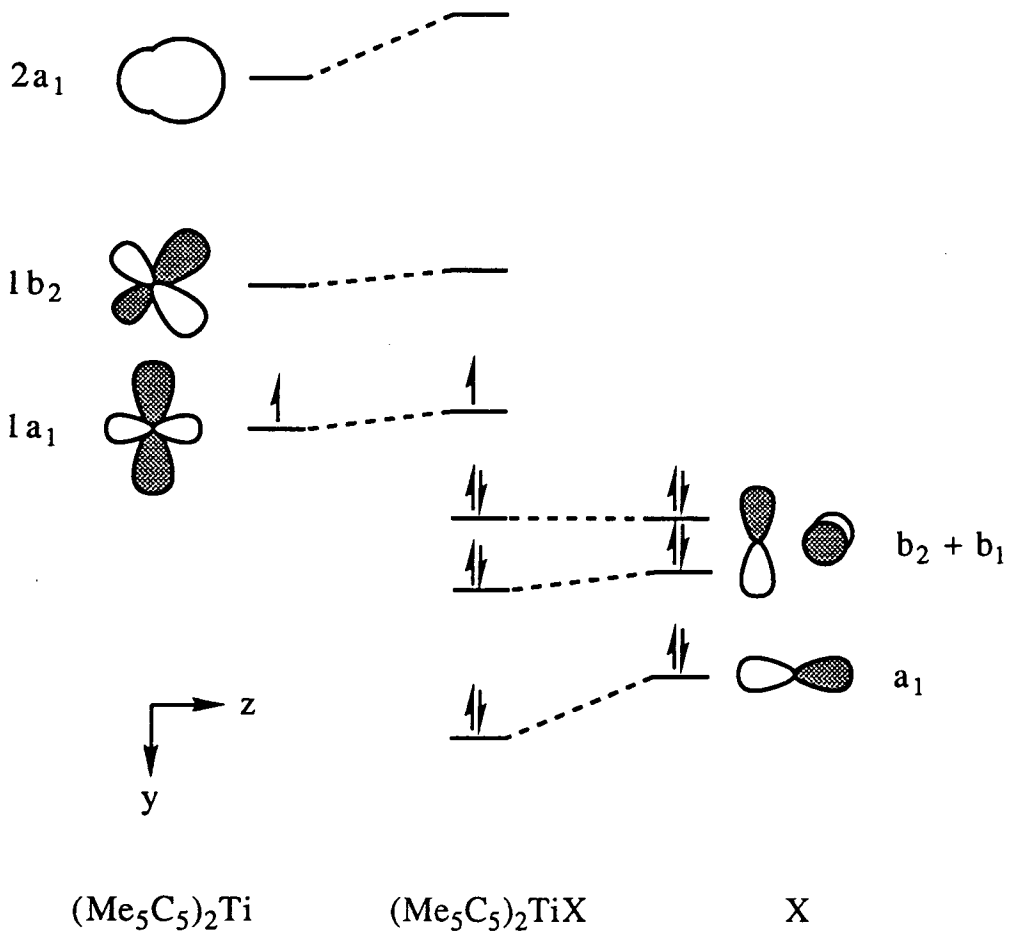

primarily metal-based character and is not involved in the Yb-Cl interaction. However, the filled molecular orbitals derived from the π symmetry orbitals of the chloride ligand should have a substantial influence on the orientation of the halide bridge. The electron density in these orbitals is directed perpendicular to the Ti-Cl bonding vector. Therefore, a linear bridge to ytterbium would not allow effective interaction of this electron density with the electropositive ytterbium center. By inducing a bent orientation of the chloride bridge, the π-electron density can be directed toward ytterbium to create a stronger donor interaction. Because the interaction should strengthen as the bending increases, the halide would be expected to maximize the amount of bending within the limits imposed by the steric requirements of the molecule.

The importance of the strength of the donor-acceptor interaction is demonstrated by a subtle detail observed in the structure of $(Me_5C_5)_2Yb(\mu\text{-}Cl)Ti(Me_5C_5)_2$. There are two distinct orientations which the bridge can assume (Figure 13). In Figure 13(a), the bend occurs in the plane that bisects the two Me_5C_5 rings on ytterbium. This forces one of the rings on titanium to lie closer to ytterbium than the other. In Figure 13(b), the bridge lies in the plane that bisects the Me_5C_5 ligands on titanium and has a perpendicular relationship with that in Figure 13(a). In this structure, a Me_5C_5 ligand on ytterbium is positioned closer to the titanium atom than its partner. The crystallographically observed orientation is clearly that shown as Figure 13(a). Because there is no disorder in the position of the chloride ligand which would suggest a

random distribution of the two orientations, there must be some factor that causes a preference for the observed geometry.

Figure 13

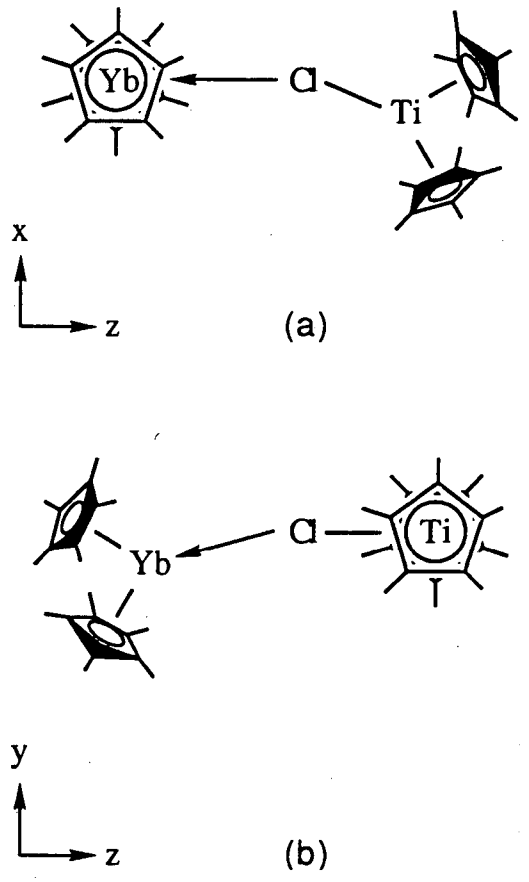

Upon formation of the titanium chloride complex, the degeneracy of the π orbitals on the chloride ligand is broken as the b_2 orbital mixes with the $1b_2$ orbital of titanium. This makes the non-interacting b_1 orbital on the chloride slightly more accessible to ytterbium. Because the b_1 orbital lies in the plane that bisects the two Me_5C_5 rings on ytterbium, the strongest interaction can occur if

the molecule bends in this plane. This then produces the orientation shown in Figure 13(a).

However, this structural preference can also be explained purely on the basis of steric effects. Because the ytterbium ion is much larger than titanium, the Me_5C_5 ligands are bound at a greater distance from the metal which provides more space in the coordination sphere around ytterbium. Therefore, moving a Me_5C_5 ligand on titanium into the wedge formed by the Me_5C_5 ligands on ytterbium should allow the bridge to bend to a greater extent than if a Me_5C_5 ligand on ytterbium moves into the more crowded coordination sphere of titanium.

The arguments concerning the tendency of the halide bridge to form a bent geometry indicate that the molecule maximizes the degree of bending in order to provide the strongest interaction with the ytterbium center. If these interpretations are valid, then the bridging angle should be dependent on the identity of the bridging atom. Therefore, examination of the bromide analogue should reveal a halide bridge with a sharper bend. Since the bromide ion is larger than the chloride ion, the bond distances to both titanium and ytterbium should be longer in the bromide complex. This should allow more freedom of movement for the two metal fragments so that the bridge can bend to a greater extent before steric repulsions become too large.

The X-ray crystallographic examination for the bromide complex, $(Me_5C_5)_2Yb(\mu\text{-}Br)Ti(Me_5C_5)_2$, shows the structure to be very similar to the chloride analogue. However, the bridging angle does sharpen to 149.53(4)° as expected. Selected bond distances and

angles are listed in Tables 6 and 7, respectively, and an ORTEP diagram is provided in Figure 14.

Table 6. Bond distances for $(Me_5C_5)_2Yb(\mu\text{-}Br)Ti(Me_5C_5)_2$ (Å)

Yb-Br	2.917 (1)	Ti-Br	2.574 (1)
Yb-Cp1	2.393	Ti-Cp3	2.060
Yb-Cp2	2.397	Ti-Cp4	2.059
Yb-C1	2.706 (7)	Ti-C21	2.360 (6)
Yb-C2	2.678 (7)	Ti-C22	2.369 (6)
Yb-C3	2.658 (7)	Ti-C23	2.359 (6)
Yb-C4	2.653 (7)	Ti-C24	2.426 (6)
Yb-C5	2.700 (6)	Ti-C25	2.402 (6)
Yb-C11	2.686 (6)	Ti-C31	2.359 (6)
Yb-C12	2.667 (6)	Ti-C32	2.374 (6)
Yb-C13	2.666 (7)	Ti-C33	2.374 (6)
Yb-C14	2.683 (7)	Ti-C34	2.407 (6)
Yb-C15	2.674 (6)	Ti-C35	2.396 (6)

Cp1, Cp2, Cp3, and Cp4 are the ring centroids of atoms C1-C5, C11-C15, C21-C25, and C31-C35, respectively.

Table 7. Bond Angles for $(Me_5C_5)_2Yb(\mu\text{-}Br)Ti(Me_5C_5)_2$ (°)

Yb-Br-Ti	149.49 (4)	Cp1-Yb-Br	109.5
		Cp2-Yb-Br	107.2
Cp1-Yb-Cp2	142.0	Cp3-Ti-Br	111.1
Cp3-Ti-Cp4	142.8	Cp4-Ti-Br	106.1

The metal-bromide distances are significantly longer than the same distances in the chloride complex. Because the metal-ring centroid distances are virtually identical in the two structures, the decrease in the bridge angle must be a consequence of the greater freedom of movement along the Ti-Br-Yb bridge. As in the chloride

Figure 14. Ortep Diagram of $(Me_5C_5)_2Yb(\mu\text{-}Br)Ti(Me_5C_5)_2$.

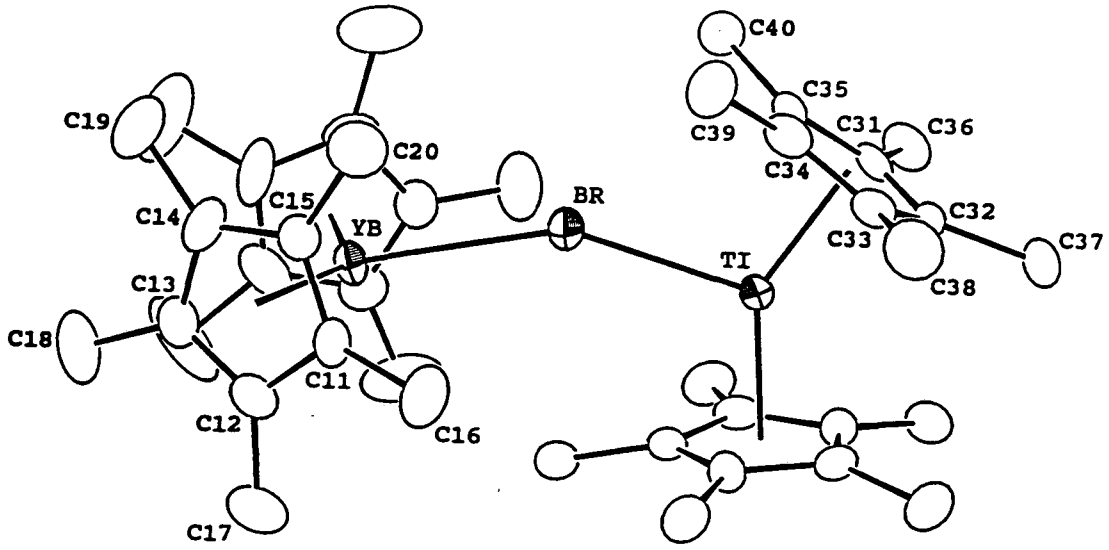

complex, the bridging interaction lies in the plane that bisects the two Me_5C_5 ligands on ytterbium. This provides further evidence that this is not a random structural feature. The crystallographic data for the bimetallic coordination complexes demonstrate that simple models can be used to predict structural features and trends in these unusual species.

The ability to obtain crystallographic data for more complex bridging ligands is especially important in that the ligand exchange processes between vanadium and ytterbium are likely to be less

straightforward than for the halides. The methyl-bridged complex, $(Me_5C_5)_2Yb(\mu\text{-}Me)Ti(Me_5C_5)_2$, is of particular interest not only in terms of the ligand exchange reaction, but also in comparison to the structures of other methyl-bridged species. As described earlier, the ytterbium methyl complexes, $(Me_5C_5)_2YbMe$ and $[(Me_5C_5)_2Yb]_2(\mu\text{-}Me)$, contain linear methyl bridges. Unfortunately, the inability to determine the locations of the hydrogen atoms on the bridging ligand prevents an examination of the subtle details of the hydrogen atom interactions.

Burns, however, was able to locate the hydrogen atoms in the beryllium complex, $(Me_5C_5)_2Yb(\mu\text{-}Me)Be(Me_5C_5)$.[20] The isotropically refined bridging methyl hydrogen atoms are arranged in a pseudo-tetrahedral geometry around the carbon atom. The coordinative interaction between the methyl group and the ytterbium center is consistent with the HOMO of the parent beryllium complex donating electron density to ytterbium through the carbon-hydrogen bonding portion of the molecular orbital (Figure 15). The simultaneous contribution from all three C-H bonds then produces a linear geometry

Figure 15

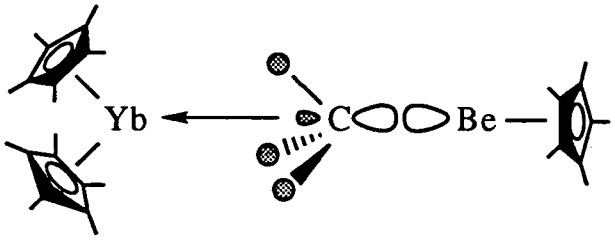

for the methyl bridge. The bridge angle is very nearly linear at 177.2(3)° despite the presence of only a single Me_5C_5 ligand on beryllium. Therefore, the reduced steric restrictions in the beryllium fragment should allow the preferred geometry to be established.

The X-ray crystal structural determination of the bimetallic complex, $(Me_5C_5)_2Yb(\mu\text{-}Me)Ti(Me_5C_5)_2$, also shows a near linear geometry for the methyl bridge. An ORTEP diagram is provided in Figure 16 and selected bond distances and angles are listed in Tables 8 and 9, respectively.

Figure 16. ORTEP Diagram of $(Me_5C_5)_2Yb(\mu\text{-}Me)Ti(Me_5C_5)_2$.

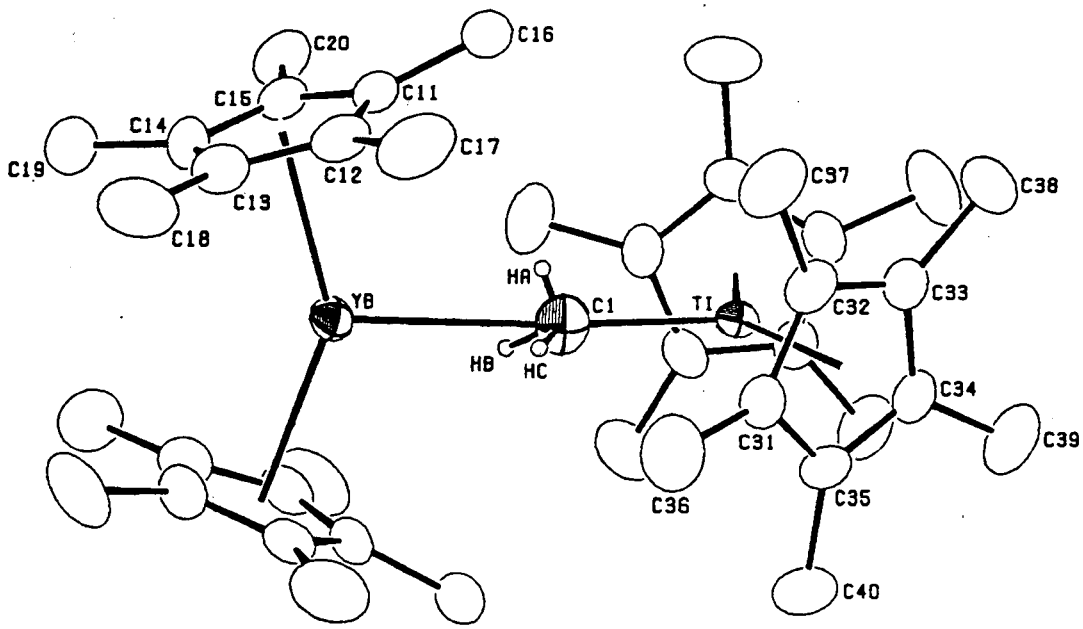

Table 8. Bond distances for $(Me_5C_5)_2Yb(\mu\text{-}Me)Ti(Me_5C_5)_2$ (Å)

Yb-C1	2.789 (7)	Ti-C1	2.196 (7)
Yb-HA	2.62 (7)	C1-HA	0.70 (7)
Yb-HB	2.39 (7)	C1-HB	0.98 (8)
Yb-HC	2.49 (7)	C1-HC	0.72 (7)
Yb-Cp1	2.396	Ti-Cp3	2.071
Yb-Cp2	2.397	Ti-Cp4	2.074
Yb-C11	2.708 (6)	Ti-C31	2.396 (6)
Yb-C12	2.671 (6)	Ti-C32	2.395 (6)
Yb-C13	2.665 (6)	Ti-C33	2.419 (6)
Yb-C14	2.680 (6)	Ti-C34	2.406 (6)
Yb-C15	2.682 (6)	Ti-C35	2.357 (6)
Yb-C21	2.702 (6)	Ti-C41	2.387 (6)
Yb-C22	2.671 (6)	Ti-C42	2.370 (6)
Yb-C23	2.677 (6)	Ti-C43	2.411 (6)
Yb-C24	2.675 (6)	Ti-C44	2.427 (6)
Yb-C25	2.673 (6)	Ti-C45	2.393 (6)

Cp1, Cp2, Cp3, and Cp4 are the ring centroids of atoms C11-C15, C21-C25, C31-C35, and C41-C45, respectively.

Table 9. Bond Angles for $(Me_5C_5)_2Yb(\mu\text{-}Me)Ti(Me_5C_5)_2$ (°)

Yb-C1-Ti	173.8 (4)	Yb-C1-HA	69 (6)
		Yb-C1-HB	56 (4)
Cp1-Yb-Cp2	143.6	Yb-C1-HC	58 (6)
Cp3-Ti-Cp4	143.3		
		Ti-C1-HA	108 (6)
Cp1-Yb-C1	108.6	Ti-C1-HB	120 (4)
Cp2-Yb-C1	107.7	Ti-C1-HC	128 (6)
Cp3-Ti-C1	108.4		
Cp4-Ti-C1	108.3	HA-C1-HB	93 (7)
		HB-C1-HC	100 (7)
		HA-C1-HC	102 (8)

The Yb-C1-Ti angle is 173.8(3)° which is slightly smaller than the angle observed in the beryllium complex. However, it is unclear what effect crystal packing forces have on these very weak bridges as the steric environments of the complexes change. The bond distances and angles in this complex are similar to those in the halide analogues. Despite the similar distances between the metal atoms and the bridging ligands for the methyl and chloride complexes, the chloride bridge bends to a much greater degree than the methyl bridge. This suggests that the tendency toward forming a bent bridge does not exist for the methyl species. This would be expected if the orbital arguments explaining the bent bridges in the halide analogues are valid.

The hydrogen atoms on the bridging methyl group have been located in the difference Fourier map and refined isotropically. Although the errors in the absolute positions of the hydrogen atoms are quite large, the atoms are clearly oriented in a pseudotetrahedral geometry around the carbon atom. This suggests that the bonding interaction is similar to that believed to exist in the beryllium methyl bridged complex. Examination of the molecular orbital diagram of the parent titanium methyl complex (Figure 17),[17,18] derived similarly to the chloride analogue, again shows that the HOMO is a metal-based orbital which should exert no influence on the nature of the bridging interaction. However, the SHOMO is a titanium-methyl bonding orbital which should have a direct effect on the coordination to the ytterbium center. Although the most effective interaction would be through donation of the electron density in the titanium-

Figure 17. Molecular Orbital Diagram for $(Me_5C_5)_2TiMe$.

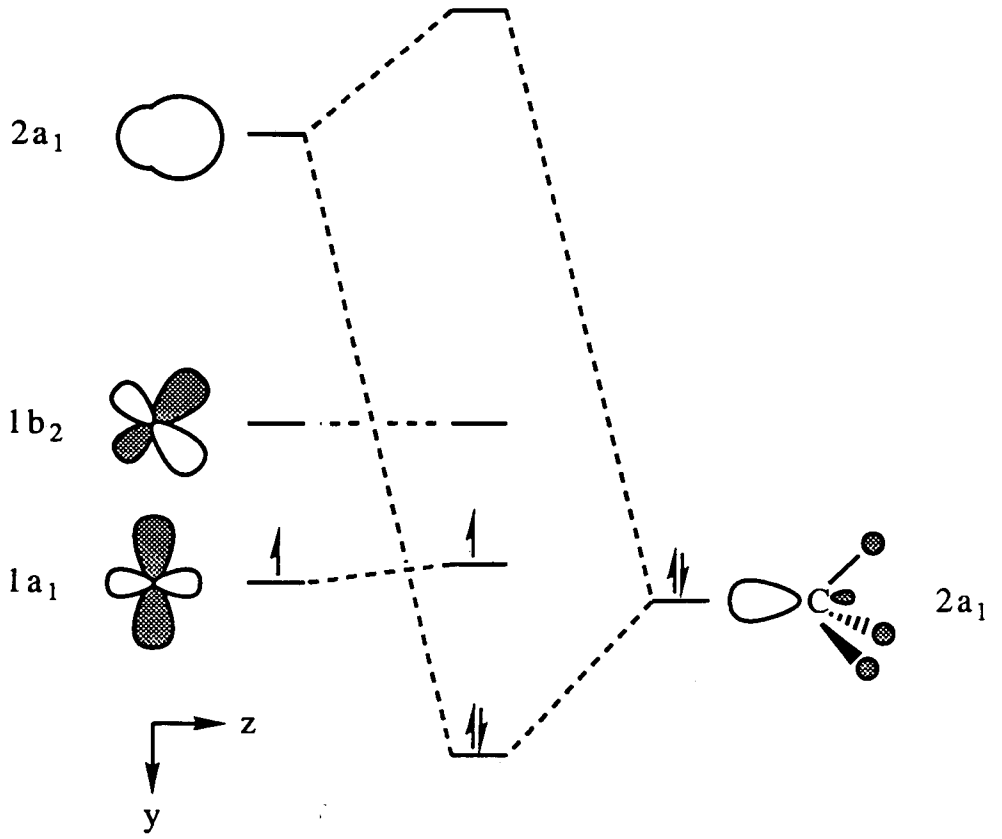

carbon bonding portion of the molecular orbital (Figure 18(a)), the steric restrictions imposed upon formation of the bimetallic complex prevent the ytterbium atom from accessing this part of the orbital. Therefore, the titanium fragment chooses to coordinate through the more diffuse carbon-hydrogen bonding portion of the molecular orbital (Figure 18(b)). This then results in the linear geometry for the methyl bridge without any tendency toward bending.

Unfortunately, the structure of the parent titanium methyl complex has never been examined so a comparison with the struc-

Figure 18

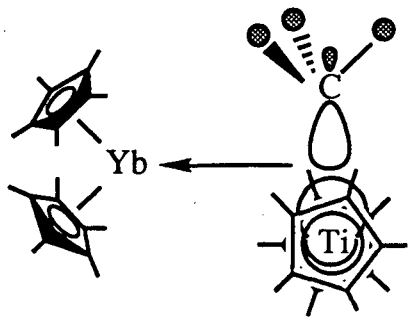

(a)

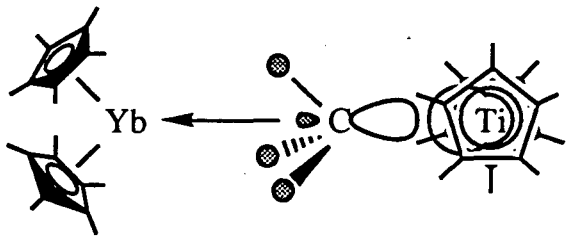

(b)

ture of the bimetallic complex cannot be made. The increase of 0.06 Å in the Ti-Cl bond length upon coordination to ytterbium indicates that the metal-ligand bonds can stretch due to the influence of ytterbium. Recently, Teuben has determined the X-ray crystal structure for the neopentyl complex, $(Me_5C_5)_2TiCH_2CMe_3$.[7] The Ti-C bond distance of 2.231(5) Å is only slightly longer than the Ti-C distance of 2.196(7) Å in the bimetallic methyl complex. The bulkiness of the neopentyl ligand might be expected to induce a significantly longer Ti-C bond length than in the simple methyl species. However, there

is not enough crystallographic data available to verify this. The beryllium bimetallic complex also could not be compared to its parent complex due to the unavailability of crystallographic data. Clearly, many more structural studies will have to be undertaken before a complete evaluation of the effects of coordination to ytterbium on metal-ligand bond lengths can be accomplished.

Models for Ligand Exchange Processes

The structurally characterized bimetallic species provide detailed views of what are likely to be the transition states in the ligand transfer reactions involving the organovanadium complexes and $(Me_5C_5)_2Yb$. The observed effects of the $(Me_5C_5)_2Yb$ fragment on the bridging ligands in the bimetallic complexes allow the mechanism for the ligand exchange process to be postulated. For the halide species, the vanadium fragment could approach the open coordination site on ytterbium (Scheme 2). It would then bind momentarily with the bridge slightly bent as in the titanium-ytterbium bimetallic complexes. As the halide maximizes its interaction with ytterbium, the vanadium-halide bond is lengthened and weakened. An electron is then transferred to the halide from ytterbium forming a direct bond which then pushes an electron back onto the vanadium center. As the vanadium-halide bond breaks, the vanadium fragment reverts to the sandwich geometry and is released since the weak coordinative interaction of the halide cannot stabilize a bent configuration for decamethylvanadocene. This then leaves the isolated trivalent ytterbium halide product.

Scheme 2

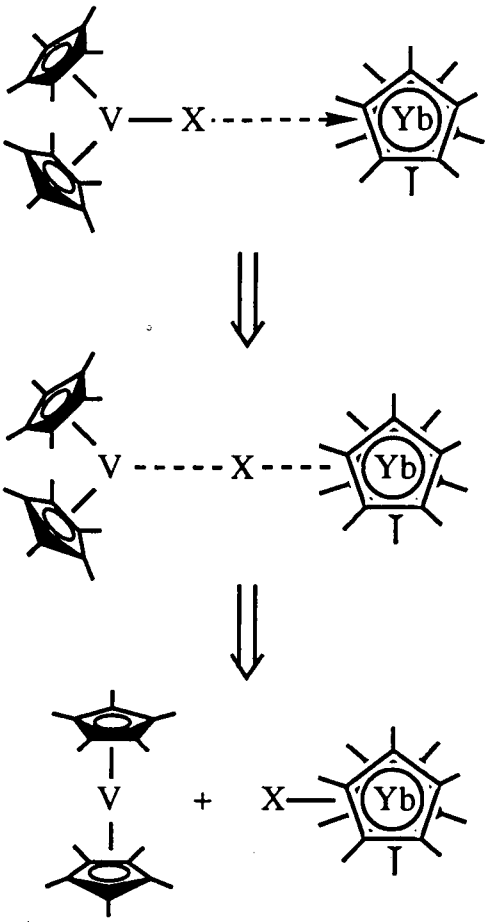

This simple halide transfer mechanism may also be applied to more complex ligands. For the borohydride exchange, if the ligand is bound to vanadium in a bidentate fashion (Figure 19), its geometry is not expected to change significantly upon transfer to ytterbium. The bridging and terminal hydrogens would simply switch identities and the borohydride ligand would be bidentate to ytterbium. This straightforward transfer is consistent with the spectroscopic data observed for the ytterbium borohydride product.

Figure 19

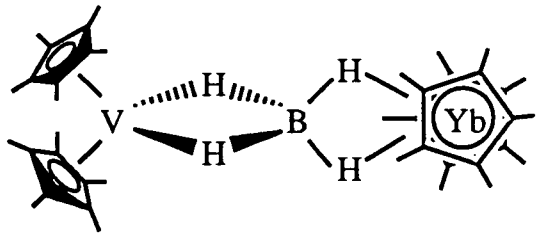

For the exchange of the methyl group from vanadium to ytterbium, the transfer process must be somewhat more complicated owing to the fact that an inversion about the methyl carbon atom must take place as the electron and ligand move from one metal tothe other. As observed in the titanium-ytterbium bimetallic complex, the geometry about the carbon atom of the methyl group remains tetrahedral as the ligand coordinates to ytterbium. Therefore, the initial coordination of the vanadium analogue probably occurs in the same manner (Scheme 3). However, as the methyl group is drawn toward ytterbium and the vanadium-methyl bond is stretched, the geometry must change to trigonal bipyramidal at some point along the reaction coordinate. This would then facilitate the transfer of an electron from ytterbium through the bridging group to vanadium. The vanadium-methyl bond would then break releasing decamethylvanadocene and producing the ytterbium methyl complex.

Scheme 3

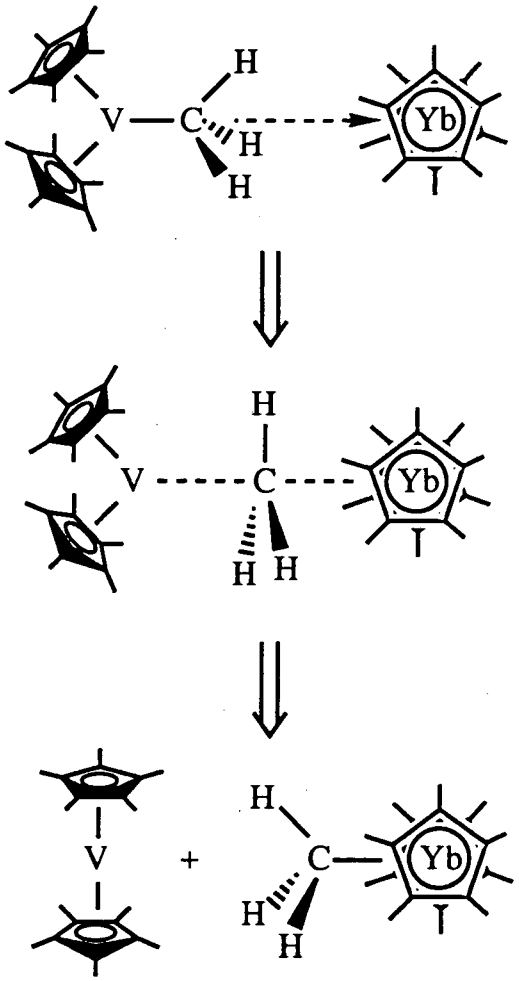

Despite the similarities between the organovanadium and organotitanium complexes, their reactions with $(Me_5C_5)_2Yb$ produce very different results. The vanadium complexes allow the reducing capabilities of $(Me_5C_5)_2Yb$ to be exploited so that a variety of novel ytterbium species can be isolated through electron-transfer processes. In contrast, the analogous titanium complexes are stable enough to resist being reduced by $(Me_5C_5)_2Yb$. Instead, they form coordination complexes which provide visual models for the

mechanism of ligand exchange between vanadium and ytterbium. Both studies provide important information on the interactions between ytterbium and organotransition metal species. In addition, the products obtained from these reactions often possess unusual characteristics such as trapped-valent magnetic behavior or linear bridge bonds. These complexes demonstrate the wide variety of chemistry which can be observed through the study of ytterbium.

References

1. Shannon, R. D., *Acta. Cryst.*, **1976**, *A32*, 751.

2. (a) Bercaw, J. E.; Marvich, R. H.; Bell, L. G.; Brintzinger, H. H., *J. Am. Chem. Soc.*, **1972**, *94*, 1219. (b) Dessy, R. E.; King, R. B.; Waldrop, M., *J. Am. Chem. Soc.*, **1966**, *88*, 5112. (c) Doisneau, R. G.; Marchon, J. C., *J. Electroanal. Chem.*, **1971**, *30*, 487. (d) Gubin, S. P.; Smirnova, S. A., *J. Organomet. Chem.*, **1969**, *229*, 241.

3. Pattiasina, J. W.; Heeres, H. J.; van Bolhuis, F.; Meetsma, A.; Teuben, J. H.; Spek, A. L., *Organometallics*, **1987**, *6*, 1004.

4. Bercaw, J. E., *J. Am. Chem. Soc.*, **1974**, *96*, 5087.

5. Lukens, W. W., Jr., personal communication.

6. Nakamoto, K., "Infrared and Raman Spectra of Inorganic and Coordination Compounds," 4th Ed., Wiley-Interscience: New York, **1986**.

7. Luinstra, G. A.; ten Cate, L. C.; Heeres, H. J.; Pattiasina, J. W.; Meetsma, A.; Teuben, J. H., *Organometallics*, **1991**, *10*, 3227.

8. (a) Pattiasina, J. W.; Hissink, C. E.; de Boer, J. L.; Meetsma, A.; Teuben, J. H.; Spek, A. L., *J. Am. Chem. Soc.*, **1985**, *107*, 7758. (b) de Boer, E. J. M.; de With, J., *J. Organomet. Chem.*, **1987**, *320*, 289. (c) Dias, A. R.; Salema, S. S.; Martinho-Simoes, J. A.; Pattiasina, J. W.; Teuben, J. H., *J. Organomet. Chem.*, **1988**, *346*, C4. (d) Bochmann, M.; Jaggar, A. J.; Wilson, L. M.; Hursthouse, M. B.; Motevalli, M., *Polyhedron*, **1989**, *8*, 1838.

9. Curtis, C. J.; Smart, J. C.; Robbins, J. L., *Organometallics*, **1985**, *4*, 1283.

10. Thompson, M. E.; Baxter, S. M.; Bulls, A. R.; Burger, B. J.; Nolan, M. C.; Santarsiero, B. D.; Schaefer, W. P.; Bercaw, J. E., *J. Am. Chem. Soc.*, **1987**, *109*, 203.

11. Drago, R. S., "Physical Methods in Chemistry," W. B. Saunders: Philadelphia, **1977**.

12. Casey, A. T.; Mitra, S., "Theory and Applications of Molecular Paramagnetism," Boudreaux, E. A.; Mulay, L. N., eds., Wiley-Interscience: New York, **1976**.

13. O'Hare, D.; Manriquez, J.; Miller, J. S., *J. Chem. Soc., Chem. Commun.*, **1988**, 491.

14. Berg, D. J., Ph.D. Thesis, University of California, Berkeley, **1987**.

15. Jungst, R.; Sekutowski, D.; Davis, J.; Luly, M.; Stucky, G., *Inorg. Chem.*, **1977**, *16*, 1645.

16. Burns, C. J.; Andersen, R. A., *J. Chem. Soc., Chem. Commun.*, **1989**, 136.

17. Albright, T. A.; Burdett, J. K.; Whangbo, M-H, "Orbital Interactions in Chemistry," Wiley-Interscience: New York, **1985**.

18. Lauher, J. W.; Hoffman, R., *J. Am. Chem. Soc.*, **1976**, *98*, 1729.

19. Green, J. C.; Payne, M. P.; Teuben, J. H., *Organometallics*, **1983**, *2*, 203.

20. Burns, C. J.; Andersen, R. A., *J. Am. Chem. Soc.*, **1987**, *109*, 5853.

Experimental Details

General

All reactions and product manipulations were carried out under an atmosphere of dry nitrogen or argon using standard Schlenk and dry box techniques. Solvents and solutions were transferred between reaction vessels *via* stainless steel tubing. Filtrations were performed by attaching filters to one inch pieces of small-bore glass tubing secured to the ends of stainless steel tubing with epoxy. Pentane, hexane, toluene, diethyl ether, and tetrahydrofuran were distilled from sodium benzophenone ketyl under nitrogen immediately prior to use. Dichloromethane was distilled from calcium hydride under nitrogen immediately prior to use. All other chemicals were of reagent grade and purified according to standard procedures as necessary.[1] Deuterated solvents for NMR measurements were distilled from potassium under nitrogen and stored over sodium. $(Me_5C_5)_2YbOEt_2$[2] and $(Me_5C_5)_2Yb$[3] were prepared according to reported procedures.

Infrared spectra were recorded on a Nicolet 5DX FTIR spectrometer or a Mattson Sirius 100 FTIR spectrometer as Nujol mulls between CsI or KBr plates. ^1H nuclear magnetic resonance spectra were measured on a JEOL FX90Q FT NMR spectrometer operating at 89.6 MHz or a departmentally built FT NMR spectrometer using Nicolet electronics and operating at 201.9 MHz at the Berkeley Department of Chemistry NMR facility. Chemical shifts were referenced to tetramethylsilane ($\delta = 0$) with positive values at higher

frequency. Electron paramagnetic resonance spectra were recorded on an IBM ER-2090D-SRC spectrometer. Melting points were measured on a Thomas-Hoover melting point apparatus in sealed capillaries and are uncorrected.

Magnetic susceptibility measurements (SQUID) were obtained from either a S.H.E. Corporation Model 905 or a Quantum Designs MPMS HP-150 superconducting magnetometer. Samples were prepared and handled according to previously reported procedures.[4] Susceptibility data were corrected for sample and container diamagnetism. Regions in the plot of $1/\chi_M$ vs. T that demonstrated Curie-Weiss behavior were fit to the Curie-Weiss law, $1/\chi_M = (T-\Theta)/C$, where Θ is the Weiss constant and C is the Curie constant, using a linear-least squares program written by Dr. E. Gamp. Electron impact mass spectra were recorded by the mass spectrometry laboratory at the University of California, Berkeley. When molecular ions were observed, the isotopic cluster was reported as follows: ion amu (observed intensity, calculated intensity). Elemental analyses were performed by the analytical laboratories at the University of California, Berkeley.

Selected Starting Materials

Bis(2,4-pentanedionato)copper(II)

This complex was synthesized according to a published procedure.[5a] To a 100 mL solution of aqueous copper(II)nitrate trihydrate (10.0 g, 41.4 mmol) was added 15 mL of concentrated aqueous ammonia. After stirring for several minutes, a dark, blue-purple solution was obtained. 2,4-pentanedione (11.0 mL, 107 mmol) was added dropwise to this solution. A light blue precipitate immediately appeared and the mixture was stirred at room temperature for an additional 10 minutes. The solid was collected in a Buchner funnel and washed three times with 50 mL portions of distilled water. The residue was washed with chloroform (20 mL), then dissolved in chloroform (150 mL) forming a deep blue solution. The solution was filtered and the filtrate was cooled to -30 °C affording light blue needles. Additional crops of crystals were obtained by concentrating the mother liquor. The yield was quantitative except for manipulative losses. The IR spectrum was identical to that of the previously reported complex.[5b,c] The product was dried under vacuum at 100 °C prior to use.

Dimethylaluminumethoxide

A solution of trimethylaluminum (40 mL, 0.42 mol) in hexane (200 mL) was cooled to -40 °C. To this was added a solution of ethanol (24 mL, 0.41 mol) in hexane (40 mL) dropwise from an addition funnel over 1.5 hours. The ethanol was distilled from mag-

nesium ethoxide immediately prior to use. After complete addition, the solution was concentrated to approximately 80 mL at 0 °C under reduced pressure. The remaining solution was transferred to a microdistillation apparatus and the remaining hexane was removed under reduced pressure. The product was vacuum distilled (10^{-2} mm Hg) with a bath temperature of 50 °C. Approximately 25 mL of a colorless, viscous product was obtained. The ^1H NMR spectrum was consistent with that for the previously observed compound.[6] ^1H NMR (C_6D_6, 24 °C): δ -0.55 (s, 6 H), 0.94 (t, 3 H, J_{HH} = 7 Hz), 3.40 (q, 2 H, J_{HH} = 7 Hz).

Methylcopper

This complex was synthesized according to a previously reported procedure.[7] The reaction must be performed in an elongated Schlenk tube to avoid splashing the unstable methylcopper on the walls of the reaction vessel. A solution of dimethylaluminumethoxide (2.5 mL, 15.3 mmol) in diethyl ether (15 mL) was added dropwise from an addition funnel to a suspension of bis(2,4-pentanedionato)copper(II) (1.00 g, 3.82 mmol) in diethyl ether (50 mL) at -40 °C. The stirring mixture was allowed to warm to -10 °C whereupon the color became lime green. The reaction vessel must be periodically vented to the nitrogen manifold to relieve the buildup of pressure. The mixture was maintained between -10 °C and -5 °C for an additional 4 hours. During this time, the suspension gradually became bright yellow. The yellow solid was allowed to settle and the subsequent purification was determined by one of two conditions.

(a) Diethyl ether must be eliminated from the subsequent reaction:

The mixture was cooled to -40 °C and the product was filtered. Any product trapped on the paper filter was carefully scraped back into the reaction vessel under a flow of nitrogen without decomposition. The residue was washed with diethyl ether, cooled to -40 °C, and three times with 40 mL portions of hexane, cooled to -40 °C. The residue was exposed to vacuum for 0.5 hour at -30 °C. The product became dark yellow-brown, but it was still reactive. The product was used as a suspension in the appropriate solvent at -40 °C. Stirring the suspension returned the product to its original fluffy, yellow appearance.

(b) Coordinating solvents do not affect the subsequent reaction:

The mixture was cooled to -40 °C. and the product was filtered. Any product trapped on the paper filter was carefully scraped back into the reaction vessel under a flow of nitrogen without decomposition. The residue was washed twice with 40 mL portions of diethyl ether at -40 °C. The product was used as a suspension in the appropriate solvent at -40 °C.

In the reactions with methylcopper, the suspension was maintained below -20 °C as the reacting species was added since the methylcopper will spontaneously decompose above 0 °C to form metallic copper.

Chapter 1

$(Me_5C_5)_2YbMe$

Methylcopper[7] (0.30 g, 3.8 mmol) was synthesized as described above. The reaction must be performed in an elongated Schlenk tube to avoid splashing the unstable methylcopper on the walls. The bright yellow product was filtered and washed once with Et_2O (60 mL) and three times with 60 mL portions of pentane at -40 °C. The solid was exposed to vacuum for 0.5 h at -30 °C. Pentane (40 mL), cooled to -30 °C, was added to the MeCu to form a suspension. To the suspension was added a solution of $(Me_5C_5)_2Yb$ (1.00 g, 2.25 mmol) in pentane (40 mL). The mixture was then allowed to warm slowly to room temperature over several hours. During this time, the mixture became deep red and a copper mirror formed on the walls of the reaction vessel. The mixture was stirred for an additional 8 hours at room temperature. In order to obtain the product cleanly, the finely divided Cu metal formed in the reaction must be allowed to settle thoroughly. The solution was filtered through a glass fiber filter (Whatman GF/D), and the filtrate was cooled to -40 °C affording red blocky crystals. Concentration of the mother liquor provided additional crops of crystals for a total yield of 0.91 g (2.0 mmol, 88%). Mp 219-221 °C (dec.). IR: 2725 (m), 2048 (vw), 1489 (w), 1260 (m), 1166 (w), 1093 (s), 1061 (m), 1023 (s), 949 (vw), 885 (s), 824 (w), 803 (m), 721 (w), 674 (m), 625 (w), 613 (w), 592 (m), 539 (w), 516 (w), 422 (w), 393 (s), 323 (s), 297 (s) cm^{-1}. ^1H NMR (C_7D_8, 22 °C): δ 16.7 ($\upsilon_{1/2}$ = 473 Hz). The protons on the ytterbium-bound methyl

group were not observed. The spectrum of a hydrolyzed sample in C_6D_6 showed resonances for Me_5C_5D only. EIMS: 455 (23, 9); 456 (63, 42); 457 (86, 70); 458 (94, 60); 459 (100, 100); 460 (40, 22); 461 (38, 38); 462 (11, 8). There was no evidence for the existence of the dimeric form in the gas phase. Magnetic Susceptibility (5 kG): Per monomer: 6-30 K, μ_{eff} = 3.65 μ_B, Θ = -0.30 K. 50-280 K, μ_{eff} = 3.91 μ_B, Θ = -9.31 K. Per dimer: 6-30 K, μ_{eff} = 5.16 μ_B, Θ = -0.30 K. 50-280 K, μ_{eff} = 5.53 μ_B, Θ = -9.31 K. Anal. Calcd for $C_{21}H_{33}Yb$: C, 55.0; H, 7.25. Found: C, 55.0; H, 7.28.

$(Me_5C_5)_2YbMe(Et_2O)$

A solution of $(Me_5C_5)_2Yb(Et_2O)$ (0.50 g, 0.97 mmol) in diethyl ether (15 mL) was added to a suspension of freshly prepared methylcopper (0.14 g, 1.8 mmol) in diethyl ether (50 mL) at -40 °C. Methylcopper was prepared as described above. The reaction must be performed in an elongated Schlenk tube to avoid splashing the unstable methylcopper on the walls. The stirring mixture was allowed to warm to room temperature over several hours and then stirred for an additional 12 hours. The red solution was filtered from the metallic Cu as in the base-free preparation, and the filtrate was concentrated to approximately 20 mL. Cooling to -20 °C afforded red blocky crystals. Several crops were obtained from the mother liquor for a combined yield of 0.47 g (0.88 mmol, 91%). Mp 196-200 °C. IR: 2725 (m), 1647 (w), 1489 (w), 1316 (w), 1288 (w), 1256 (vw), 1187 (m), 1146 (m), 1108 (m), 1093 (s), 1045 (s), 1023 (m), 1001 (s), 950 (w), 894 (s), 828 (w), 799 (m), 774 (s), 724 (w), 673 (m), 626 (w), 617 (w), 595 (m), 519 (m), 478 (w), 393 (s), 324 (m),

295 (s) cm^{-1}. ^1H NMR (C_6D_6, 23 °C): δ 5.95 (30 H, $\upsilon_{1/2}$ = 387 Hz), 38.90 (6 H, $\upsilon_{1/2}$ = 308 Hz). The methylene protons of diethyl ether were not observed. The ^1H NMR spectrum of a hydrolyzed sample verified the 2:1 stoichiometry of Me_5C_5H to Et_2O in the product. Anal. Calcd for $C_{25}H_{43}OYb$: C, 56.4; H, 8.14. Found: C, 56.0; H, 8.02.

$(Me_5C_5)_2YbMe(THF)$

A sample of $(Me_5C_5)_2YbMe$ (0.15 g, 0.33 mmol) was dissolved in tetrahydrofuran (10 mL) forming a red-orange solution. The tetrahydrofuran was then removed under reduced pressure and the resulting residue was extracted with hexane (15 mL). The solution was filtered, concentrated to approximately 10 mL, and cooled to -80 °C. A mass of red-orange needles was isolated (0.10 g, 0.19 mmol, 58%). The ^1H NMR and IR spectra were identical to those of the previously reported complex.[3] Mp 162-165 °C (Lit. 162-163 °C).

$(Me_5C_5)_2Yb(\mu\text{-}Me)_2AlMe_2$

Trimethylaluminum (0.19 mL of a 1.15 M hexane solution, 0.22 mmol) was added by syringe to a solution of $(Me_5C_5)_2YbMe$ (0.10 g, 0.22 mmol) in hexane (10 mL). Upon mixing, the solution immediately changed color from red to purple. After stirring at room temperature for 0.5 hour, a purple precipitate was observed in the mixture. The volatile materials were completely removed under reduced pressure and the residue was extracted with toluene (10 mL). The purple solution was filtered and the filtrate was concentrated to approximately 3 mL. The solution was warmed to redissolve the precipitates. The solution was cooled to -40 °C

affording purple crystals that lost solvent upon exposure to vacuum (0.10 g, 0.19 mmol, 84%). The IR spectrum was identical to that of the previously reported compound.[4] Mp 214-218 °C (Lit. 220-222 °C).

Polymerization of ethylene by $(Me_5C_5)_2YbMe$

A solution of $(Me_5C_5)_2YbMe$ (0.05 g, 0.11 mmol) in hexane (20 mL) was placed in a Fischer-Porter thick-walled pressure bottle. The bottle was pressurized with ethylene (7 atm) and the mixture was stirred at room temperature. A white solid quickly formed and the pressure returned to approximately 1 atm in 5 minutes. The mixture had a slightly pinkish tint due to the presence of the ytterbium complex. The mixture was then hydrolyzed with dilute aqueous hydrochloric acid and collected on a filter frit. The white solid was then washed with additional dilute hydrochloric acid, distilled water, and acetone and thoroughly air dried. The yield of polymer was 0.72 g. The polycrystalline polymer melted at 131 °C.

$[(Me_5C_5)_2Yb]_2(\mu\text{-}H)$

A solution of $(Me_5C_5)_2YbMe$ (0.12 g, 0.26 mmol) in hexane (20 mL) was placed in a Fischer-Porter thick-walled pressure bottle. The atmosphere was flushed three times with hydrogen before a static pressure of hydrogen (10 atm) was applied to the system. Upon stirring, the solution quickly changed color from red to purple. The solution was stirred at room temperature for 3 hours during which time a purple solid appeared. The pressure was then released and the mixture was transferred to a Schlenk tube. The solid was

filtered and residual solvent was removed under reduced pressure leaving a purple powder (0.07 g, 0.08 mmol, 60%). The IR spectrum was identical to that of the previously observed compound obtained from $(Me_5C_5)_2YbCH(SiMe_3)_2$ and hydrogen.[3]

$[(Me_5C_5)_2Yb]_2(\mu\text{-}D)$

A solution of $(Me_5C_5)_2YbMe$ (0.08 g, 0.2 mmol) in hexane (15 mL) was placed in a Fischer-Porter thick-walled pressure bottle. The atmosphere was flushed three times with deuterium before a static pressure of deuterium (13 atm) was applied to the system. Upon stirring, the solution quickly changed color from red to purple and a purple precipitate appeared after a few minutes. After stirring at room temperature for 5 hours, the mixture was transferred to a Schlenk tube and filtered. The yield of the purple powder was 0.05 g (0.06 mmol, 64%). The IR spectrum was identical to that of the previously observed compound obtained from $(Me_5C_5)_2YbCH(SiMe_3)_2$ and deuterium.[3]

$[(Me_5C_5)_2Yb]_2(\mu\text{-}Me)$

(a) From $(Me_5C_5)_2YbMe$

A solution of $(Me_5C_5)_2Yb$ (0.18 g, 0.41 mmol) in pentane (10 mL) was added to a solution of $(Me_5C_5)_2YbMe$ (0.19 g, 0.41 mmol) in pentane (5 mL). Upon addition, a brick red precipitate immediately formed. After stirring at room temperature for 1 hour, the product was filtered and residual solvent was removed from the residue under reduced pressure. Recrystallization of the residue

from toluene (5 mL) afforded dark red crystals (0.33 g, 0.37 mmol, 90%), whose physical properties were identical to those obtained in the synthesis described below.

(b) From Methylcopper

Methylcopper (0.063 g, 0.80 mmol) was synthesized as described above. The reaction must be performed in an elongated Schlenk tube to avoid splashing the unstable methylcopper on the walls. The bright yellow product was filtered and washed once with Et_2O (60 mL) and three times with 60 mL portions of pentane at -40 °C. The solid was exposed to vacuum for 40 min. at -30 °C. Pentane (30 mL), cooled to -30 °C, was added to the methylcopper to form a suspension. To the suspension was added a solution of $(Me_5C_5)_2Yb$ (0.57 g, 1.3 mmol) in pentane (30 mL). The mixture was then allowed to warm slowly to room temperature over several hours. During this time, the mixture became deep red and a copper mirror formed on the walls of the reaction vessel. The mixture was stirred for an additional 8 hours at room temperature. The solid was filtered and residual solvent was removed from the residue under reduced pressure. The residue was extracted with toluene (40 mL), and the product was filtered twice using glass fiber filters (Whatman GF/D) to separate it from the finely divided metallic copper. The filtrate was then concentrated to approximately 20 mL and cooled to -40 °C producing brick red crystals. Concentration of the mother liquor provided additional crops of crystals for a total yield of 0.32 g (0.35 mmol, 55%). Mp 223-225 °C (dec). IR: 2725 (m), 2038 (w), 1653 (w), 1489 (m), 1259 (w), 1162 (w), 1099 (vw), 1061 (w), 1023

(m), 957 (s), 803 (m), 724 (w), 696 (w), 661 (s), 623 (m), 588 (m), 554 (w), 431 (m), 380 (m), 358 (m), 327 (s), 302 (m), 276 (s) cm^{-1}. ^1H NMR (C_7D_8, 30 °C): δ = 5.46 ($\upsilon_{1/2}$ = 150 Hz). The protons on the ytterbium-bound methyl group were not observed. The highest isotopic cluster in the mass spectrum was centered at 768 amu (M^+-Me_5C_5). Magnetic Susceptibility (5 kG): 6-30 K, μ_{eff} = 4.56 μ_B, Θ = -0.45 K. 50-280 K, μ_{eff} = 4.75 μ_B, Θ = -5.85 K. Anal. Calcd for $C_{41}H_{63}Yb_2$: C, 54.6; H, 7.04. Found: C, 54.7; H, 7.21.

$(Me_5C_5)_2YbNH_2(NH_3)$

(a) From $(Me_5C_5)_2YbMe$

A solution of $(Me_5C_5)_2YbMe$ (0.27 g, 0.59 mmol) in hexane (15 mL) was frozen in a liquid nitrogen bath. An excess of anhydrous ammonia was then vacuum transferred into the reaction vessel. The mixture was allowed to warm to room temperature while the system was vented to the nitrogen manifold to release excess ammonia. While warming, an orange solid formed which then redissolved as the mixture reached room temperature. The deep orange solution was stirred for a additional 0.5 hour before the hexane was completely removed under reduced pressure. The residue was extracted with pentane (25 mL) and filtered. Slow cooling of the filtrate to -80 °C afforded yellow-orange needles (0.20 g, 0.42 mmol, 71%), whose physical properties were identical to those obtained in the synthesis described below.

(b) From $(Me_5C_5)_2YbCH(SiMe_3)_2$

A solution of $(Me_5C_5)_2YbCH(SiMe_3)_2$[3] (0.41 g, 0.75 mmol) in hexane (10 mL) was frozen in a liquid nitrogen bath. An excess of ammonia was condensed onto the frozen solid. The mixture was allowed to warm to room temperature while vented to the nitrogen manifold to release excess ammonia. The mixture remained red until approximately 0 °C whereupon it quickly turned bright orange and an orange precipitate appeared. The orange solid was stirred at room temperature for 1 hour before the volatile materials were completely removed under reduced pressure. The residue was extracted with pentane (40 mL) and filtered. The filtrate was concentrated to approximately 15 mL with slight warming to redissolve the solid. Slow cooling to room temperature and then further cooling to -80 °C afforded a mass of yellow-orange needles (0.25 g, 0.52 mmol, 70%). The compound did not melt to 330 °C. IR: 3361 (m), 3280 (m), 2725 (m), 1590 (m), 1522 (s), 1493 (w), 1261 (w), 1183 (s), 1097 (w), 1061 (w), 1021 (m), 951 (w), 819 (vw), 803 (m), 722 (w), 644 (m), 628 (vw), 620 (vw), 593 (w), 552 (vw), 498 (s), 423 (s), 385 (vw), 301 (s) cm^{-1}. ^1H NMR (C_6D_6, 25 °C): δ 2.76 ($\upsilon_{1/2}$ = 30 Hz). Neither the protons of the amide nor the ammonia ligands were observed in the ^1H NMR spectrum. The highest isotopic cluster in the mass spectrum was centered at 460 amu (M^+-NH_3). Anal. Calcd for $C_{20}H_{35}N_2Yb$: C, 50.4; H, 7.40; N, 5.88. Found: C, 50.1; H, 7.36; N, 5.73.

$(Me_5C_5)_2YbND_2(ND_3)$

A solution of $(Me_5C_5)_2YbMe$ (0.21 g, 0.46 mmol) in hexane (10 mL) was frozen in a liquid nitrogen bath. An excess of anhydrous ammonia-d_3 was then vacuum transferred into the reaction vessel. The mixture was allowed to warm to room temperature while the system was vented to the nitrogen manifold to release excess ammonia-d_3. While warming, an orange solid formed which then redissolved as the mixture reached room temperature. The deep orange solution was stirred for a additional 3 hours before the volatile materials were removed under reduced pressure. The residue was extracted with pentane (20 mL) and filtered. The filtrate was concentrated to approximately 5 mL with warming to redissolve the solid and slowly cooled to -80 °C to produce yellow-orange needles (0.16 g, 0.33 mmol, 70%). The compound did not melt to 330 °C. IR: 2725 (m), 2504 (m), 2449 (w), 2408 (w), 2380 (m), 2311 (vw), 2044 (vw), 1653 (w), 1524 (w), 1491 (w), 1342 (m), 1262 (w), 1238 (m), 1166 (m), 1130 (s), 1097 (m), 1061 (w), 1023 (m), 992 (s), 915 (s), 802 (m), 723 (m), 645 (m), 629 (w), 618 (w), 593 (w), 555 (w), 491 (m), 469 (s), 387 (s, br), 354 (m), 301 (s, br) cm^{-1}. ^1H NMR (C_6D_6, 25 °C): δ 2.78 ($\upsilon_{1/2}$ = 30 Hz). EIMS: 478 (37, 9); 479 (63, 42); 480 (92, 70); 481 (90, 60); 482 (100, 100); 483 (82, 22); 484 (75, 38); 485 (50, 8).

$(Me_5C_5)_2Yb(\mu\text{-}NH_2)_2AlMe_2$

To a solution of $(Me_5C_5)_2YbNH_2(NH_3)$ (0.12 g, 0.25 mmol) in hexane (10 mL) was added dropwise <u>via</u> syringe 0.22 mL (0.25 mmol) of a 1.15 M hexane solution of trimethylaluminum. Upon

mixing, the color immediately changed from bright orange to deep red and gas evolution was observed. After stirring at room temperature for 0.5 hour, the solution was filtered and the filtrate was cooled to -40 °C to produce deep red crystals (0.10 g, 0.19 mmol, 75%). Mp 195-197 °C (dec). IR: 3385 (m), 3331 (m), 2725 (m), 1790 (vw), 1645 (vw), 1586 (m), 1489 (m), 1422 (w), 1262 (vw), 1188 (s), 1164 (vw), 1090 (vw), 1059 (vw), 1023 (m), 949 (vw), 867 (vw), 800 (vw), 773 (s), 738 (s), 652 (m), 624 (m), 617 (s), 593 (m), 522 (m), 507 (m), 413 (m), 382 (m), 347 (m), 304 (s) cm^{-1}. ^1H NMR (C_6D_6, 24 °C): δ 4.86 (30 H), -22.5 (6 H). The protons on the amide ligands were not observed. EIMS: 529 (9, 8); 530 (41, 41); 531 (69, 70); 532 (61, 61); 533 (100, 100); 534 (24, 24); 535 (36, 38); 536 (9, 9). Anal. Calcd for $C_{22}H_{40}N_2AlYb$: C, 49.6; H, 7.57; N, 5.26. Found: C, 48.9; H, 7.63; N, 4.40.

Polymerization of ethylene by $(Me_5C_5)_2YbCH(SiMe_3)_2$

A solution of $(Me_5C_5)_2YbCH(SiMe_3)_2$[3] (0.22 g, 0.36 mmol) in hexane (15 mL) was added to a Fischer-Porter thick-walled pressure bottle. The system was pressurized with ethylene (8 atm) and the solution was stirred at room temperature. Polymerization did not start immediately but required a period of about 1 hour before the polymer formed and the pressure dropped to approximately 1 atm. The purple mixture was hydrolyzed with dilute aqueous hydrochloric acid and collected on a filter frit. The white solid was washed with distilled water and acetone and dried thoroughly in air. The white polymer was not polycrystalline but instead formed one large continuous mass. The yield of polymer was 0.31 g.

$(Me_5C_5)_2YbNPh_2$

Hexane (15 mL) was added to a mixture of $(Me_5C_5)_2Yb$-$CH(SiMe_3)_2$[3] (0.50 g, 0.83 mmol) and diphenylamine (0.14 g, 0.83 mmol). The resulting purple solution was stirred at room temperature for 3 days before the volatile materials were removed under reduced pressure. The residue was extracted with pentane (20 mL) and filtered. The filtrate was concentrated to approximately 5 mL and cooled to -68 °C producing a mass of dark brown needles (0.22 g, 0.36 mmol, 43%). Mp 214-219 °C. IR: 3065 (w), 2725 (w), 2554 (vw), 2526 (vw), 1940 (vw), 1921 (vw), 1886 (vw), 1634 (vw), 1581 (s), 1559 (m), 1483 (s), 1332 (s), 1313 (s), 1263 (w), 1244 (vw), 1212 (m), 1171 (m), 1152 (w), 1099 (sh), 1083 (w), 1026 (m), 992 (w), 985 (m), 976 (vw), 888 (m), 862 (vw), 844 (m), 806 (w), 749 (s), 724 (vw), 702 (m), 692 (s), 661 (w), 588 (w), 522 (m), 500 (m), 411 (vw), 396 (w), 374 (w), 317 (s) cm^{-1}. ^1H NMR (C_6D_6, 24 °C): δ 8.55 (30 H, $\upsilon_{1/2}$ = 700 Hz), 19.02 (2 H, $\upsilon_{1/2}$ = 45 Hz), 20.63 (4 H, $\upsilon_{1/2}$ = 110 Hz). The ortho protons on the phenyl rings were not observed. EIMS: 609 (38, 40); 610 (70, 70); 611 (57, 64); 612 (100, 100); 614 (37, 38). Anal. Calcd for $C_{32}H_{40}NYb$: C, 62.8; H, 6.59; N, 2.29. Found: C, 62.5; H, 6.58; N, 2.24.

Reaction of $(Me_5C_5)_2Yb$ with Me_3SiCH_2Cu

A solution of $(Me_5C_5)_2Yb$ (0.50 g, 1.1 mmol) in hexane (40 mL) was added to a solution of Me_3SiCH_2Cu[8] (0.17 g, 1.1 mmol) in hexane (15 mL). The mixture was stirred for 4 hours at room temperature in the absence of light during which time a copper mirror formed on the walls of the flask and the mixture took on a purple coloration.

The mixture was filtered and the volatile materials were removed under reduced pressure. The residue was extracted with hexamethyl-disiloxane (15 mL) and filtered. Cooling the filtrate to -40 °C produced a mass of poorly formed purple crystals (0.21 g). Mp 101-108 °C. IR: 2725 (m), 2076 (w), 1257 (s), 1245 (s), 1239 (s), 1099(s), 1024 (s), 990 (sh), 969 (s), 908 (s), 902 (s), 857 (vs), 820 (vs), 744 (s), 714 (s), 678 (s), 672 (s), 602 (w), 590 (m), 574 (m), 529 (sh), 520 (m), 474 (m), 383 (m), 313 (s) cm^{-1}. ^1H NMR (C_7D_8, 29 °C): δ 10.69 ($\upsilon_{1/2}$ = 170 Hz, 15 H), 3.81 ($\upsilon_{1/2}$ = 35 Hz, 15 H), -4.30 ($\upsilon_{1/2}$ = 25 Hz, 9 H). No other resonances were observed. EIMS: 528 (51, 39); 529 (84, 69); 530 (82, 63); 531 (100, 100); 532 (39, 30); 533 (37, 40). Anal. Calcd for $C_{24}H_{41}SiYb$: C, 54.3; H, 7.79. Found: C, 50.5; H, 7.37.

Chapter 2

$(Me_5C_5)_2VF$

A solution of $(Me_5C_5)_2V$[9] (1.0 g, 3.2 mmol) in hexane (50 mL) was added to a suspension of silver(I)fluoride (0.40 g, 3.2 mmol) in hexane (50 mL). The silver(I)fluoride was purified by extraction with anhydrous hydrogen fluoride prior to use. The mixture was stirred at room temperature for 14 hours in the absence of light producing a deep blue solution and finely divided silver metal. The solution was filtered and the filtrate was concentrated to approximately 25 mL. Cooling to -20 °C afforded dark blue columns. A second crop of crystals was isolated by concentrating and cooling the mother liquor to -20 °C. The total yield was 0.71 g (2.1 mmol, 65%). Mp 257-261 °C. IR: 2725 (w), 2045 (vw), 1501 (vw), 1264 (vw), 1161 (w), 1099 (vw), 1067 (m), 1024 (s), 951 (w), 803 (w), 722 (w), 630 (m), 614 (m), 517 (s), 428 (s), 423 (s), 409 (s), 304 (m) cm^{-1}. ^1H NMR (C_6D_6, 30 °C): δ 18.1 ($\upsilon_{1/2}$ = 154 Hz). EIMS: 340 (100, 100); 341 (30, 22); 342 (3.2, 2.4). Magnetic Susceptibility (5 kG, 5-300 K): μ_{eff} = 2.78 μ_B, Θ = -0.48 K. Anal. Calcd for $C_{20}H_{30}FV$: C, 70.6; H, 8.88. Found: C, 70.7; H, 9.07.

$(Me_5C_5)_2VCl$

Hexane (100 mL) was added to a Schlenk tube containing $(Me_5C_5)_2V$ (0.92 g, 3.0 mmol) and copper(I)chloride (0.30, 3.0 mmol). The copper(I)chloride was purified according to a published procedure[10] and dried under vacuum at 100 °C for 12 hours prior to use.

The mixture was stirred at room temperature for 6 hours during which time the color changed from red to deep blue. The blue solution was filtered from the copper metal which formed in the reaction. The filtrate was concentrated to approximately 60 mL. Warming of the solution to dissolve the solid followed by slow cooling to -40 °C afforded deep blue blocks. Several crops of crystals were obtained for a total yield of 0.98 g (2.8 mmol, 91%). Mp 233 °C. ^{1}H NMR (C_6D_6, 29 °C): δ 7.31 ($\upsilon_{1/2}$ = 185 Hz). The IR spectrum was identical to that of the previously reported compound.[11]

$(Me_5C_5)_2VBr$

Hexane (100 mL) was added to a Schlenk tube containing $(Me_5C_5)_2V$ (0.65 g, 2.0 mmol) and copper(I)bromide (0.29 g, 2.0 mmol). Copper(I)bromide was purified according to a published procedure[10] and dried under vacuum at 100 °C for 12 hours prior to use. The mixture was stirred at room temperature for 6 hours producing a blue-green solution and metallic copper. The solution was filtered, and the filtrate was concentrated to approximately 50 mL. Warming of the solution to dissolve the solid followed by slow cooling to -40 °C afforded blue-green blocks. Several crops of crystals were isolated in a combined yield of 0.71 g (1.8 mmol, 87 %). Mp 249-252 °C. IR: 2763 (vw), 2717 (w), 2038 (vw), 1480 (vw), 1157 (m), 1068 (m), 1019 (s), 949 (w), 803 (w), 723 (w), 620 (m), 607 (w), 596 (w), 421 (s), 397 (m), 345 (m) cm^{-1}. ^{1}H NMR (C_6D_6, 30 °C): δ 6.07 ($\upsilon_{1/2}$ = 229 Hz). EIMS: 400 (99, 100); 401 (29, 23); 402 (100, 100); 403 (25, 22). Anal. Calcd for $C_{20}H_{30}BrV$: C, 59.9; H, 7.54.

Found: C, 60.3; H, 7.63. This complex has been previously reported although no spectroscopic data were published.[12]

$(Me_5C_5)_2VI$

A solution of $(Me_5C_5)_2V$ (0.59 g, 1.8 mmol) in hexane (50 mL) was added to a suspension silver(I)iodide (0.43 g, 1.8 mmol) in hexane (50 mL). The silver(I)iodide was dried under vacuum at 100 °C for 12 hours and used without further purification. The mixture was stirred at room temperature in the absence of light for 12 hours during which time a deep green solution and metallic silver was produced. The solution was filtered, and the filtrate was concentrated to approximately 30 mL. Cooling to -20 °C afforded a mass of green blocks. Several crops of crystals were obtained in a total yield of 0.63 g (1.4 mmol, 77%). Mp 266-267 °C. IR: 2764 (vw), 2717 (w), 2032 (vw), 1408 (vw), 1264 (vw), 1158 (m), 1097 (vw), 1067 (w), 1018 (s), 949 (w), 803 (w), 723 (w), 619 (w), 608 (w), 594 (w), 550 (w), 415 (s), 399 (w), 341 (w) cm^{-1}. ^1H NMR (C_6D_6, 30 °C): δ 5.23 ($\upsilon_{1/2}$ = 211 Hz). EIMS: 448 (100, 100); 449 (23, 22). Anal. Calcd for $C_{20}H_{30}IV$: C, 53.6; H, 6.75. Found: C, 54.0; H, 6.74. This complex has been previously reported although no spectroscopic data was published.[11b]

$(Me_5C_5)_2VPh$

To a solution of $(Me_5C_5)_2VCl$ (0.61 g, 1.7 mmol) in diethyl ether was added 2.2 mL of a 0.99 M diethyl ether solution of phenyllithium. Phenyllithium was synthesized from phenyl bromide and lithium metal in diethyl ether. The solution was filtered from excess

lithium and the filtrate was titrated with 1.0 N aqueous hydrochloric acid immediately prior to use. The mixture was stirred for 14 hours at room temperature before the volatile materials were removed under reduced pressure. The residue was extracted with pentane (40 mL) and filtered. The filtrate was concentrated to approximately 20 mL and cooled to -80 °C affording black needles (0.51 g, 1.3 mmol, 75%). Mp 203-210 °C. IR: 3123 (w), 3107 (m), 3045 (s), 2762 (vw), 2725 (m), 2571 (vw), 2528 (vw), 2471 (vw), 2387 (vw), 2326 (vw), 2226 (vw), 2199 (vw), 2045 (w), 1951 (w), 1938 (w), 1924 (w), 1870 (w), 1857 (w), 1827 (w), 1814 (w), 1789 (w), 1768 (w), 1749 (w), 1625 (w), 1582 (w), 1560 (s), 1552 (m), 1485 (sh), 1468 (sh), 1433 (sh), 1415 (sh), 1366 (s), 1261 (m), 1237 (m), 1177 (w), 1167 (w), 1113 (w), 1099 (w), 1067 (m), 1051 (m), 1024 (s), 1013 (s), 994 (w), 975 (m), 964 (w), 948 (w), 894 (m), 854 (m), 824 (m), 805 (m), 779 (w), 730 (s), 711 (s), 638 (m), 617 (w), 611 (vw), 595 (w), 549 (w), 487 (m), 463 (w), 420 (s), 396 (m), 353 (w) cm^{-1}. ^1H NMR (C_6D_6, 30 °C): δ 24.4 ($\upsilon_{1/2}$ = 229 Hz). The protons on the phenyl ligand were not observed. EIMS: 398 (100, 100); 399 (29, 29); 400 (18, 4). Anal. Calcd for $C_{26}H_{35}V$: C, 78.4; H, 8.85. Found: C, 75.7; H, 8.74.

$(Me_5C_5)_2VBH_4$

A mixture of $(Me_5C_5)_2VCl$ (0.66 g, 1.9 mmol) and lithium borohydride (0.05 g, 2.3 mmol) in tetrahydrofuran (40 mL) was stirred for 2 days at room temperature. After the volatile materials were removed under reduced pressure, the residue was extracted with hexane (50 mL). Filtration of the purple solution followed by cooling of the filtrate to -40 °C afforded dark purple crystals.

Additional crops of crystals were obtained from the mother liquor in a combined yield of 0.60 g (1.8 mmol, 96%). Mp 255-260 °C. IR: 2717 (m), 2607 (vw), 2444 (s), 2407 (m), 2363 (m), 1936 (m,br), 1832 (w), 1759 (w), 1611 (m), 1486 (m), 1397 (s), 1265 (vw), 1191 (s), 1154 (vw), 1066 (m), 1021 (s), 948 (w), 844 (w), 800 (w), 726 (w), 623 (w), 601 (w), 549 (w), 468 (m),446 (w), 424 (m), 336 (w) cm^{-1}. ^1H NMR (C_6D_6, 26 °C): δ 2.34 ($\upsilon_{1/2}$ = 37 Hz). The protons on the borohydride ligand were not observed. The highest isotopic cluster in the mass spectrum was centered at 321 amu (M^+-BH_4). Anal. Calcd for $C_{20}H_{34}BV$: C, 71.4; H, 10.2. Found: C, 71.4; H, 10.2.

$(Me_5C_5)_2VBD_4$

A mixture of $(Me_5C_5)_2VCl$ (0.55 g, 1.5 mmol) and lithium borodeuteride (0.06 g, 2 mmol) in tetrahydrofuran (40 mL) was stirred for 1.5 days at room temperature. After the volatile materials were removed under reduced pressure, the residue was extracted with hexane (30 mL). The solution was filtered, and the filtrate was concentrated to 10 mL. Cooling to -40 °C afforded dark purple crystals. Further concentration of the mother liquor provided additional crops of crystals in a combined yield of 0.27 g (0.79 mmol, 51%). Mp 240-245 °C. IR: 2765 (vw), 2725 (w), 2437 (w), 2388 (w), 2044 (vw), 1841 (m), 1801 (m), 1745 (m), 1700 (vw), 1481 (m), 1318 (vw), 1304 (vw), 1262 (vw), 1160 (w), 1097 (vw), 1066 (w), 1021 (s), 951 (vw), 882 (w), 859 (w), 821 (w), 805 (w), 722 (W), 654 (w), 621 (w), 611 (vw), 595 (w), 550 (vw), 463 (vw), 428 (m) cm^{-1}.

Reaction of $(Me_5C_5)_2VBH_4$ with ammonia

A solution of $(Me_5C_5)_2VBH_4$ (0.09 g, 0.27 mmol) in hexane (10 mL) was frozen in a liquid nitrogen bath. An excess of ammonia was condensed onto the frozen solid. The mixture was allowed to warm to room temperature while vented to the nitrogen manifold to release excess ammonia. A purple solid formed as the solution was stirred at room temperature for 0.5 hour. The volatile materials were removed under reduced pressure and the residue was extracted with diethyl ether (15 mL). The purple solution was filtered, and the filtrate was concentrated to approximately 3 mL. Cooling to -80 °C afforded green-brown crystals (0.08 g, 0.25 mmol, 93%). The IR spectrum was identical to that of the previously reported hydride complex, $(Me_5C_5)_2VH$.[11a]

$(Me_5C_5)_2VO$

A solution of $(Me_5C_5)_2V$ (1.07 g, 3.33 mmol) in hexane (15 mL) was placed in a Fischer-Porter thick-walled pressure bottle. The atmosphere above the solution was flushed three times with nitrous oxide before a static pressure of nitrous oxide (4 atm) was applied to the system. The mixture was stirred at room temperature for 4 hours during which time the color changed from deep red to green-brown. The mixture was transferred to a Schlenk tube and the volatile materials were removed under reduced pressure. The residue was extracted with pentane (25 mL) and filtered. The residue contained a significant amount of a black powder. Concentration of the pentane filtrate to approximately 10 mL followed by cooling to -40 °C afforded green-brown crystals (0.50 g, 1.5 mmol, 45%). The

compound did not melt to 330 °C. IR: 2762 (vw), 2725 (w), 2044 (vw), 1504 (m), 1445 (m), 1375 (s), 1262 (vw), 1163 (w), 1099 (vw), 1066 (w), 1024 (m), 953 (w), 852 (vs), 802 (m), 758 (vw), 722 (w), 621 (w), 595 (vw), 550 (w), 529 (w), 444 (s), 376 (s) cm^{-1}. No resonances were observed in the ^1H NMR spectrum in C_6D_6 at room temperature. EIMS: 337 (100, 100); 338 (25, 22). Magnetic Susceptibility (5 kG, 5-300 K): μ_{eff} = 1.95 μ_B, Θ = -0.49 K. Anal. Calcd for $C_{20}H_{30}OV$: C, 71.2; H, 8.96. Found: C, 71.3; H, 8.99.

The dark residue noted above was washed with pentane (10 mL) and filtered. Residual solvent was removed from the residue under reduced pressure leaving a black-green solid. The IR and mass spectra were identical to those of the cluster complex, $(Me_5C_5)_4V_4O_6$, observed by Bottomley.[13]

$(Me_5C_5)_2YbF$

A solution of $(Me_5C_5)_2Yb$ (0.40 g, 0.90 mmol) in pentane (20 mL) was added to a solution of $(Me_5C_5)_2VF$ (0.31 g, 0.90 mmol) in pentane (10 mL). Upon mixing, a purple precipitate immediately appeared. The mixture was stirred at room temperature for 1 hour and filtered. The solid was washed with pentane (30 mL), and filtered. Residual solvent was removed from the residue under reduced pressure leaving a purple powder (0.32 g, 0.69 mmol, 77%). Mp 285 °C (dec.). IR: 2725 (w), 1646 (w), 1490 (vw), 1256 (w), 1167 (w), 1099 (w), 1064 (w), 1029 (m), 954 (vw), 803 (m), 722 (w), 668 (vw), 636 (vw), 617 (w), 593 (w), 552 (w), 485 (m), 412 (s), 385 (m), 369 (m), 320 (s), 299 (s) cm^{-1}. No resonances were observed in the ^1H NMR spectrum in C_7D_8 at room temperature.

EIMS: 460 (43, 42); 461 (67, 70); 462 (57, 60); 463 (100, 100); 464 (21, 21); 465 (38, 38). Anal. Calcd for $C_{20}H_{30}FYb$: C, 51.9; H, 6.54. Found: C, 52.1; H, 6.63. The filtrate from the reaction mixture was concentrated to 10 mL and cooled to -20 °C giving $(Me_5C_5)_2V$.

$(Me_5C_5)_2YbF(THF)$

Tetrahydrofuran (5 mL) was added to $(Me_5C_5)_2YbF$ (0.10 g, 0.22 mmol) forming a red-orange solution. After complete dissolution, the tetrahydrofuran was removed under reduced pressure. The residue was extracted with pentane (10 mL) and filtered. The filtrate was concentrated to 5 mL and cooling to -80 °C afforded red-orange, flaky crystals (0.07 g, 0.1 mmol, 61%). The IR and ^1H NMR spectra were identical to those of the previously reported compound.[3] Mp 160-163 °C (Lit. 158-162 °C).

$(Me_5C_5)_2YbCl$

A solution of $(Me_5C_5)_2Yb$ (1.57 g, 3.54 mmol) in hexane (50 mL) was added to a solution of $(Me_5C_5)_2VCl$ (1.26 g, 3.53 mmol) in hexane (30 mL). The mixture was stirred at room temperature for 2 hours producing a blue-purple precipitate. The precipitate was filtered and the residue was washed with pentane (20 mL). Residual solvent was removed from the residue under reduced pressure leaving a blue-purple powder (1.55 g, 3.24 mmol, 91%). Mp 280 °C (dec.). IR : 2725 (w), 1606 (w), 1487 (w), 1264 (w), 1167 (w), 1099 (w), 1064 (w), 1024 (m), 954 (w), 803 (w), 725 (w), 630 (vw), 614 (w), 593 (w), 552 (vw), 388 (m), 331 (s), 304 (s), 258 (s) cm^{-1}. ^1H NMR (C_7D_8, 28 °C): δ 19.75 ($\upsilon_{1/2}$ = 295 Hz). EIMS: 475 (4.3, 7.1); 476

(30, 34); 477 (58, 59); 478 (64, 60); 479 (100, 100); 480 (30, 33); 481 (57, 57); 482 (7.9, 12); 483 (8.4, 11); 484 (0.5, 2.2). Anal. Calcd for $C_{20}H_{30}ClYb$: C, 50.2; H, 6.31. Found: C, 53.8; H, 6.81. The filtrate from the reaction mixture was concentrated to 20 mL and cooled to -20 °C giving $(Me_5C_5)_2V$.

$(Me_5C_5)_2YbCl(THF)$

Tetrahydrofuran (10 mL) was added to $(Me_5C_5)_2YbCl$ (0.18 g, 0.38 mmol) forming a magenta solution. After complete dissolution, the tetrahydrofuran was removed under reduced pressure. The residue was extracted with a 2:1 mixture of pentane/toluene (30 mL) and filtered. Cooling of the filtrate to -80 °C afforded purple needles (0.08 g, 0.15 mmol, 39%). The IR spectrum was identical to that of the previously reported compound.[14] Mp 218-220 °C (Lit. 221-223 °C).

$(Me_5C_5)_2YbBr$

A solution of $(Me_5C_5)_2Yb$ (0.25 g, 0.56 mmol) in hexane (15 mL) was added to a solution of $(Me_5C_5)_2VBr$ (0.23 g, 0.57 mmol) in hexane (15 mL). The mixture was stirred at room temperature for 1 hour producing a blue precipitate which was filtered and washed with pentane (15 mL). Residual solvent was removed from the residue under reduced pressure leaving a blue powder (0.23 g, 0.44 mmol, 78%). Mp 275 °C (dec.). IR: 2725 (w), 1596 (vw), 1261 (vw), 1164 (w), 1098 (vw), 1064 (w), 1022 (m), 954 (vw), 802 (w), 721 (w), 614 (vw), 590 (w), 551 (vw), 423 (vw), 389 (w), 328 (s), 305 (s) cm^{-1}. ^1H NMR (C_7D_8, 30 °C): δ 14.35 ($\upsilon_{1/2}$ = 316 Hz). EIMS: 520 (15,

25); 521 (33, 47); 322 (60, 60); 323 (100, 100); 324 (42, 47); 325 (65, 80); 326 (12, 17); 327 (19, 22). Anal. Calcd for $C_{20}H_{30}BrYb$: C, 45.9; H, 5.78. Found: C, 46.9; H, 5.87. The filtrate from the reaction mixture was concentrated to 10 mL and cooled to -20 °C giving $(Me_5C_5)_2V$.

$(Me_5C_5)_2YbI$

A solution of $(Me_5C_5)_2Yb$ (0.25 g, 0.56 mmol) in pentane (30 mL) was added to a solution of $(Me_5C_5)_2VI$ (0.25 g, 0.56 mmol) in pentane (10 mL). The mixture was stirred at room temperature for 1 hour during which time a blue precipitate appeared. The solid was filtered and washed with pentane (10 mL). Residual solvent was removed from the residue under reduced pressure leaving a blue powder (0.25 g, 0.44 mmol, 78%). Mp 258 °C (dec.). IR: 2725 (w), 1486 (w), 1165 (w), 1098 (w), 1061 (w), 1020 (m), 957 (w), 805 (w), 770 (w), 723 (w), 614 (vw), 597 (m), 384 (m), 308 (s) cm^{-1}. EIMS: 567 (8.3, 8.7); 568 (42, 42); 569 (73, 70); 570 (61, 60); 571 (100, 100); 572 (21, 21); 573 (37, 38); 574 (7.4, 8.0). Anal. Calcd for $C_{20}H_{30}IYb$: C, 42.1; H, 5.30. Found: C, 40.6; H, 5.15. The filtrate from the reaction mixture was concentrated to 10 mL and slowly cooled to -20 °C giving $(Me_5C_5)_2V$.

$(Me_5C_5)_2YbI(THF)$

A sample of $(Me_5C_5)_2YbI$ (0.35 g, 0.61 mmol) was dissolved in tetrahydrofuran (10 mL) forming a deep purple solution. The solution was filtered and the filtrate was concentrated to approximately 5 mL. Cooling to -80 °C produced a mass of purple crystals

(0.15 g, 0.23 mmol, 38%). The IR spectrum was identical to that of the previously reported compound.[2]

$(Me_5C_5)_2YbBH_4$

A solution of $(Me_5C_5)_2Yb$ (0.23 g, 0.52 mmol) in hexane (15 mL) was added to a solution of $(Me_5C_5)_2VBH_4$ (0.17 g, 0.51 mmol) in hexane (15 mL). After stirring at room temperature for 0.5 hour, the solvent was removed under reduced pressure. The residue was extracted with hexane (10 mL). The purple powder that did not dissolve in hexane was crystallized from toluene (5 mL) at -40 °C affording purple needles (0.12 g, 0.26 mmol, 50%). Mp 210-212 °C. IR: 2725 (m), 2337 (s), 2198 (s), 1606 (m), 1493 (m), 1263 (vw), 1219 (m), 1178 (m), 1118 (w), 1064 (w), 1023 (m), 957 (vw), 803 (w), 727 (m), 696 (m), 626 (vw), 614 (vw), 595 (w), 557 (vw), 466 (m), 384 (m), 330 (s), 305 (s) cm^{-1}. ^1H NMR (C_7D_8, 30 °C): δ 13.4 ($\upsilon_{1/2}$ = 124 Hz). The protons on the borohydride ligand were not observed. EIMS: 455 (19, 18); 456 (62, 56); 457 (80, 81); 458 (83, 81); 459 (100, 100); 460 (27, 29); 461 (37, 38). Anal. Calcd for $C_{20}H_{34}BYb$: C, 52.4; H, 7.48. Found: C, 52.6; H, 7.47.

$(Me_5C_5)_2YbBD_4$

A solution of $(Me_5C_5)_2Yb$ (0.16 g, 0.36 mmol) in pentane (5 mL) was added to a solution of $(Me_5C_5)_2VBD_4$ (0.12 g, 0.35 mmol) in pentane (5 mL). The purple mixture was stirred at room temperature for 1 hour before the volatile materials were removed under reduced pressure. The residue was extracted with toluene (5 mL) and filtered. The filtrate was concentrated to approximately 2

mL and cooled to -40 °C producing a purple powder (0.11 g, 0.24 mmol, 66%). Mp 194-198 °C. IR: 2766 (vw), 2725 (m), 2367 (w), 2176 (w), 1952 (vw), 1727 (s), 1638 (m), 1563 (m), 1262 (m), 1203 (vw), 1164 (vw), 1098 (m), 1064 (m), 1023 (s), 959 (w), 918 (m), 868 (vw), 804 (m), 729 (w), 695 (w), 590 (w), 463 (m), 424 (w), 388 (m), 331 (s), 303(s) cm^{-1}.

Reaction of $(Me_5C_5)_2Yb$ with $(Me_5C_5)_2VN_3$

A solution of $(Me_5C_5)_2Yb$ (0.12 g, 0.27 mmol) in hexane (10 mL) was added to a solution of $(Me_5C_5)_2VN_3$[15] (0.10 g, 0.28 mmol) in hexane (10 mL). Upon mixing, a light purple precipitate immediately appeared. After stirring at room temperature for 1 hour, the solid was filtered and washed with hexane (15 mL). Residual solvent was removed from the residue under reduced pressure giving 0.12 g of a purple powder. The physical properties of this product were identical to those of the material obtained from the reaction of $(Me_5C_5)_2Yb$ with trimethylsilylazide described below.

Reaction of $(Me_5C_5)_2Yb$ with trimethylsilylazide

Trimethylsilylazide (0.14 mL, 1.1 mmol) was added to a solution of $(Me_5C_5)_2Yb$ (0.24 g, 0.54 mmol) in pentane (20 mL). The mixture was stirred for 12 hours at room temperature producing a purple precipitate. The precipitate was filtered and washed with pentane (10 mL). Residual solvent was removed from the residue under reduced pressure giving 0.14 g of a purple powder. The product did not melt to 330 °C IR: 2725 (m), 2155 (vs, br), 2088 (s), 1656 (vw), 1489 (w), 1267 (vw), 1165 (w), 1098 (w), 1061 (w), 1022

(m), 952 (vw), 802 (w), 723 (w), 635 (vw), 601 (m), 594 (w), 584 (m), 566 (vw), 552 (vw), 434 (w), 390 (m), 316 (s), 298 (s) cm^{-1}. The highest isotopic cluster in the mass spectrum was centered at 444 amu corresponding to $(Me_5C_5)_2Yb$. Anal. Calcd for $C_{20}H_{30}N_3Yb$: C, 49.5; H, 6.23; N, 8.66. Found: C, 49.9; H, 6.37; N, 9.63.

$[(Me_5C_5)_2Yb]_2(\mu\text{-}F)$

A solution of $(Me_5C_5)_2Yb$ (0.07 g, 0.2 mmol) in pentane (10 mL) was added to a suspension of $(Me_5C_5)_2YbF$ (0.07 g, 0.2 mmol) in pentane (5 mL). The mixture was stirred at room temperature for 1 h producing a brown solid. The product was filtered and residual solvent was removed under reduced pressure leaving a brown powder (0.09 g, 0.1 mmol, 66 %). The IR spectrum was identical to that of the previously reported compound.[16a] Mp 289-295 °C (Lit. 290 °C). There was no evidence for the formation of the tetrameric complex, $(Me_5C_5)_6Yb_4(\mu\text{-}F)_4$.[16b]

$[(Me_5C_5)_2Yb]_2(\mu\text{-}Cl)$

A solution of $(Me_5C_5)_2VCl$ (0.18 g, 0.50 mmol) in hexane (20 mL) was added to a solution of $(Me_5C_5)_2Yb$ (0.44 g, 0.99 mmol) in hexane (10 mL). The mixture was stirred at room temperature for 12 hours during which time a brown microcrystalline precipitate appeared. The solid was filtered and the residue was dissolved in toluene (10 mL). Filtration followed by cooling of the filtrate to -20 °C afforded dark brown blocks (0.41 g, 0.44 mmol, 90%). Mp 282 °C (dec.). IR : 2725 (w), 2040 (vw), 1796 (vw), 1655 (w), 1488 (w), 1164 (w), 1100 (vw), 1062 (w), 1024 (m), 951 (w), 803 (w),

727 (w), 692 (w), 658 (w), 628 (vw), 616 (vw), 590 (w), 552 (w), 464 (w), 392 (m), 384 (m), 362 (m), 331 (s), 274 (s) cm^{-1}. ^1H NMR (C_7D_8, 31 °C): δ 11.02 ($\upsilon_{1/2}$ = 153 Hz). A molecular ion is not observed in the mass spectrum. The highest isotopic cluster is centered at 823 amu which does not correspond to any simple fragmentation pattern. However, there is an ion at 479 amu corresponding to $(Me_5C_5)_2YbCl$. Magnetic Susceptibility (5 kG): 5-60 K, μ_{eff} = 3.83 μ_B, Θ = -0.93 K; 120-300 K, μ_{eff} = 4.32 μ_B, Θ = -26 K. Anal. Calcd for $C_{40}H_{60}ClYb_2$: C, 52.1; H, 6.56. Found: C, 52.2; H, 6.54.

$[(Me_5C_5)_2Yb]_2(\mu\text{-}Br)$

A solution of $(Me_5C_5)_2VBr$ (0.22 g, 0.55 mmol) in hexane (20 mL) was added to a solution of $(Me_5C_5)_2Yb$ (0.49 g, 1.1 mmol) in hexane (10 mL.) Upon mixing, a brown microcrystalline precipitate immediately appeared. After stirring at room temperature for 12 hours, the solid was filtered and washed with pentane (20 mL.) Residual solvent was removed from the residue under reduced pressure and the residue was crystallized from toluene (10 mL) at -20 °C affording dark brown blocks (0.37 g, 0.38 mmol, 70%.) Mp 252 °C (dec.). IR: 2725 (m), 2040 (w), 1652 (w), 1484 (w), 1265 (vw), 1163 (w), 1087 (vw), 1063 (w), 1024 (m), 948 (vw), 802 (w), 723 (w), 633 (vw), 617 (vw), 587 (w), 554 (w), 468 (vw), 392 (w), 362 (w), 329 (s), 276 (s) cm^{-1}. ^1H NMR (C_7D_8, 30 °C): δ 13.66 ($\upsilon_{1/2}$ = 150 Hz). A molecular ion is not observed in the mass spectrum. The highest isotopic cluster is centered at 911 amu which does not correspond to any simple fragmentation pattern. However, there is an ion at 523 amu corresponding to $(Me_5C_5)_2YbBr$. Magnetic

Susceptibility (5 kG): 5-60 K, $\mu_{eff} = 3.68\ \mu_B$, Θ = - 1.1 K; 120-300 K, $\mu_{eff} = 4.23\ \mu_B$, Θ = -30 K. Anal. Calcd for $C_{40}H_{60}BrYb_2$: C, 49.7; H, 6.25. Found: C, 49.8; H, 6.23.

$[(Me_5C_5)_2Yb]_2(\mu$-Me) from $(Me_5C_5)_2VMe$

A solution of $(Me_5C_5)_2VMe$[11a] (0.11 g, 0.33 mmol) in hexane (5 mL) was added to a solution of $(Me_5C_5)_2Yb$ (0.29 g, 0.65 mmol) in hexane (10 mL). Upon addition, a red-brown precipitate immediately formed. After stirring at room temperature for 1 hour, the solid was filtered and the residue was washed with hexane (5 mL). Crystallization of the residue from toluene (5 mL) at -20 °C afforded brick red crystals (0.21 g, 0.23 mmol, 71%). The IR and ^1H NMR spectra were identical to those of the compound obtained from the reaction of $(Me_5C_5)_2Yb$ with methylcopper as described above.

$[(Me_5C_5)_2Yb]_2(\mu$-$BH_4)$

A solution of $(Me_5C_5)_2VBH_4$ (0.07 g, 0.2 mmol) in pentane (10 mL) was added to a solution of $(Me_5C_5)_2Yb$ (0.18 g, 0.41 mmol) in pentane (10 mL). Upon mixing, a brown microcrystalline precipitate appeared. After stirring for 1 hour at room temperature, the product was filtered and the residue was washed with pentane (20 mL). Crystallization of the residue from toluene (3 mL) at -20 °C afforded green-brown crystals (0.13 g, 0.14 mmol, 71%). Mp 294 °C (dec). IR: 2725 (m), 2389 (m), 2323 (s), 2194 (s), 2142 (m), 1891 (w), 1652 (w), 1600 (vw), 1484 (w), 1229 (s), 1163 (w), 1099 (vw), 1088 (vw), 1064 (w), 1022 (m), 948 (w), 802 (w), 728 (w), 695 (vw), 667 (vw), 632 (vw), 618 (vw), 588 (w), 552 (w), 409 (m), 390 (m),

357 (w), 332 (s), 274 (s) cm^{-1}. ^1H NMR (C_7D_8, 30 °C): δ 8.97 ($\upsilon_{1/2}$ = 73 Hz). The protons on the borohydride ligand were not observed. The highest isotopic cluster in the mass spectrum was centered at 751 amu (M^+-Me_5C_5). Magnetic Susceptibility (5 kG): 5-50 K, μ_{eff} = 4.41 μ_B, Θ = -1.14 K; 120-300 K, μ_{eff} = 4.78 μ_B, Θ = -12 K. Anal. Calcd for $C_{40}H_{64}BYb_2$: C, 53.3; H, 7.15. Found: C, 52.9; H, 7.18.

$[(Me_5C_5)_2Yb]_2(\mu\text{-}BD_4)$

A solution of $(Me_5C_5)_2VBD_4$ (0.10 g, 0.29 mmol) in pentane (5 mL) was added to a solution of $(Me_5C_5)_2Yb$ (0.26 g, 0.59 mmol) in pentane (5 mL). After stirring for 1 hour at room temperature, the pentane was completely removed under reduced pressure. The residue was extracted with toluene (5 mL) and filtered. Concentration of the filtrate to approximately 3 mL followed by cooling to -40 °C afforded green-brown crystals (0.14 g, 0.15 mmol, 53%). The product did not melt to 330 °C. IR: 2725 (m), 2389 (w), 2328 (w), 2149 (w), 2037 (vw), 1792 (w), 1750 (sh), 1714 (s), 1633 (m), 1559 (s), 1483 (sh), 1261 (w), 1163 (w), 1099 (vw), 1062 (w), 1023 (m), 969 (m), 923 (m), 800 (w), 730 (w), 695 (w), 659 (w), 632 (vw), 598 (w), 553 (w), 465 (vw), 389 (m), 359 (m), 331 (s), 272 (s) cm^{-1}.

Chapter 3

$(Me_5C_5)_2TiBr$

$(Me_5C_5)_2TiCl$ was synthesized from $TiCl_3(THF)_3$ and $Na(Me_5C_5)$ similarly to the previously reported procedure.[17] To a solution of $(Me_5C_5)_2TiCl$ (1.18 g, 3.34 mmol) in diethyl ether (50 mL) was added 0.44 mL of bromotrimethylsilane (3.3 mmol) via syringe. The blue solution was stirred at room temperature for 24 hours. The volatile materials were removed under reduce pressure and the residue was exposed to vacuum for an additional hour. The residue was treated with bromotrimethylsilane (3.3 mmol) a second time exactly as described above. The residue was extracted with pentane (60 mL) and filtered. The blue-green filtrate was concentrated to approximately 25 mL and cooled to -25 °C affording blue-green crystals (1.00 g, 2.51 mmol, 75%). Mp 262-264 °C. The IR and mass spectra were identical to those of the previously reported complex.[17]

$(Me_5C_5)_2TiI$

$(Me_5C_5)_2TiCl$ was synthesized from $TiCl_3(THF)_3$ and $Na(Me_5C_5)$ similarly to the previously reported procedure.[17] To a solution of $(Me_5C_5)_2TiCl$ (0.88 g, 2.5 mmol) in diethyl ether (30 mL) was added 0.35 mL of iodotrimethylsilane (2.5 mmol) via syringe. After stirring at room temperature for 24 hours, the volatile materials were removed under reduced pressure. The green residue was exposed to vacuum for an additional 2 hours. The residue was then treated a second time with iodotrimethylsilane (2.5 mmol) exactly as described

above. The residue was extracted with pentane (40 mL) and filtered. The green filtrate was concentrated to approximately 20 mL and cooled to -20 °C affording green crystals (0.92 g, 2.1 mmol, 83%). Mp 299-300 °C. The IR and mass spectra were identical to those of the previously reported complex.[17]

$(Me_5C_5)_2TiMe$

$(Me_5C_5)_2TiCl$ was synthesized from $TiCl_3(THF)_3$ and $Na(Me_5C_5)$ similarly to the previously reported procedure.[17] To a solution of $(Me_5C_5)_2TiCl$ (1.30 g, 3.67 mmol) in diethyl ether (50 mL) was added 3.0 mL of a 0.63 M diethyl ether solution of dimethylmagnesium (1.9 mmol). Upon mixing, the solution became deep green and a thick precipitate immediately appeared. After stirring at room temperature for 12 hours, the diethyl ether was removed under reduced pressure. The residue was extracted with pentane (50 mL) and filtered. The filtrate was concentrated to approximately 5 mL and cooled to -40 °C affording dark green columns (0.96 g, 2.9 mmol, 79%). Mp 256-257 °C. Anal. Calcd for $C_{21}H_{33}Ti$: C, 75.7; H, 9.98. Found: C, 75.7; H, 10.0. The IR spectrum was identical to that of the previously reported compound.[18]

$(Me_5C_5)_2TiH$

A solution of $(Me_5C_5)_2TiMe$ (0.86 g, 2.6 mmol) in pentane(15 mL) was added to a Fischer-Porter high pressure reaction vessel. The atmosphere was pressurized and flushed with H_2 five times before a static pressure of H_2 (10 atm) was applied. Upon mixing, the solution quickly changed from green to red. After stirring at

room temperature for 2 hours, the pressure was released and the solution transferred to a Schlenk tube. The solution was concentrated to approximately 5 mL and cooled to -40 °C affording deep red plates (0.79 g, 2.5 mmol, 96%). Mp 234-237 °C. IR: 2768 (vw), 2725 (m), 1512 (s), 1489 (s), 1436 (sh), 1261 (w), 1161 (w), 1099 (w), 1064 (w), 1023 (s), 951 (vw), 827 (m), 800 (m), 722 (w), 636 (vw), 625 (vw), 614 (w), 571 (m), 555 (vw), 460 (s), 436 (w), 407 (w), 296 (m) cm^{-1}. ^1H NMR (C_6D_6, 30 °C): δ 22.45 ($\upsilon_{1/2}$ = 95 Hz); (C_7D_8, 30 °C): δ 22.64 ($\upsilon_{1/2}$ = 128 Hz). The highest isotopic cluster in the mass spectrum was centered around 317 amu (M^+-H). Magnetic Susceptibility (5 kG): 5-100 K, μ_{eff} = 1.72 μ_B, Θ = -2.12 K; 180 - 300 K, μ_{eff} = 1.97 μ_B, Θ = -42.32 K. Anal. Calcd for $C_{20}H_{31}TiYb$: C, 75.2; H, 9.78. Found: C, 75.3; H, 9.84.

Reaction of $(Me_5C_5)_2TiMe$ with D_2

A solution of $(Me_5C_5)_2TiMe$ (3.88 g, 11.6 mmol) in hexane (40 mL) was placed in a Fischer-Porter high pressure reaction vessel. After flushing the apparatus five times with deuterium, a static pressure of deuterium (6 atm) was applied to the system. Upon stirring, the solution quickly changed from green to red. The system was flushed and repressurized with fresh deuterium every 12 hours. After a total reaction time of 5 days, the solution was transferred to a Schlenk tube and the volatile materials were removed under reduced pressure. The residue was extracted with pentane (40 mL) and filtered. The filtrate was concentrated to approximately 25 mL and cooled to -40 °C affording deep red plates. Additional crops of crystals were obtained from the mother liquor

for a combined yield of 3.81 g. Mp 226-231 °C. IR: 2226 (m), 2193 (s), 2143 (s), 2119 (s), 2061 (m), 1510 (s), 1277 (s), 1152 (w), 1094 (m), 1048 (m), 889 (vw), 833 (m), 723 (w), 601 (m), 570 (m), 451 (s), 390 (m), 283 (m) cm^{-1}. The IR spectrum recorded in halocarbon oil indicated that the H/D exchange was approximately 80-90% complete. The extent of H/D exchange was estimated by comparison of the relative intensities of the C-H stretches at 2953 and 2909 cm^{-1} and the resolved C-D stretches at 2238, 2201, 2120, and 2068 cm^{-1} in the IR spectra.

$(Me_5C_5)_2Yb(\mu\text{-}Cl)Ti(Me_5C_5)_2$

All manipulations were performed under dry argon and all solvents were purged with argon prior to use. A solution of $(Me_5C_5)_2Yb$ (0.25 g, 0.57 mmol) in pentane (10 mL) was added to a solution of $(Me_5C_5)_2TiCl$[17] (0.20 g, 0.57 mmol) in pentane (20 mL). Upon mixing, a dark green precipitate formed. After stirring at room temperature for 10 hours, the precipitate was filtered and the residue was washed with pentane (20 mL). Removal of residual solvent under reduced pressure left a brown-green solid. Crystallization of the solid from toluene at -20 °C afforded brown-green crystals (0.41 g, 0.51 mmol, 91%). Mp 244-248 °C. IR: 2725 (m), 2040 (vw), 1655 (vw), 1488 (m), 1379 (s), 1165 (w), 1065 (w), 1022 (s), 951 (vw), 804 (w), 799 (w), 728 (w), 694 (vw), 656 (w), 634 (vw), 625 (vw), 607 (vw), 596 (vw), 588 (vw), 552 (vw), 438 (s), 404 (w), 357 (s), 276 (s) cm^{-1}. Magnetic Susceptibility (5 kG): 5-100 K, μ_{eff} = 1.79 μ_B, Θ = -1.24 K; 180-300 K, μ_{eff} = 1.85 μ_B, Θ = -10.57 K. Anal. Calcd for $C_{40}H_{60}ClTiYb$: C, 60.3; H, 7.59. Found: C, 60.1; H, 7.55.

When this reaction was performed under nitrogen, an additional absorption of medium intensity was observed in the IR spectrum at 1892 cm^{-1}. If the product was exposed to vacuum for several hours, the intensity of this absorption decreased. Furthermore, when samples synthesized under argon were exposed to an atmosphere of nitrogen for 1 week, the absorption was observed in the subsequent IR spectrum. These results suggest that a dinitrogen complex may have been isolated. However, no additional evidence has so far been obtained.

$(Me_5C_5)_2Yb(\mu\text{-}Br)Ti(Me_5C_5)_2$

All manipulations were performed under dry argon and all solvents were purged with argon prior to use. A solution of $(Me_5C_5)_2Yb$ (0.20 g, 0.45 mmol) in pentane (15 mL) was added to a solution of $(Me_5C_5)_2TiBr$ (0.18 g, 0.45 mmol) in pentane (10 mL). Upon mixing, a dark brown-green precipitate formed. After stirring at room temperature for 1 hour, the precipitate was filtered and the residue was washed with pentane (20 mL). Crystallization of the residue from toluene at -40 °C gave brown-green crystals (0.31 g, 0.37 mmol, 82%). mp 238-242 °C (dec). IR: 2725 (m), 2042 (vw), 1651 (vw), 1486 (m), 1380 (s), 1164 (w), 1099 (vw), 1064 (w), 1023 (s), 955 (vw), 804 (w), 797 (w), 725 (w), 656 (w), 632 (vw), 625 (vw), 608 (vw), 595 (vw), 588 (vw), 550 (w), 440 (m), 406 (w), 361 (w), 348 (m), 276 (s) cm^{-1}. Magnetic Susceptibility (5 kG): 5 - 100 K, μ_{eff} = 1.85 μ_B, Θ = -1.59 K; 180-300 K, μ_{eff} = 2.07 μ_B, Θ = -39.66 K. Anal. Calcd for $C_{40}H_{60}BrTiYb$: C, 57.1; H, 7.18. Found: C, 56.9; H, 7.20.

When this reaction was performed under nitrogen, an additional absorption of strong intensity was observed in the IR spectrum at 1888 cm^{-1}.

Reaction of $(Me_5C_5)_2Yb$ with $(Me_5C_5)_2TiI$

All manipulations were performed under dry argon and all solvents were purged with argon prior to use. A solution of $(Me_5C_5)_2Yb$ (0.50 g, 1.1 mmol) in pentane (30 mL) was added to a solution of $(Me_5C_5)_2TiI$ (0.50 g, 1.1 mmol) in pentane (10 mL). Upon addition, a brown precipitate appeared which was stirred at room temperature for 2 hours. The precipitate was filtered and residual solvent was removed from the residue under reduced pressure. Attempts to crystallize the residue from toluene resulted in the isolation of poorly formed crystals that were always contaminated with a small amount of a green colored impurity even after repeated crystallizations. Mp 214-218 C°. IR: 2725 (m), 2038 (vw), 1653 (vw), 1486 (m), 1162 (w), 1064 (w), 1023 (m), 951 (vw), 881 (w), 799 (w), 727 (w), 595 (w), 551 (w), 519 (vw), 437 (m), 403 (m), 346 (m), 276 (s) cm^{-1}. Anal. Calcd for $C_{40}H_{60}ITiYb$: C, 54.1; H, 6.80. Found: C, 52.5; H, 6.70.

$(Me_5C_5)_2Yb(\mu\text{-}H)Ti(Me_5C_5)_2$

All manipulations were performed under dry argon and all solvents were purged with argon prior to use. A solution of $(Me_5C_5)_2Yb$ (0.45 g, 1.0 mmol) in pentane (10 mL) was added to a solution of $(Me_5C_5)_2TiH$ (0.32 g, 1.0 mmol) in pentane (5 mL). Upon mixing, a brown precipitate formed. After stirring at room temper-

ature for 1 hour, the pentane was removed from the suspension under reduced pressure. The residue was extracted with toluene (15 mL) and filtered. Concentration of the filtrate to approximately 5 mL followed by cooling to -40 °C afforded brown-green crystals (0.44 g, 0.58 mmol, 58%). Mp 155-160 °C. IR: 2725 (m), 1491 (m), 1460 (s), 1393 (m), 1381 (s), 1254 (s,br) 1163 (m), 1099 (w), 1057 (w), 1021 (m), 975 (vw), 948 (w) 857 (w), 799 (sh),790 (m), 726 (w), 693 (vw), 663 (m), 617 (w), 608 (w), 590 (w), 566 (w), 551 (w), 472 (m), 447 (m), 402 (w), 366 (w), 263 (s) cm^{-1}. Magnetic Susceptibility (5 kG): 5-100 K, μ_{eff} = 2.18 μ_B, Θ = -2.36 K; 180-300 K, μ_{eff} = 2.40 μ_B, Θ = -28.97 K. Anal. Calcd for $C_{40}H_{61}TiYb$: C, 63.0; H, 8.06. Found: C, 62.4; H, 7.92.

$(Me_5C_5)_2Yb(\mu\text{-}Me)Ti(Me_5C_5)_2$

All manipulations were performed under dry argon and all solvents were purged with argon prior to use. A solution of $(Me_5C_5)_2Yb$ (0.33 g, 0.75 mmol) in pentane (10 mL) was added to a solution of $(Me_5C_5)_2TiMe$ (0.25 g, 0.75 mmol) in pentane (20 mL). A brown microcrystalline precipitate formed upon mixing. After stirring at room temperature for 2 hours, the precipitate was filtered and the residue was washed with pentane (15 mL). Crystallization of the residue from toluene at -20 °C afforded dark brown crystals (0.41 g, 0.53 mmol, 71%). Mp 176-178 °C (dec). IR: 2723 (m), 2037 (vw), 1926 (vw), 1648 (vw), 1492 (m), 1380 (s), 1263 (vw), 1163 (w), 1098 (vw), 1065 (w), 1024 (s), 995 (s), 949 (vw), 804 (w), 723 (w), 663 (w), 632 (vw), 626 (vw), 610 (vw), 588 (w), 551 (w), 454 (m), 435 (m), 401 (w), 359 (m), 274 (s) cm^{-1}. Magnetic Susceptibility

(5 kG): 5-100 K, μ_{eff} = 2.02 μ_B, Θ = -2.12 K; 180-300 K, μ_{eff} = 2.25 μ_B, Θ = -38.51 K. Anal. Calcd for $C_{41}H_{63}TiYb$: C, 63.4; H, 8.17. Found: C, 63.3; H, 8.05.

When this reaction was performed under nitrogen, an additional absorption of medium intensity was observed in the IR spectrum at 1898 cm^{-1}.

$(Me_5C_5)_2Yb(\mu\text{-}BH_4)Ti(Me_5C_5)_2$

All manipulations were performed under dry argon and all solvents were purged with argon prior to use. A solution of $(Me_5C_5)_2Yb$ (0.41 g, 0.93 mmol) in pentane (20 mL) was added to a solution of $(Me_5C_5)_2TiBH_4$[17] (0.31 g, 0.93 mmol) in pentane (5 mL). Upon mixing, a dark green precipitate formed. After stirring at room temperature for 1 hour, the precipitate was filtered and the residue washed with pentane (20 mL). Crystallization of the residue from toluene at -20 °C afforded dark green-brown crystals (0.62 g, 0.80 mmol, 86%). Mp 302-305 °C (dec). IR: 2725 (m), 2386 (w), 2325 (s), 2152 (w), 2072 (s), 1652 (vw), 1488 (m), 1380 (s), 1235 (s), 1164 (w), 1065 (w), 1022 (m), 801 (w), 728 (w), 632 (vw), 611 (vw), 591 (w), 551 (w), 438 (m), 407 (w), 361 (w), 269 (s) cm^{-1}. Magnetic Susceptibility (5 kG): 5-100 K,μ_{eff} = 1.84 μ_B, Θ = -0.76 K; 180-300 K, μ_{eff} = 1.89 μ_B, Θ = -4.60 K. Anal. Calcd for $C_{40}H_{64}BTiYb$: C, 61.9; H, 8.31. Found: C, 61.5; H, 8.27.

X-ray Crystallographic Studies

$(Me_5C_5)_2YbMe$

Red rectangular plates of the complex were grown from a pentane solution at -80 °C. A crystal of approximate dimensions 0.31 mm × 0.14 mm × 0.10 mm was isolated and placed in Paratone N oil.[19] The crystal was mounted on the end of a cut quartz capillary tube and placed under a flow of cold nitrogen on an Enraf-Nonius CAD4 diffractometer.[20] The solidified oil held the crystal in place and protected it from decomposition. The temperature was stabilized at -100 °C with an automated cold flow apparatus.

After centering the crystal in the X-ray beam, a set of accurate cell dimensions and an orientation matrix were determined by a least-squares fit to the setting angles of the unresolved MoKα components of 24 symmetry related reflections. The dimensions and volume of the unit cell suggested monoclinic symmetry with four molecules in the unit cell. Details of the unit cell, collection parameters, and structure refinement are listed in Table 1.

A set of three standard reflections (4, 12, -3; 6, 4, 0; 2, -5, -8) was chosen to monitor intensity and crystal orientation. The intensity was checked after every hour of X-ray exposure time and showed no appreciable decay over the course of the data collection. The crystal orientation was checked after every 200 reflections and was reoriented if any of the standard reflections were offset from

their predicted position by more than 0.1°. The crystal orientation matrix was reoriented seven times during the data collection.

The 5675 raw data were converted to structure factor amplitudes and their esds by correction for scan speed, background, and Lorentz-polarization effects.[21,22,23] An empirical absorption correction was applied to the data based on averaged azimuthal psi scans for three reflections with $\chi > 80°$.[24] Examination of the azimuthal scans showed a variation of $I_{min}/I_{max} = 0.74$ for the average relative intensity curve. Analysis of the data revealed the following systematic absences: h 0 l, l odd; 0 k 0, k odd, consistent with the space group $P2_1/C$.

The coordinates of the two independent ytterbium atoms were determined by Patterson methods. The locations of all non-hydrogen atoms were determined through the use of standard Fourier techniques and refined by least-squares methods. All non-hydrogen atoms were refined anisotropically. A difference Fourier map revealed the positions of all hydrogen atoms associated with the permethylcyclopentadienyl rings. These atoms were placed in calculated positions and included in the structure factor calculations but not refined. All hydrogen atoms were given isotropic thermal parameters 1.3 times the B(iso) of the atom to which they were bonded. The positions of the hydrogen atoms on metal-bound methyl groups could not be clearly determined. Therefore, these atoms were not included in the structure solution.

Final refinement of the 398 variables using the 3919 data for which $F_o^2 > 3\sigma(F_o^2)$ gave residuals of $R = 0.0379$ and $R_w = 0.0486$. The R value based on all 5570 unique data was 0.0972 and the goodness-

of-fit parameter was 1.322. The least-squares program minimized the expression, $\Sigma w(|F_o| - |F_c|)^2$, where w is the weight of a given observation. A value of 0.05 for the p-factor was used to reduce the weight of intense reflections in the refinements.[25] The analytical forms of the scattering factor tables for the neutral atoms[26] were used and all non-hydrogen scattering factors were corrected for both real and imaginary components of anomalous dispersion.[27]

The data were evaluated through the residuals over ranges of $\sin\Theta/\lambda$, $|F_o|$, parity, and individual indices. No unusual features or trends were observed. Prior to the final refinement, three reflections were rejected as "bad" data due to their high values of $w \times \Delta^2$. The highest and lowest peaks in the final difference Fourier map had electron densities of 1.011 and -0.247 e/Å^3, respectively, and were associated with the ytterbium atoms.

Table 1. Crystal Data for $(Me_5C_5)_2YbMe$

Formula	$C_{42}H_{66}Yb_2$
FW	917.07
Space Group	$P2_1/C$ (No. 14)
a, Å	10.820 (2)
b, Å	26.986 (9)
c, Å	14.224 (2)
β, deg.	108.85 (2)
V, $Å^3$	3930 (4)
Z	4
F(000)	458
d(calc.), g/cm^3	1.553
μ(calc.), 1/cm	47.51
size, mm	0.31 × 0.14 × 0.10
temp. °C	-100 °C
diffractometer	Enraf-Nonius CAD4
radiation	MoKα (0.71073 Å)
monochromator	highly oriented graphite
scan range, type	$3.0° \leq 2\Theta \leq 45°$, $\Theta - 2\Theta$
scan width, deg.	$\Delta\Theta = 0.80 + 0.35\ (\tan\Theta)$
octants collected	+ h, + k, ± l
reflections collected	5675
unique reflections	5570
reflections, $F_o^2 > 3\sigma(F_o^2)$	3919
variables	398
R	0.0379
R_w	0.0486
R_{all}	0.0972
GOF	1.322
largest Δ/σ in final LS cycle	0.00

$[(Me_5C_5)_2Yb]_2(\mu\text{-}Me)$

Red parallelopipeds of the complex were grown from a toluene solution at -20 °C. The crystals were placed in Paratone N oil[19] and one was selected and cut to approximate dimensions of 0.42 mm × 0.40 mm × 0.38 mm. The crystal was mounted on the end of a cut quartz capillary tube and placed under a flow of cold nitrogen on an Enraf-Nonius CAD4 diffractometer.[20] The solidified oil held the crystal in place and protected it from decomposition. The temperature was stabilized at -118 °C with an automated cold flow apparatus.

After centering the crystal in the X-ray beam, a set of accurate cell dimensions and an orientation matrix were determined by a least-squares fit to the setting angles of the unresolved MoKα components of 24 symmetry related reflections. The dimensions and volume of the unit cell suggested triclinic symmetry with two molecules in the unit cell. Details of the unit cell, collection parameters, and structure refinement are listed in Table 2.

A set of three standard reflections (4, -1, -6; 1, -5, -7; 5, 4, 5) was chosen to monitor intensity and crystal orientation. The intensity was checked after every hour of X-ray exposure time and showed no appreciable decay over the course of the data collection. The crystal orientation was checked after every 200 reflections and was reoriented if any of the standard reflections were offset from their predicted position by more than 0.1°. The crystal orientation matrix was reoriented six times during the data collection.

The 5060 raw data were converted to structure factor amplitudes and their esds by correction for scan speed, background,

and Lorentz-polarization effects.[21,22,23] An empirical absorption correction was applied to the data based on averaged azimuthal psi scans for three reflections with $\chi > 80°$.[24] Examination of the azimuthal scans showed a variation of $I_{min}/I_{max} = 0.81$ for the average relative intensity curve.

The coordinates of the two independent ytterbium atoms were determined by Patterson methods. The locations of all non-hydrogen atoms were determined through the use of standard Fourier techniques and refined by least-squares methods. All non-hydrogen atoms were refined anisotropically. A difference Fourier map revealed the positions of all hydrogen atoms associated with the permethylcyclopentadienyl rings. These atoms were placed in calculated positions and included in the structure factor calculations but not refined. All hydrogen atoms were given isotropic thermal parameters 1.2 times the B(iso) of the atom to which they were bonded. The positions of the hydrogen atoms on the metal-bound methyl group could not be clearly determined. Therefore, these atoms were not included in the structure solution.

Final refinement of the 388 variables using the 4500 data for which $F_o^2 > 3\sigma(F_o^2)$ gave residuals of $R = 0.0286$ and $R_w = 0.0421$. The R value based on all 4996 unique data was 0.0340 and the goodness-of-fit parameter was 2.289. The least-squares program minimized the expression, $\Sigma w(|F_o| - |F_c|)^2$, where w is the weight of a given observation. A value of 0.03 for the p-factor was used to reduce the weight of intense reflections in the refinements.[25] The analytical forms of the scattering factor tables for the neutral atoms[26] were

used and all non-hydrogen scattering factors were corrected for both real and imaginary components of anomalous dispersion.[27]

The data were evaluated through the residuals over ranges of $\sin\Theta/\lambda$, $|F_o|$, parity, and individual indices. No unusual features or trends were observed. The highest and lowest peaks in the final difference Fourier map had electron densities of 1.855 and -1.140 e/Å^3, respectively, and were associated with the ytterbium atoms.

Table 2. Crystal Data for $[(Me_5C_5)_2Yb]_2(\mu\text{-Me})$

Formula	$C_{41}H_{63}Yb_2$
FW	903.02
Space Group	$P\bar{1}$ (No. 2)
a, Å	10.638 (3)
b, Å	11.378 (2)
c, Å	16.720 (4)
α, deg.	76.93 (2)
β, deg.	76.93 (2)
γ, deg.	84.91 (2)
V, Å^3	1919 (1)
Z	2
F(000)	449
d(calc.), g/cm^3	1.561
μ(calc.), 1/cm	58.55
size, mm	0.42 × 0.40 × 0.38
temp. °C	-118 °C
diffractometer	Enraf-Nonius CAD4
radiation	MoKα (0.71073 Å)
monochromator	highly oriented graphite
scan range, type	$3.0° \leq 2\Theta \leq 45°$, $\Theta - 2\Theta$
scan width, deg.	$\Delta\Theta = 0.75 + 0.35\ (\tan\Theta)$
octants collected	+ h, ± k, ± l
reflections collected	5068
unique reflections	4996
reflections, $F_o^2 > 3\sigma(F_o^2)$	4500
variables	388
R	0.0286
R_w	0.0421
R_{all}	0.0340
GOF	2.289
largest Δ/σ in final LS cycle	0.02

$(Me_5C_5)_2Yb(\mu\text{-}NH_2)_2AlMe_2$

Red plate-like crystals of the complex were grown from a toluene/hexamethyldisiloxane solution. A crystal of approximate dimensions 0.35 mm × 0.21 mm × 0.12 mm was isolated and placed in Paratone N oil.[19] The crystal was mounted on the end of a cut quartz capillary tube and placed under a flow of cold nitrogen on an Enraf-Nonius CAD4 diffractometer.[20] The solidified oil held the crystal in place and protected it from decomposition. The temperature was stabilized at -110 °C with an automated cold flow apparatus.

After centering the crystal in the X-ray beam, a set of accurate cell dimensions and an orientation matrix were determined by a least-squares fit to the setting angles of the unresolved MoKα components of 24 symmetry related reflections. The dimensions and volume of the unit cell suggested triclinic symmetry with two molecules in the unit cell. Details of the unit cell, collection parameters, and structure refinement are listed in Table 3.

A set of three standard reflections (-2, -3, 5; 2, 6, 1; 5, -1, -3) was chosen to monitor intensity and crystal orientation. The intensity was checked after every hour of X-ray exposure time and showed no appreciable decay over the course of the data collection. The crystal orientation was checked after every 200 reflections and was reoriented if any of the standard reflections were offset from their predicted position by more than 0.1°. The crystal orientation matrix did not require reorientation during the data collection.

The 3046 raw data were converted to structure factor amplitudes and their esds by correction for scan speed, background,

and Lorentz-polarization effects.[21,22,23] An empirical absorption correction was applied to the data based on averaged azimuthal psi scans for three reflections with $\chi > 80°$.[24] Examination of the azimuthal scans showed a variation of $I_{min}/I_{max} = 0.63$ for the average relative intensity curve.

The coordinates of the ytterbium atom were determined by Patterson methods. The locations of all non-hydrogen atoms were determined through the use of standard Fourier techniques and refined by least-squares methods. All non-hydrogen atoms were refined anisotropically. A difference Fourier map revealed the positions of all hydrogen atoms associated with the permethylcyclopentadienyl rings. These atoms were placed in calculated positions and included in the structure factor calculations but not refined. All hydrogen atoms were given isotropic thermal parameters 1.3 times the B(iso) of the atom to which they were bonded. Subsequent difference Fourier maps revealed positions for the hydrogen atoms on the bridging amide groups. These coordinates were input and refined isotropically.

Final refinement of the 251 variables using the 2663 data for which $F_o^2 > 3\sigma(F_o^2)$ gave residuals of $R = 0.0408$ and $R_w = 0.0509$. The R value based on all 2986 unique data was 0.0461 and the goodness-of-fit parameter was 2.497. The least-squares program minimized the expression, $\Sigma w(|F_o| - |F_c|)^2$, where w is the weight of a given observation. A value of 0.03 for the p-factor was used to reduce the weight of intense reflections in the refinements.[25] The analytical forms of the scattering factor tables for the neutral atoms[26] were

used and all non-hydrogen scattering factors were corrected for both real and imaginary components of anomalous dispersion.[27]

The data were evaluated through the residuals over ranges of $\sin\Theta/\lambda$, $|F_o|$, parity, and individual indices. No unusual features or trends were observed. The highest and lowest peaks in the final difference Fourier map had electron densities of 2.62 and -0.37 e/Å^3, respectively, and were associated with the ytterbium atoms.

Table 3. Crystal Data for $(Me_5C_5)_2Yb(\mu\text{-}NH_2)_2AlMe_2$

Formula	$C_{22}H_{40}N_2AlYb$
FW	532.59
Space Group	$P\bar{1}$ (No. 2)
a, Å	10.197 (3)
b, Å	10.213 (2)
c, Å	11.252 (3)
α, deg.	85.86 (2)
β, deg.	85.82 (2)
γ, deg.	80.81 (2)
V, Å^3	1152 (8)
Z	2
F(000)	269
d(calc.), g/cm^3	1.536
μ(calc.), 1/cm	40.94
size, mm	0.35 × 0.21 × 0.12
temp. °C	-110 °C
diffractometer	Enraf-Nonius CAD4
radiation	MoKα (0.71073 Å)
monochromator	highly oriented graphite
scan range, type	$3.0° \leq 2\Theta \leq 45°$, $\Theta - 2\Theta$
scan width, deg.	$\Delta\Theta = 0.80 + 0.35\ (\tan\Theta)$
octants collected	+ h, ± k, ± l
reflections collected	3046
unique reflections	2986
reflections, $F_o^2 > 3\sigma(F_o^2)$	2663
variables	251
R	0.0408
R_w	0.0509
R_{all}	0.0461
GOF	2.497
largest Δ/σ in final LS cycle	0.07

$(Me_5C_5)_2Yb(\mu\text{-}Cl)Ti(Me_5C_5)_2$

Brown-green columns of the complex were grown from a toluene solution at -20 °C. The crystals were placed in Paratone N oil[19] and one was selected and cut to approximate dimensions of 0.51 mm × 0.34 mm × 0.31 mm. The crystal was mounted on the end of a cut quartz capillary tube and placed under a flow of cold nitrogen on an Enraf-Nonius CAD4 diffractometer.[20] The solidified oil held the crystal in place and protected it from decomposition. The temperature was stabilized at -100 °C with an automated cold flow apparatus.

After centering the crystal in the X-ray beam, a set of accurate cell dimensions and an orientation matrix were determined by a least-squares fit to the setting angles of the unresolved MoKα components of 24 symmetry related reflections. The dimensions and volume of the unit cell suggested monoclinic symmetry with four molecules in the unit cell. Details of the unit cell, collection parameters, and structure refinement are listed in Table 4.

A set of three standard reflections (5, 1, -8; -2, -4, 8; 8, 3, -4) was chosen to monitor intensity and crystal orientation. The intensity was checked after every hour of X-ray exposure time. Over the course of the data collection, a slight linear intensity decay was observed. The decay was expressed as a linear function and a correction was applied to the data. The crystal orientation was checked after every 200 reflections and was reoriented if any of the standard reflections were offset from their predicted position by

more than 0.1°. The crystal orientation matrix was reoriented twice during the data collection.

The 5406 raw data were converted to structure factor amplitudes and their esds by correction for scan speed, background, and Lorentz-polarization effects.[21,22,23] An empirical absorption correction was applied to the data based on averaged azimuthal psi scans for three reflections with $\chi > 80°$.[24] Examination of the azimuthal scans showed a variation of $I_{min}/I_{max} = 0.93$ for the average relative intensity curve. Analysis of the data revealed the following systematic absences: h 0 l, l odd; 0 k 0, k odd, consistent with the space group $P2_1/C$.

The coordinates of the ytterbium atom were determined by Patterson methods. The locations of all non-hydrogen atoms were determined through the use of standard Fourier techniques and refined by least-squares methods. The data were evaluated through the residuals over ranges of $\sin\Theta/\lambda$, $|F_o|$, parity, and individual indices. This revealed sections of poor data throughout the data set. A total of 117 data were rejected as "bad" before the structure refined properly. The problem resulted from overlap of closely spaced peaks within the scan window. All non-hydrogen atoms were refined anisotropically. A difference Fourier map revealed the positions of all hydrogen atoms associated with the permethylcyclopentadienyl rings. These atoms were placed in calculated positions and included in the structure factor calculations but not refined. All hydrogen atoms were given isotropic thermal parameters 1.3 times the B(iso) of the atom to which they were bonded.

Final refinement of the 389 variables using the 4513 data for which $F_o^2 > 3\sigma(F_o^2)$ gave residuals of R = 0.0306 and R_w = 0.0438. The R value based on all 4896 unique data was 0.0373 and the goodness-of-fit parameter was 3.008. The least-squares program minimized the expression, $\Sigma w(|F_o| - |F_c|)^2$, where w is the weight of a given observation. A value of 0.02 for the p-factor was used to reduce the weight of intense reflections in the refinements.[25] The analytical forms of the scattering factor tables for the neutral atoms[26] were used and all non-hydrogen scattering factors were corrected for both real and imaginary components of anomalous dispersion.[27]

There was evidence for secondary extinction in the low angle, high intensity data so a correction was applied to the data.[28] The secondary extinction coefficient was refined to a value of 4.4×10^{-8} e^{-2}. The highest and lowest peaks in the final difference Fourier map had electron densities of 0.61 and -0.98 e/Å^3, respectively, and were associated with the ytterbium atoms.

Table 4. Crystal Data for $(Me_5C_5)_2Yb(\mu\text{-}Cl)Ti(Me_5C_5)_2$

Formula	$C_{40}H_{60}ClTiYb$
FW	797.31
Space Group	$P2_1/C$ (No. 14)
a, Å	15.992 (3)
b, Å	14.547 (3)
c, Å	16.222 (2)
β, deg.	93.60 (1)
V, Å^3	3750 (2)
Z	4
F(000)	409
d(calc.), g/cm^3	1.412
μ(calc.), 1/cm	27.78
size, mm	0.51 × 0.34 × 0.31
temp. °C	-100 °C
diffractometer	Enraf-Nonius CAD4
radiation	MoKα (0.71073 Å)
monochromator	highly oriented graphite
scan range, type	$3.0° \leq 2\Theta \leq 45°$, $\Theta - 2\Theta$
scan width, deg.	$\Delta\Theta = 0.65 + 0.35\ (\tan\Theta)$
octants collected	+ h, + k, ± l
reflections collected	5406
unique reflections	4896
reflections, $F_o^2 > 3\sigma(F_o^2)$	4513
variables	389
R	0.0306
R_w	0.0438
R_{all}	0.0373
GOF	3.008
largest Δ/σ in final LS cycle	0.00

$(Me_5C_5)_2Yb(\mu\text{-}Br)Ti(Me_5C_5)_2$

Brown-green crystals of the complex were grown from a toluene solution at -40 °C. The crystals were placed in Paratone N oil[19] and a large block was cut several times to approximate dimensions of 0.36 mm × 0.33 mm × 0.28 mm. The crystal was mounted on the end of a cut quartz capillary tube and placed under a flow of cold nitrogen on an Enraf-Nonius CAD4 diffractometer.[20] The solidified oil held the crystal in place and protected it from decomposition. The temperature was stabilized at -88 °C with an automated cold flow apparatus.

After centering the crystal in the X-ray beam, a set of accurate cell dimensions and an orientation matrix were determined by a least-squares fit to the setting angles of the unresolved MoKα components of 24 symmetry related reflections. The dimensions and volume of the unit cell suggested monoclinic symmetry with four molecules in the unit cell. Details of the unit cell, collection parameters, and structure refinement are listed in Table 5.

A set of three standard reflections (-6, -6, 4; 8, -1, 4; -3, -2, 9) was chosen to monitor intensity and crystal orientation. The intensity was checked after every hour of X-ray exposure time. Over the course of the data collection, a slight linear intensity decay was observed. The decay was expressed as a linear function and a correction was applied to the data. The crystal orientation was checked after every 200 reflections and was reoriented if any of the standard reflections were offset from their predicted position by

more than 0.1°. The crystal did not require reorientation during the data collection.

The 5505 raw data were converted to structure factor amplitudes and their esds by correction for scan speed, background, and Lorentz-polarization effects.[21,22,23] An empirical absorption correction was applied to the data based on averaged azimuthal psi scans for two reflections with $\chi > 80°$.[24] Examination of the azimuthal scans showed a variation of $I_{min}/I_{max} = 0.84$ for the average relative intensity curve. Analysis of the data revealed the following systematic absences: h 0 l, l odd; 0 k 0, k odd, consistent with the space group $P2_1/C$. Rejection of the systematic absences left a total of 4962 unique data.

The coordinates of the ytterbium atom were determined by Patterson methods. The locations of all non-hydrogen atoms were determined through the use of standard Fourier techniques and refined by least-squares methods. All non-hydrogen atoms were refined anisotropically. A difference Fourier map revealed the positions of almost all of hydrogen atoms associated with the permethylcyclopentadienyl rings. These atoms were placed in calculated positions and included in the structure factor calculations but not refined. All hydrogen atoms were given isotropic thermal parameters 1.3 times the B(iso) of the atom to which they were bonded.

Final refinement of the 388 variables using the 3996 data for which $F_o^2 > 3\sigma(F_o^2)$ gave residuals of $R = 0.0335$ and $R_w = 0.0400$. The R value based on all 4962 unique data was 0.0470 and the goodness-of-fit parameter was 1.811. The least-squares program minimized

the expression, $\Sigma w(|F_o| - |F_c|)^2$, where w is the weight of a given observation. A value of 0.03 for the p-factor was used to reduce the weight of intense reflections in the refinements.[25] The analytical forms of the scattering factor tables for the neutral atoms[26] were used and all non-hydrogen scattering factors were corrected for both real and imaginary components of anomalous dispersion.[27]

The data were evaluated through the residuals over ranges of $\sin\Theta/\lambda$, $|F_o|$, parity, and individual indices. No unusual features or trends were observed. The highest and lowest peaks in the final difference Fourier map had electron densities of 0.84 and -0.17 e/Å^3, respectively, and were associated with the ytterbium atom.

Table 5. Crystal Data for $(Me_5C_5)_2Yb(\mu\text{-}Br)Ti(Me_5C_5)_2$

Formula	$C_{40}H_{60}BrTiYb$
FW	841.76
Space Group	$P2_1/C$ (No. 14)
a, Å	15.917 (3)
b, Å	14.710 (6)
c, Å	16.307 (4)
β, deg.	94.60 (2)
V, Å^3	3806 (4)
Z	4
F(000)	427
d(calc.), g/cm^3	1.468
μ(calc.), 1/cm	37.04
size, mm	0.36 × 0.33 × 0.28
temp. °C	-88 °C
diffractometer	Enraf-Nonius CAD4
radiation	MoKα (0.71073 Å)
monochromator	highly oriented graphite
scan range, type	$3.0° \leq 2\Theta \leq 45°$, $\Theta - 2\Theta$
scan width, deg.	$\Delta\Theta = 0.80 + 0.35\ (\tan\Theta)$
octants collected	+ h, + k, ± l
reflections collected	5505
unique reflections	4962
reflections, $F_o^2 > 3\sigma(F_o^2)$	3996
variables	388
R	0.0335
R_w	0.0400
R_{all}	0.0470
GOF	1.811
largest Δ/σ in final LS cycle	0.01

$(Me_5C_5)_2Yb(\mu\text{-}Me)Ti(Me_5C_5)_2$

Brown crystals of the complex were grown from a toluene solution at -20 °C. The crystals were placed in Paratone N oil[19] and one was selected and cut to approximate dimensions of 0.32 mm × 0.30 mm × 0.21 mm. The crystal was mounted on the end of a cut quartz capillary tube and placed under a flow of cold nitrogen on an Enraf-Nonius CAD4 diffractometer.[20] The solidified oil held the crystal in place and protected it from decomposition. The temperature was stabilized at -103 °C with an automated cold flow apparatus.

After centering the crystal in the X-ray beam, a set of accurate cell dimensions and an orientation matrix were determined by a least-squares fit to the setting angles of the unresolved MoKα components of 24 symmetry related reflections. The dimensions and volume of the unit cell suggested triclinic symmetry with two molecules in the unit cell. Details of the unit cell, collection parameters, and structure refinement are listed in Table 6.

A set of three standard reflections (4, -4, 4; 0, -6, 4; -3, 1, 9) was chosen to monitor intensity and crystal orientation. The intensity was checked after every hour of X-ray exposure time. Examination of the intensity standards showed a slight linear decay over the course of the data collection. The decay was expressed as a linear function and a correction was applied to the data. The crystal orientation was checked after every 200 reflections and was reoriented if any of the standard reflections were offset from their predicted position by more than 0.1°. The crystal orientation matrix was reoriented four times during the data collection.

The 5026 raw data were converted to structure factor amplitudes and their esds by correction for scan speed, background, and Lorentz-polarization effects.[21,22,23] An empirical absorption correction was applied to the data based on averaged azimuthal psi scans for three reflections with $\chi > 80°$.[24] Examination of the azimuthal scans showed a variation of $I_{min}/I_{max} = 0.93$ for the average relative intensity curve.

The coordinates of the ytterbium atom were determined by Patterson methods. The locations of all non-hydrogen atoms were determined through the use of standard Fourier techniques and refined by least-squares methods. All non-hydrogen atoms were refined anisotropically. A difference Fourier map revealed the positions of all hydrogen atoms associated with the permethylcyclopentadienyl rings. These atoms were placed in calculated positions and included in the structure factor calculations but not refined. All hydrogen atoms were given isotropic thermal parameters 1.2 times the B(iso) of the atom to which they were bonded. Subsequent difference Fourier maps revealed positions for the three hydrogen atoms on the bridging methyl group. These coordinates were input and refined isotropically.

Final refinement of the 400 variables using the 4493 data for which $F_o^2 > 3\sigma(F_o^2)$ gave residuals of $R = 0.0298$ and $R_w = 0.0399$. The R value based on all 4954 unique data was 0.0344 and the goodness-of-fit parameter was 1.982. The least-squares program minimized the expression, $\Sigma w(|F_o| - |F_c|)^2$, where w is the weight of a given observation. A value of 0.03 for the p-factor was used to reduce the weight of intense reflections in the refinements.[25] The

analytical forms of the scattering factor tables for the neutral atoms[26] were used and all non-hydrogen scattering factors were corrected for both real and imaginary components of anomalous dispersion.[27]

The data were evaluated through the residuals over ranges of $\sin\Theta/\lambda$, $|F_o|$, parity, and individual indices. No unusual features or trends were observed. The highest and lowest peaks in the final difference Fourier map had electron densities of 1.018 and -0.147 e/Å^3, respectively.

Table 6. Crystal Data for $(Me_5C_5)_2Yb(\mu\text{-}Me)Ti(Me_5C_5)_2$

Formula	$C_{41}H_{63}TiYb$
FW	776.89
Space Group	$P\bar{1}$ (No. 2)
a, Å	10.956 (2)
b, Å	11.029 (3)
c, Å	16.280 (3)
α, deg.	94.35 (2)
β, deg.	102.46 (2)
γ, deg.	96.14 (2)
V, $Å^3$	1900 (2)
Z	2
F(000)	401
d(calc.), g/cm^3	1.358
μ(calc.), 1/cm	26.72
size, mm	0.32 × 0.30 × 0.21
temp. °C	-103 °C
diffractometer	Enraf-Nonius CAD4
radiation	MoKα (0.71073 Å)
monochromator	highly oriented graphite
scan range, type	$3.0° \leq 2\Theta \leq 45°$, $\Theta - 2\Theta$
scan width, deg.	$\Delta\Theta = 0.75 + 0.35 (\tan\Theta)$
octants collected	+ h, ± k, ± l
reflections collected	5026
unique reflections	4954
reflections, $F_o^2 > 3\sigma(F_o^2)$	4493
variables	400
R	0.0298
R_w	0.0399
R_{all}	0.0344
GOF	1.982
largest Δ/σ in final LS cycle	0.01

References

1. Perrin, D. D.; Armarego, W. L. F.; Perrin, D. R., "Purification of Laboratory Materials," Pergamon: Oxford, **1980**. (b) Gordon, A. J.; Ford, R. A., "The Chemist's Companion: A Handbook of Practical Data, Techniques, and References," Wiley-Interscience: New York, **1972**.

2. Tilley, T. D., Ph.D. Thesis, University of California, Berkeley, **1982**.

3. Burns, C. J., Ph.D. Thesis, University of California, Berkeley, **1987**.

4. Berg, D. J., Ph.D. Thesis, University of California, Berkeley, **1987**.

5. (a) Jones, M. M., *J. Am. Chem. Soc.*, **1959**, *81*, 3188. (b) Mikami, M.; Nakagawa, I.; Shimanouchi, T., *Spectrochim. Acta.*, **1967**, *23A*, 1037. (c) Nakamoto, K., "Infrared and Raman Spectra of Inorganic and Coordination Compounds," 4th Ed., Wiley-Interscience: New York, **1986**.

6. Hoffman, E. G., *Trans. Faraday Soc.*, **1962**, *58*, 642.

7. Ikariya, T.; Yamamoto, A., *J. Organomet. Chem.*, **1974**, *72*, 145.

8. (a) Lappert, M. F.; Pearce, R., *J. Chem. Soc., Chem. Commun.*, **1973**, 24. (b) Jarvis, J. A. J.; Pearce, R.; Lappert, M. F., *J. Chem. Soc., Dalton Trans.*, **1977**, 999.

9. Robbins, J. L.; Edelstein, N.; Spencer, B.; Smart, J. C., *J. Am. Chem. Soc.*, **1982**, *104*, 1882.

10. Keller, R. N.; Wycoff, H. D. in "Inorganic Syntheses," Vol. II, Fernelius, W. C., ed., McGraw-Hill: New York, **1946**, p. 1.

11. (a) Curtis, C. J.; Smart, J. C.; Robbins, J. L., *Organometallics*, **1985**, *4*, 1283. (b) Gambarotta, S.; Floriani, C.; Chiesi-Villa, A.; Guastini, C.; *Inorg. Chem.*, **1984**, *23*, 1739.

12. Bottomley, F.; Darkwa, J.; White, P. S., *Organometallics*, **1985**, *4*, 961.

13. (a) Bottomley, F.; Magill, C. P.; Zhao, B, *Organometallics*, **1990**, *9*, 1700. (b) Bottomley, F.; Magill, C. P.; Zhao, B., *Organometallics*, **1991**, *10*, 1946.

14. (a) Tilley, T. D.; Andersen, R. A., *Inorg. Chem.*, **1981**, *20*, 3267. (b) Watson, P. L.; Whitney, J. F.; Harlow, R. L., *Inorg. Chem.*, **1981**, *20*, 3271.

15. Osborne, J. H.; Rheingold, A. L.; Trogler, W. C., *J. Am Chem. Soc.*, **1985**, *107*, 7945.

16. (a) Burns, C. J.; Andersen, R. A., *J. Chem. Soc., Chem. Commun.*, **1989**, 136. (b) Burns, C. J.; Berg, D. J.; Andersen, R. A., *J. Chem. Soc., Chem. Commun.*, **1987**, 272.

17. Pattiasina, J. W.; Heeres, H. J.; van Bolhuis, F.; Meetsma, A.; Teuben, J. H.; Spek, A. L., *Organometallics*, **1987**, *6*, 1004.

18. Luinstra, G. A.; ten Cate, L. C.; Heeres, H. J.; Pattiasina, J. W.; Meetsma, A.; Teuben, J. H., *Organometallics*, **1991**, *10*, 3227.

19. Paratone N oil is a viscous commercial oil available from Exxon Chemical Company, Houston, TX. The oil was degassed prior to use.

20. Instrumentation at the University of California Chemistry Department X-ray Crystallographic Facility (CHEXRAY) consists of two Enraf-Nonius CAD-4 diffractometers controlled by a DEC Microvax II and equipped with departmentally constructed low temperature systems. Both use Enraf-Nonius software as described in the "CAD-4 Operations Manual, Version 5.0," Enraf-Nonius, Delft, The Netherlands, **1977**, updated **1989**.

21. All calculations were performed on a DEC Microvax II or a DEC Microvax 4000 using locally modified Nonius-SDP software operating under Micro-VMS operating system.

22. (a) Frenz, B. A., "Structure Determination Package Users Guide," Texas A & M University and Enraf-Nonius: College Station, TX and The Netherlands, **1985**. (b) Fair, C. K., "MolEN Molecular Structure Solution Procedures," Enraf-Nonius, Delft Instruments, X-ray Diffraction B. V., The Netherlands, **1990**.

23. The data reduction formulae are:

$$F_o^2 = \frac{\omega}{L_p}(C - 2B) \qquad \sigma_o(F_o^2) = \frac{\omega}{L_p}(C + 4B)^{1/2}$$

$$F_o = (F_o^2)^{1/2} \qquad \sigma_o(F) = [F_o^2 + \sigma_o(F_o^2)]^{1/2} - F_o$$

where C is the total count in the scan, B is the sum of the two background counts, ω is the scan speed used in deg/min, and

$$\frac{1}{L_p} = \frac{\sin 2\Theta(1 + \cos^2 2\Theta_m)}{1 + \cos^2 2\Theta_m - \sin^2 2\Theta}$$

is the correction for Lorentz and polarization effects for a reflection with scattering angle 2Θ and radiation monochromatized with a 50% perfect single-crystal monochromator with scattering angle $2\Theta_m$.

24. Reflections used for azimuthal scans were located near $\chi = 90°$ and the intensities were measured at 10° increments of rotation of the crystal about the diffraction vector.

25. $$R = \frac{\Sigma||F_o| - |F_c||}{\Sigma|F_o|} \qquad wR = \sqrt{\frac{\Sigma w(|F_o| - |F_c|)^2}{\Sigma w F_o^2}}$$

$$GOF = \sqrt{\frac{\Sigma w(|F_o| - |F_c|)^2}{(n_o - n_v)}}$$

where n_o is the number of observations, n_v is the number of variable parameters, and the weights, w, were given by

$$w = \frac{1}{\sigma^2(F_o)} \qquad \sigma(F_o^2) = \sqrt{\sigma_o^2(F_o^2) + (pF^2)^2}$$

where $\sigma^2(F_o)$ was calculated as above from $\sigma(F_o^2)$ and where p is the factor used to lower the weight of intense reflections.

26. Cromer, D. T.; Waber, J. T., "International Tables for X-ray Crystallography," Vol. IV, The Kynoch Press: Birmingham, England, **1974**, Table 2.2B.

27. Cromer, D. T., *ibid.*, Table 2.3.1.

28. Zachariesen, W. H., *Acta. Cryst.*, **1983**, *16*, 1139.

Appendix I. Tables of Positional and Thermal Parameters

$(Me_5C_5)_2YbMe$

Table of Positional Parameters and Their Estimated Standard Deviations

Atom	x	y	z	B(A2)
YB1	Ø.17397(5)	Ø.62724(2)	Ø.89942(4)	1.78(1)
YB2	-Ø.16798(5)	Ø.64534(2)	Ø.54869(4)	1.78(1)
C1	-Ø.ØØ1(1)	Ø.6389(4)	Ø.7415(8)	1.9(3)
C2	-Ø.Ø42(1)	Ø.71Ø4(4)	Ø.5135(9)	2.7(3)
C11	-Ø.289(1)	Ø.7138(4)	Ø.6177(8)	2.4(3)
C12	-Ø.337(1)	Ø.6687(5)	Ø.6413(8)	2.3(3)
C13	-Ø.413(1)	Ø.6465(5)	Ø.549(1)	3.3(3)
C14	-Ø.4Ø9(1)	Ø.6782(4)	Ø.472Ø(8)	2.7(3)
C15	-Ø.337(1)	Ø.7199(4)	Ø.5124(9)	2.8(3)
C16	-Ø.216(1)	Ø.7521(5)	Ø.6918(9)	3.4(3)
C17	-Ø.322(1)	Ø.65Ø9(5)	Ø.744(1)	3.9(3)
C18	-Ø.497(1)	Ø.6Ø15(7)	Ø.545(1)	6.Ø(5)
C19	-Ø.493(2)	Ø.6726(7)	Ø.366(1)	7.3(5)
C2Ø	-Ø.324(1)	Ø.7649(5)	Ø.455(1)	4.8(4)
C21	-Ø.Ø35(1)	Ø.5629(4)	Ø.5413(8)	2.6(3)
C22	-Ø.168(1)	Ø.5491(4)	Ø.5188(8)	2.5(3)
C23	-Ø.236(1)	Ø.5689(5)	Ø.4236(9)	2.9(3)
C24	-Ø.146(1)	Ø.5979(5)	Ø.3922(9)	3.Ø(3)
C25	-Ø.Ø21(1)	Ø.593Ø(5)	Ø.4633(8)	2.4(3)
C26	Ø.Ø78(1)	Ø.542Ø(5)	Ø.626Ø(9)	3.3(3)
C27	-Ø.222(1)	Ø.5133(5)	Ø.575(1)	4.7(4)
C28	-Ø.369(2)	Ø.553Ø(6)	Ø.357(1)	5.7(4)
C29	-Ø.175(1)	Ø.6215(5)	Ø.292(1)	4.6(4)
C3Ø	Ø.1Ø1(1)	Ø.6126(5)	Ø.45Ø(1)	4.2(4)
C31	Ø.Ø35(1)	Ø.5941(4)	1.ØØØ8(8)	2.3(3)
C32	Ø.Ø27(1)	Ø.5569(4)	Ø.9292(8)	2.1(3)
C33	Ø.153(1)	Ø.5368(4)	Ø.954Ø(8)	2.8(3)
C34	Ø.236(1)	Ø.5598(5)	1.Ø395(8)	2.5(3)
C35	Ø.163(1)	Ø.5954(4)	1.Ø673(8)	2.5(3)
C36	-Ø.Ø76(1)	Ø.627Ø(5)	1.ØØ7(1)	4.2(3)
C37	-Ø.Ø94(1)	Ø.537Ø(5)	Ø.853(1)	3.8(3)
C38	Ø.192(1)	Ø.4923(5)	Ø.9Ø2(1)	4.3(4)
C39	Ø.371(1)	Ø.54Ø7(6)	1.1ØØ(1)	4.9(4)
C4Ø	Ø.2Ø2(1)	Ø.6269(6)	1.163(1)	4.8(4)
C41	Ø.325(1)	Ø.666Ø(4)	Ø.8126(8)	1.9(2)
C42	Ø.4Ø6(1)	Ø.6374(4)	Ø.8911(8)	2.Ø(2)
C43	Ø.411(1)	Ø.66Ø3(5)	Ø.9834(9)	2.8(3)
C44	Ø.329(1)	Ø.7Ø28(4)	Ø.9577(9)	2.5(3)
C45	Ø.276(1)	Ø.7Ø54(4)	Ø.8519(8)	2.1(3)
C46	Ø.3Ø6(1)	Ø.6569(5)	Ø.7Ø38(9)	3.7(3)
C47	Ø.485(1)	Ø.5927(5)	Ø.885(1)	4.2(4)
C48	Ø.5Ø8(1)	Ø.65Ø7(6)	1.ØØØ(1)	4.8(4)
C49	Ø.317(1)	Ø.74Ø9(5)	1.Ø31(1)	4.9(4)
C5Ø	Ø.191(1)	Ø.7465(5)	Ø.794(1)	4.Ø(4)

Starred atoms were included with isotropic thermal parameters.
The thermal parameter given for anisotropically refined atoms is the isotropic equivalent thermal parameter defined as:
(4/3) * [a2*B(1,1) + b2*B(2,2) + c2*B(3,3) + ab(cos gamma)*B(1,2) + ac(cos beta)*B(1,3) + bc(cos alpha)*B(2,3)]
where a,b,c are real cell parameters, and B(i,j) are anisotropic betas.

Table of Anisotropic Thermal Parameters - B's

Name	B(1,1)	B(2,2)	B(3,3)	B(1,2)	B(1,3)	B(2,3)	Beqv
YB1	1.61(2)	1.91(2)	1.56(2)	-0.39(2)	0.16(1)	0.32(2)	1.78(1)
YB2	1.75(2)	1.87(2)	1.48(2)	0.48(2)	0.19(1)	-0.22(2)	1.78(1)
C1	2.8(5)	1.6(5)	0.9(4)	0.5(4)	-0.1(4)	0.9(4)	1.9(3)
C2	1.9(5)	2.4(5)	3.7(6)	0.4(4)	0.8(4)	0.0(5)	2.7(3)
C11	2.2(5)	2.9(5)	2.3(5)	1.0(4)	0.7(4)	-0.2(4)	2.4(3)
C12	1.9(4)	3.7(6)	1.4(4)	-0.0(4)	0.8(3)	0.3(4)	2.3(3)
C13	0.6(4)	2.5(5)	6.6(7)	0.5(4)	0.9(4)	-1.1(5)	3.3(3)
C14	2.3(5)	3.5(6)	1.6(5)	1.5(4)	-0.2(4)	-0.7(4)	2.7(3)
C15	2.5(4)	3.1(5)	3.4(5)	2.3(4)	1.9(3)	0.5(4)	2.8(3)
C16	3.8(6)	3.2(6)	3.4(5)	0.8(5)	1.4(4)	-0.9(5)	3.4(3)
C17	4.0(6)	4.1(7)	4.1(6)	1.6(5)	1.9(4)	0.9(5)	3.9(3)
C18	2.8(6)	6.4(9)	10(1)	-0.4(6)	2.8(5)	-1.5(8)	6.0(5)
C19	5.8(8)	11(1)	3.3(7)	4.8(7)	-0.9(6)	-3.0(7)	7.3(5)
C20	5.2(6)	5.7(7)	4.2(6)	3.2(6)	2.5(5)	3.3(5)	4.8(4)
C21	4.0(5)	2.4(5)	1.0(4)	1.0(4)	0.3(4)	-1.0(4)	2.6(3)
C22	4.7(6)	1.4(5)	1.5(4)	0.2(4)	1.2(4)	-0.9(4)	2.5(3)
C23	2.6(5)	2.8(5)	2.5(5)	0.5(4)	-0.3(4)	-1.7(4)	2.9(3)
C24	3.9(5)	2.2(5)	2.6(5)	1.2(4)	0.8(4)	0.1(4)	3.0(3)
C25	2.7(5)	2.8(5)	1.8(4)	0.7(4)	0.7(4)	-0.0(4)	2.4(3)
C26	3.7(5)	3.2(6)	2.4(5)	1.9(5)	0.3(4)	-0.6(5)	3.3(3)
C27	5.8(7)	2.4(6)	5.4(8)	-1.1(6)	1.2(6)	0.2(6)	4.7(4)
C28	5.3(8)	5.7(8)	4.5(7)	-0.4(7)	-0.6(6)	-2.0(6)	5.7(4)
C29	5.9(7)	4.4(7)	2.9(6)	1.7(6)	0.7(5)	0.7(6)	4.6(4)
C30	5.5(7)	4.0(7)	3.1(6)	1.1(5)	1.4(5)	-1.0(5)	4.2(4)
C31	3.4(5)	1.2(5)	2.6(5)	-0.7(4)	1.3(4)	0.3(4)	2.3(3)
C32	1.8(4)	1.6(5)	2.2(5)	-0.2(4)	-0.2(4)	1.0(4)	2.1(3)
C33	3.4(5)	2.6(5)	2.5(5)	-0.0(4)	1.2(4)	1.8(4)	2.8(3)
C34	1.9(5)	3.5(6)	1.9(5)	-0.2(4)	0.1(4)	1.0(4)	2.5(3)
C35	3.8(5)	2.2(5)	1.4(4)	-2.1(4)	0.9(4)	-0.4(4)	2.5(3)
C36	6.2(6)	2.7(6)	5.2(6)	-0.2(5)	3.9(4)	0.8(5)	4.2(3)
C37	4.3(6)	3.0(6)	2.8(6)	-1.2(5)	-0.7(5)	0.2(5)	3.8(3)
C38	7.1(7)	2.0(6)	4.6(6)	0.3(5)	3.0(5)	0.8(5)	4.3(4)
C39	2.3(6)	7.1(8)	4.7(6)	0.2(5)	0.1(5)	4.3(5)	4.9(4)
C40	5.4(7)	5.2(8)	3.4(6)	-2.3(6)	1.0(5)	-0.8(6)	4.8(4)
C41	1.9(4)	1.7(5)	2.5(5)	-0.7(4)	1.1(3)	-0.2(4)	1.9(2)
C42	2.5(4)	1.3(5)	2.8(5)	-0.3(4)	1.5(3)	0.6(4)	2.0(2)
C43	2.7(5)	3.3(6)	2.6(5)	-1.1(4)	1.1(4)	-0.4(4)	2.8(3)
C44	2.3(4)	2.3(5)	3.3(5)	-1.3(4)	1.1(4)	-1.0(4)	2.5(3)
C45	2.5(5)	1.3(5)	2.4(5)	-0.4(4)	0.5(4)	0.6(4)	2.1(3)
C46	4.2(5)	5.0(7)	2.4(5)	-0.8(5)	1.9(4)	0.5(5)	3.7(3)
C47	2.9(5)	4.1(7)	5.7(7)	1.0(5)	1.4(5)	1.6(6)	4.2(4)
C48	3.0(5)	7.2(8)	3.2(6)	-3.5(5)	-0.5(5)	0.3(6)	4.8(4)
C49	5.8(7)	3.4(7)	5.7(8)	-1.6(6)	2.1(6)	-1.8(6)	4.9(4)
C50	2.3(5)	2.4(6)	6.6(8)	-0.2(5)	0.5(5)	1.3(6)	4.0(4)

The form of the anisotropic temperature factor is:
exp[-0.25(h2a2B(1,1) + k2b2B(2,2) + l2c2B(3,3) + 2hkabB(1,2) + 2hlacB(1,3) + 2klbcB(2,3))] where a,b, and c are reciprocal lattice constants.

$[(Me_5C_5)_2Yb]_2(\mu\text{-}Me)$

Table of Positional Parameters and Their Estimated Standard Deviations

Atom	x	y	z	B(A2)
YB1	Ø.39431(2)	-Ø.37792(2)	Ø.24862(1)	1.715(6)
YB2	Ø.Ø55ØØ(2)	-Ø.ØØ3387(2)	Ø.25759(2)	2.ØØ17(6)
C1	Ø.25Ø6(5)	-Ø.2ØØ2(5)	Ø.2585(3)	1.5(1)
C11	Ø.4165(6)	-Ø.3975(5)	Ø.4Ø24(4)	2.Ø(1)
C12	Ø.5Ø93(6)	-Ø.4798(5)	Ø.3684(3)	1.9(1)
C13	Ø.4416(6)	-Ø.5718(5)	Ø.3531(4)	2.2(1)
C14	Ø.3ØØ2(6)	-Ø.5447(5)	Ø.3742(4)	2.1(1)
C15	Ø.2932(6)	-Ø.4382(6)	Ø.4Ø67(4)	2.Ø(1)
C16	Ø.4467(7)	-Ø.2913(6)	Ø.4327(4)	3.4(2)
C17	Ø.6511(6)	-Ø.4776(7)	Ø.3639(4)	3.1(2)
C18	Ø.5Ø17(8)	-Ø.6892(6)	Ø.33Ø9(4)	3.3(2)
C19	Ø.2Ø23(7)	-Ø.6178(6)	Ø.3668(4)	3.3(2)
C2Ø	Ø.1656(6)	-Ø.3864(7)	Ø.4492(4)	3.Ø(2)
C21	Ø.5536(6)	-Ø.29ØØ2(6)	Ø.1136(4)	2.3(1)
C22	Ø.5861(6)	-Ø.4167(6)	Ø.1314(3)	2.1(1)
C23	Ø.4822(6)	-Ø.4788(6)	Ø.1213(4)	2.2(1)
C24	Ø.3878(6)	-Ø.3911(6)	Ø.ØØ961(4)	2.3(1)
C25	Ø.4319(6)	-Ø.2759(6)	Ø.ØØØ6(4)	2.2(1)
C26	Ø.6339(7)	-Ø.1914(7)	Ø.1181(5)	3.8(2)
C27	Ø.7153(7)	-Ø.47Ø8(7)	Ø.146Ø(4)	3.5(2)
C28	Ø.4787(8)	-Ø.61Ø9(6)	Ø.1239(4)	3.6(2)
C29	Ø.2675(7)	-Ø.4175(7)	Ø.Ø723(4)	3.6(2)
C3Ø	Ø.3727(7)	-Ø.1565(7)	Ø.Ø531(4)	3.6(2)
C31	Ø.Ø5ØØ(6)	Ø.2Ø27(5)	Ø.2481(4)	2.4(1)
C32	Ø.1632(6)	Ø.18Ø8(6)	Ø.19Ø1(4)	2.8(1)
C33	Ø.251Ø(6)	Ø.113Ø(5)	Ø.2364(4)	2.6(1)
C34	Ø.192Ø(6)	Ø.ØØ915(6)	Ø.3223(4)	2.3(1)
C35	Ø.ØØ674(6)	Ø.1471(6)	Ø.3292(4)	2.6(1)
C36	-Ø.ØØ619(8)	Ø.2875(7)	Ø.2289(6)	4.8(2)
C37	Ø.187Ø(8)	Ø.225Ø(8)	Ø.ØØ964(5)	4.8(2)
C38	Ø.3895(7)	Ø.ØØ775(7)	Ø.1997(5)	4.2(2)
C39	Ø.2554(7)	Ø.ØØ296(7)	Ø.3931(5)	3.7(2)
C4Ø	-Ø.ØØ253(8)	Ø.1559(7)	Ø.41Ø7(5)	3.9(2)
C41	-Ø.2ØØ4(6)	-Ø.ØØ553(5)	Ø.289Ø(4)	2.2(1)
C42	-Ø.1588(6)	-Ø.ØØ3Ø6(6)	Ø.2ØØ8(4)	2.7(1)
C43	-Ø.ØØ848(6)	-Ø.1319(6)	Ø.1781(4)	2.3(1)
C44	-Ø.ØØ832(6)	-Ø.2196(5)	Ø.2525(4)	2.1(1)
C45	-Ø.1514(6)	-Ø.1714(5)	Ø.3215(4)	2.Ø(1)
C46	-Ø.2937(7)	Ø.ØØ216(6)	Ø.3399(4)	3.3(2)
C47	-Ø.1994(7)	Ø.ØØ783(7)	Ø.1398(5)	3.7(2)
C48	-Ø.ØØ259(7)	-Ø.1477(7)	Ø.ØØØ8(4)	3.5(2)
C49	-Ø.ØØ254(6)	-Ø.3468(6)	Ø.2575(4)	3.1(2)
C5Ø	-Ø.1739(7)	-Ø.2328(6)	Ø.4129(4)	2.9(2)

Starred atoms were included with isotropic thermal parameters.
The thermal parameter given for anisotropically refined atoms is the isotropic equivalent thermal parameter defined as:
(4/3) * [a2*B(1,1) + b2*B(2,2) + c2*B(3,3) + ab(cos gamma)*B(1,2) + ac(cos beta)*B(1,3) + bc(cos alpha)*B(2,3)]
where a,b,c are real cell parameters, and B(i,j) are anisotropic betas.

Table of Anisotropic Thermal Parameters - B's

Name	B(1,1)	B(2,2)	B(3,3)	B(1,2)	B(1,3)	B(2,3)	Beqv
Y81	1.87(1)	1.97(1)	1.335(9)	0.133(9)	-0.423(8)	-0.426(8)	1.715(6)
Y82	1.80(1)	1.87(1)	2.62(1)	-0.022(9)	-0.777(9)	-0.676(9)	2.017(6)
C1	1.5(2)	1.0(2)	1.3(2)	0.8(2)	-0.1(2)	0.3(2)	1.5(1)
C11	2.4(2)	2.5(2)	1.5(2)	0.3(2)	-0.7(2)	-0.7(2)	2.0(1)
C12	2.2(2)	2.5(2)	1.2(2)	0.2(2)	-0.9(2)	-0.2(2)	1.9(1)
C13	3.0(3)	2.0(2)	1.5(2)	0.7(2)	-0.7(2)	-0.3(2)	2.2(1)
C14	2.4(2)	2.2(2)	1.6(2)	-0.3(2)	-0.7(2)	0.0(2)	2.1(1)
C15	2.1(2)	2.7(3)	1.4(2)	0.6(2)	-0.7(2)	-0.6(2)	2.0(1)
C16	4.3(3)	3.8(3)	2.7(3)	-0.5(3)	-1.6(2)	-1.1(2)	3.4(2)
C17	2.4(3)	4.7(3)	2.4(3)	0.3(3)	-1.0(2)	-0.5(2)	3.1(2)
C18	5.3(4)	2.3(3)	2.6(3)	0.6(3)	-1.1(3)	-1.2(2)	3.3(2)
C19	4.1(3)	3.2(3)	2.6(3)	-1.2(2)	-0.9(2)	-0.2(2)	3.3(2)
C20	2.4(3)	4.2(3)	2.0(3)	1.1(3)	-0.1(2)	-0.5(2)	3.0(2)
C21	2.4(2)	2.8(3)	1.7(2)	-0.8(2)	-0.4(2)	-0.6(2)	2.3(1)
C22	2.1(2)	3.3(3)	1.1(2)	-0.1(2)	-0.3(2)	-0.8(2)	2.1(1)
C23	2.3(3)	2.7(3)	1.5(2)	-0.1(2)	0.2(2)	-0.8(2)	2.2(1)
C24	1.6(2)	3.8(3)	1.8(2)	-0.2(2)	-0.2(2)	-1.1(2)	2.3(1)
C25	2.7(3)	2.8(3)	1.3(2)	0.1(2)	-0.4(2)	-0.5(2)	2.2(1)
C26	3.3(3)	4.7(3)	3.4(3)	-1.5(3)	0.1(3)	-1.4(3)	3.8(2)
C27	2.5(3)	5.3(4)	2.6(3)	0.6(3)	-0.6(2)	-1.0(3)	3.5(2)
C28	4.9(4)	3.5(3)	2.6(3)	-0.8(3)	-0.4(3)	-1.1(2)	3.6(2)
C29	2.9(3)	5.7(3)	2.9(3)	-0.0(3)	-0.8(2)	-2.4(2)	3.6(2)
C30	3.8(3)	4.2(3)	2.2(3)	0.3(3)	-0.6(2)	0.5(3)	3.6(2)
C31	2.4(2)	1.8(2)	3.6(3)	-0.3(2)	-1.1(2)	-1.1(2)	2.4(1)
C32	3.4(3)	2.9(3)	2.1(2)	-1.3(2)	-0.5(2)	-0.6(2)	2.8(1)
C33	2.8(3)	2.1(2)	2.9(3)	-0.3(2)	0.1(2)	-1.4(2)	2.6(1)
C34	2.4(2)	2.2(2)	2.5(2)	-0.2(2)	-0.9(2)	-0.5(2)	2.3(1)
C35	2.4(3)	2.3(2)	3.0(3)	-0.4(2)	-0.0(2)	-1.1(2)	2.6(1)
C36	4.4(3)	2.2(3)	8.7(4)	0.4(3)	-3.6(3)	-1.0(3)	4.8(2)
C37	6.3(4)	5.5(4)	2.9(3)	-2.5(3)	-1.6(3)	-0.1(3)	4.8(2)
C38	3.1(3)	3.7(3)	6.0(4)	-0.8(3)	0.7(3)	-2.8(2)	4.2(2)
C39	4.4(3)	3.3(3)	3.8(3)	-0.2(3)	-1.8(2)	-0.5(3)	3.7(2)
C40	3.9(3)	4.3(3)	3.9(3)	-1.1(3)	0.6(3)	-2.6(2)	3.9(2)
C41	1.6(2)	2.0(2)	3.2(3)	0.0(2)	-0.6(2)	-1.3(2)	2.2(1)
C42	2.0(2)	3.1(3)	3.1(3)	-0.6(2)	-1.1(2)	-0.2(2)	2.7(1)
C43	1.7(2)	3.0(3)	2.4(2)	-0.3(2)	-0.6(2)	-0.7(2)	2.3(1)
C44	1.9(2)	2.2(2)	2.5(2)	-0.1(2)	-0.8(2)	-0.8(2)	2.1(1)
C45	1.8(2)	2.5(2)	1.8(2)	-0.2(2)	-0.5(2)	-0.8(2)	2.0(1)
C46	2.7(3)	3.6(3)	3.8(3)	0.1(2)	-0.6(2)	-1.7(2)	3.3(2)
C47	3.6(3)	3.7(3)	4.1(3)	-0.2(3)	-2.1(2)	0.1(3)	3.7(2)
C48	2.6(3)	5.4(4)	2.6(3)	-0.5(3)	-0.5(2)	-1.1(3)	3.5(2)
C49	2.5(3)	2.9(3)	4.3(3)	0.2(2)	-1.0(2)	-1.6(2)	3.1(2)
C50	3.0(3)	3.2(3)	2.6(3)	-0.4(2)	-0.7(2)	-0.7(2)	2.9(2)

The form of the anisotropic temperature factor is:
exp[-0.25(h2a2B(1,1) + k2b2B(2,2) + l2c2B(3,3) + 2hkabB(1,2) + 2hlacB(1,3) + 2klbcB(2,3))] where a,b, and c are reciprocal lattice constants.

$(Me_5C_5)_2Yb(\mu\text{-}NH_2)_2AlMe_2$

Table of Positional Parameters and Their Estimated Standard Deviations

Atom	x	y	z	B(A2)
YB	Ø.21263(4)	Ø.28732(4)	Ø.25ØØ2(3)	1.162(7)
AL	Ø.ØØ85(3)	Ø.4718(3)	Ø.75Ø2(3)	1.78(6)
N1	Ø.ØØ69(8)	Ø.4558(8)	Ø.3658(6)	1.8(2)
N2	Ø.ØØ52(8)	Ø.4Ø28(8)	Ø.1341(7)	1.8(2)
C1	Ø.211(1)	Ø.49Ø(1)	Ø.6935(9)	2.7(2)
C2	Ø.ØØ9(1)	Ø.289(1)	Ø.8ØØ7(9)	2.6(2)
C11	Ø.178(1)	Ø.1Ø46(9)	Ø.4214(8)	1.8(2)
C12	Ø.2546(9)	Ø.ØØ82(9)	Ø.3276(8)	1.8(2)
C13	Ø.174(1)	Ø.ØØ37(9)	Ø.2296(8)	1.7(2)
C14	Ø.ØØ8(1)	Ø.1119(9)	Ø.2637(8)	1.9(2)
C15	Ø.ØØ91(9)	Ø.1494(9)	Ø.3823(8)	1.7(2)
C16	Ø.222(1)	Ø.112(1)	Ø.5435(9)	2.5(2)
C17	Ø.384(1)	-Ø.ØØ55(1)	Ø.344(1)	2.8(2)
C18	Ø.214(1)	-Ø.Ø18(1)	Ø.1123(9)	2.8(2)
C19	-Ø.Ø73(1)	Ø.126(1)	Ø.191(1)	2.9(2)
C2Ø	-Ø.Ø67(1)	Ø.2Ø4(1)	Ø.4631(9)	2.6(2)
C21	Ø.3959(9)	Ø.322(1)	Ø.Ø788(8)	1.8(2)
C22	Ø.3518(9)	Ø.45Ø5(9)	Ø.1174(8)	1.7(2)
C23	Ø.3869(9)	Ø.4539(9)	Ø.2363(8)	1.9(2)
C24	Ø.453(1)	Ø.326(1)	Ø.27ØØ9(8)	1.9(2)
C25	Ø.4615(9)	Ø.2453(9)	Ø.1718(8)	1.6(2)
C26	Ø.387(1)	Ø.279(1)	-Ø.Ø441(8)	2.6(2)
C27	Ø.296(1)	Ø.567(1)	Ø.ØØ37(1)	2.8(2)
C28	Ø.374(1)	Ø.573(1)	Ø.3Ø75(9)	2.9(2)
C29	Ø.517(1)	Ø.287(1)	Ø.3875(9)	2.9(2)
C3Ø	Ø.554(1)	Ø.116(1)	Ø.1552(9)	2.8(2)
HA	Ø.154(9)	Ø.5Ø4(9)	Ø.384(8)	2(2)*
HB	Ø.ØØ53(9)	Ø.417(9)	Ø.437(8)	3(2)*
HD	Ø.ØØ8(1)	Ø.44(1)	Ø.ØØ7(1)	5(3)*
HC	-Ø.ØØØ8(8)	Ø.356(8)	Ø.118(7)	1(2)*

Starred atoms were included with isotropic thermal parameters.
The thermal parameter given for anisotropically refined atoms is the isotropic equivalent thermal parameter defined as:
(4/3) * [a2*B(1,1) + b2*B(2,2) + c2*B(3,3) + ab(cos gamma)*B(1,2) + ac(cos beta)*B(1,3) + bc(cos alpha)*B(2,3)]
where a,b,c are real cell parameters, and B(i,j) are anisotropic betas.

Table of Anisotropic Thermal Parameters - B's

Name	B(1,1)	B(2,2)	B(3,3)	B(1,2)	B(1,3)	B(2,3)	Beqv
Y8	1.85(1)	1.26(1)	0.51(1)	-0.66(1)	0.24(1)	-0.26(1)	1.162(7)
AL	2.3(1)	1.7(1)	1.3(1)	-0.34(9)	0.24(9)	-0.11(9)	1.78(6)
N1	2.4(3)	2.0(3)	1.1(3)	-0.8(3)	0.3(3)	-0.4(3)	1.8(2)
N2	2.2(3)	2.1(3)	1.3(3)	-1.3(3)	0.3(3)	-0.3(3)	1.8(2)
C1	3.2(5)	3.3(5)	1.4(4)	-0.4(4)	-0.0(4)	0.2(4)	2.7(2)
C2	3.8(5)	2.3(4)	1.6(4)	-0.6(4)	1.0(4)	-0.5(3)	2.6(2)
C11	3.1(4)	1.2(4)	1.3(4)	-0.7(3)	0.2(3)	-0.3(3)	1.8(2)
C12	2.0(4)	1.9(4)	1.3(4)	-0.4(3)	0.5(3)	-0.0(3)	1.8(2)
C13	3.2(4)	1.0(3)	1.2(3)	-1.2(3)	0.4(3)	-0.4(3)	1.7(2)
C14	2.9(4)	1.9(4)	1.2(4)	-1.3(3)	-0.1(3)	0.1(3)	1.9(2)
C15	2.3(4)	1.1(3)	1.7(4)	-1.2(3)	0.8(3)	0.1(3)	1.7(2)
C16	3.5(5)	2.8(4)	1.4(4)	-1.0(4)	0.1(4)	-0.0(4)	2.5(2)
C17	3.1(5)	2.2(4)	2.9(5)	-0.5(4)	0.6(4)	0.3(4)	2.8(2)
C18	4.6(5)	2.2(4)	2.0(4)	-1.6(4)	0.3(4)	-0.7(4)	2.8(2)
C19	3.5(5)	2.8(4)	2.8(5)	-1.7(4)	-0.7(4)	0.4(4)	2.9(2)
C20	3.2(5)	2.0(4)	2.4(4)	-1.0(4)	1.3(4)	-0.1(4)	2.6(2)
C21	1.4(4)	3.0(4)	1.1(3)	-1.1(3)	0.0(3)	-0.0(3)	1.8(2)
C22	2.0(4)	2.2(4)	1.1(3)	-1.3(3)	0.6(3)	0.3(3)	1.7(2)
C23	2.2(4)	2.1(4)	1.6(4)	-1.5(3)	0.6(3)	-0.3(3)	1.9(2)
C24	2.5(4)	2.3(4)	1.0(3)	-0.9(3)	0.2(3)	0.1(3)	1.9(2)
C25	2.3(4)	1.6(4)	0.9(3)	-0.5(3)	0.2(3)	0.4(3)	1.6(2)
C26	3.6(5)	3.5(5)	0.8(4)	-1.2(4)	1.0(4)	-0.6(4)	2.6(2)
C27	2.7(4)	2.9(5)	2.7(4)	-1.0(4)	0.7(4)	0.2(4)	2.8(2)
C28	3.2(5)	3.4(5)	2.4(4)	-1.9(4)	0.8(4)	-1.2(4)	2.9(2)
C29	2.7(4)	4.6(5)	2.0(4)	-1.8(4)	-0.5(4)	-0.2(4)	2.9(2)
C30	3.1(5)	2.5(4)	2.5(4)	-0.3(4)	1.0(4)	-0.2(4)	2.8(2)

The form of the anisotropic temperature factor is:
exp[-0.25(h2a2B(1,1) + k2b2B(2,2) + l2c2B(3,3) + 2hkabB(1,2) + 2hlacB(1,3) + 2klbcB(2,3))] where a,b, and c are reciprocal lattice constants.

$(Me_5C_5)_2Yb(\mu\text{-}Cl)Ti(Me_5C_5)_2$

Table of Positional Parameters and Their Estimated Standard Deviations

Atom	x	y	z	B(A2)
YB	0.25938(2)	0.39881(2)	0.17816(2)	1.759(6)
TI	0.23968(8)	0.73736(7)	0.10701(6)	1.46(2)
CL	0.2472(1)	0.5714(1)	0.10502(9)	2.15(4)
C11	0.4123(5)	0.4043(4)	0.2597(4)	2.4(2)
C12	0.3886(4)	0.3119(5)	0.2597(4)	2.4(2)
C13	0.3855(5)	0.2792(4)	0.1755(5)	3.1(2)
C14	0.4076(4)	0.3527(5)	0.1257(4)	2.5(2)
C15	0.4278(4)	0.4292(4)	0.1787(4)	1.8(1)
C16	0.4286(5)	0.4615(6)	0.3364(4)	3.9(2)
C17	0.3789(5)	0.2528(6)	0.3353(5)	5.0(2)
C18	0.3755(5)	0.1809(5)	0.1491(6)	4.9(2)
C19	0.4119(5)	0.3517(6)	0.0341(5)	4.4(2)
C20	0.4654(5)	0.5192(5)	0.1508(5)	3.2(2)
C21	0.1168(4)	0.3598(4)	0.2467(4)	1.9(1)
C22	0.1468(4)	0.2739(4)	0.2211(4)	2.3(2)
C23	0.1428(5)	0.2709(4)	0.1338(4)	2.7(2)
C24	0.1089(4)	0.3552(4)	0.1045(4)	2.0(1)
C25	0.0904(4)	0.4103(4)	0.1727(4)	1.8(1)
C26	0.1070(5)	0.3901(5)	0.3339(5)	3.6(2)
C27	0.1636(5)	0.1927(5)	0.2771(5)	3.8(2)
C28	0.1609(5)	0.1900(5)	0.0807(5)	3.9(2)
C29	0.0944(5)	0.3823(5)	0.0145(4)	3.2(2)
C30	0.0460(5)	0.5010(5)	0.1685(4)	2.7(2)
C31	0.2826(4)	0.8494(4)	0.2108(4)	1.8(1)
C32	0.3107(4)	0.7608(4)	0.2383(4)	1.8(1)
C33	0.2379(4)	0.7077(4)	0.2497(3)	1.2(1)
C34	0.1655(4)	0.7609(4)	0.2278(4)	1.6(1)
C35	0.1941(4)	0.8495(4)	0.2044(4)	1.9(1)
C36	0.3402(5)	0.9314(5)	0.2071(4)	3.1(2)
C37	0.4006(5)	0.7334(5)	0.2576(4)	2.9(2)
C38	0.2366(5)	0.6145(4)	0.2901(4)	2.3(2)
C39	0.0758(5)	0.7346(5)	0.2358(4)	2.5(2)
C40	0.1369(5)	0.9316(5)	0.1915(4)	2.9(2)
C41	0.2839(4)	0.7162(4)	-0.0301(4)	1.7(1)
C42	0.3121(4)	0.8034(4)	-0.0010(3)	1.6(1)
C43	0.2397(4)	0.8583(4)	0.0090(3)	1.6(1)
C44	0.1669(4)	0.8038(4)	-0.0104(4)	1.8(1)
C45	0.1956(4)	0.7163(4)	-0.0354(4)	2.1(2)
C46	0.3399(5)	0.6401(5)	-0.0563(4)	2.7(2)
C47	0.4016(5)	0.8354(5)	0.0062(4)	2.8(2)
C48	0.2392(5)	0.9618(4)	0.0168(4)	3.1(2)
C49	0.0776(5)	0.8354(5)	-0.0167(4)	3.4(2)
C50	0.1403(5)	0.6394(5)	-0.0683(4)	3.0(2)

Starred atoms were included with isotropic thermal parameters.
The thermal parameter given for anisotropically refined atoms is the isotropic equivalent thermal parameter defined as:
(4/3) * [a2*B(1,1) + b2*B(2,2) + c2*B(3,3) + ab(cos gamma)*B(1,2) + ac(cos beta)*B(1,3) + bc(cos alpha)*B(2,3)]
where a,b,c are real cell parameters, and B(i,j) are anisotropic betas.

Table of Anisotropic Thermal Parameters - B's

Name	B(1,1)	B(2,2)	B(3,3)	B(1,2)	B(1,3)	B(2,3)	Beqv
YB	1.68(2)	1.47(1)	2.22(1)	0.04(1)	0.25(1)	0.49(1)	1.759(6)
TI	1.80(6)	1.17(4)	1.43(4)	0.02(4)	0.22(4)	0.03(4)	1.46(2)
CL	3.2(1)	1.40(6)	1.85(6)	0.07(6)	0.35(6)	0.18(5)	2.15(4)
C11	2.1(4)	3.0(3)	2.1(3)	0.3(3)	0.0(3)	-0.1(2)	2.4(2)
C12	0.3(3)	3.7(3)	3.2(3)	-0.1(3)	-0.5(3)	1.6(3)	2.4(2)
C13	2.7(4)	1.5(3)	5.1(4)	0.3(3)	0.4(3)	0.2(3)	3.1(2)
C14	2.1(4)	2.7(3)	2.7(3)	0.4(3)	0.5(3)	-0.2(3)	2.5(2)
C15	0.5(3)	2.0(3)	2.8(3)	0.0(2)	-0.1(2)	0.4(2)	1.8(1)
C16	2.6(4)	6.2(4)	2.6(3)	2.3(3)	-1.5(3)	-0.7(3)	3.9(2)
C17	2.2(5)	7.5(5)	5.3(4)	-0.5(4)	-0.7(3)	3.8(3)	5.0(2)
C18	1.6(4)	2.7(3)	10.3(6)	0.4(3)	-1.2(4)	-1.2(4)	4.9(2)
C19	2.8(4)	7.1(5)	3.3(3)	0.6(4)	0.9(3)	-1.4(3)	4.4(2)
C20	1.6(4)	2.9(3)	5.1(4)	-0.3(3)	0.1(3)	1.4(3)	3.2(2)
C21	1.5(4)	2.3(3)	2.0(2)	0.1(3)	-0.2(2)	0.6(2)	1.9(1)
C22	1.2(4)	2.0(3)	3.5(3)	-0.6(2)	-0.5(3)	0.5(2)	2.3(2)
C23	3.6(4)	1.5(3)	3.0(3)	-0.5(3)	1.0(3)	-0.2(2)	2.7(2)
C24	1.3(4)	2.2(3)	2.5(3)	-0.3(3)	-0.2(2)	-0.3(2)	2.0(1)
C25	0.6(3)	1.9(3)	2.7(3)	-0.1(2)	-0.6(2)	-0.1(2)	1.8(1)
C26	3.2(4)	4.3(4)	3.4(3)	-1.0(3)	1.2(3)	0.2(3)	3.6(2)
C27	3.8(5)	2.5(3)	5.1(4)	-0.4(3)	0.4(3)	1.6(3)	3.8(2)
C28	3.7(5)	2.3(3)	5.5(4)	0.6(3)	0.3(3)	-1.0(3)	3.9(2)
C29	3.1(4)	3.8(3)	2.6(3)	-0.3(3)	-0.1(3)	-0.1(3)	3.2(2)
C30	1.7(4)	2.2(3)	4.0(3)	0.2(3)	-0.8(3)	-0.2(3)	2.7(2)
C31	1.8(3)	1.7(2)	1.9(2)	-0.5(2)	0.6(2)	-0.4(2)	1.8(1)
C32	1.5(3)	2.3(3)	1.5(2)	0.4(2)	0.0(2)	-0.6(2)	1.8(1)
C33	0.4(3)	1.9(2)	1.2(2)	-0.1(2)	-0.2(2)	-0.2(2)	1.2(1)
C34	0.9(3)	2.2(3)	1.7(2)	-0.0(2)	0.3(2)	-0.2(2)	1.6(1)
C35	2.5(4)	1.5(2)	1.8(2)	-0.1(2)	0.8(2)	-0.3(2)	1.9(1)
C36	3.9(4)	2.3(3)	3.1(3)	-1.0(3)	0.9(3)	-0.5(3)	3.1(2)
C37	2.2(4)	3.9(3)	2.6(3)	0.7(3)	-0.1(3)	-0.8(3)	2.9(2)
C38	3.0(4)	2.2(3)	1.8(2)	0.2(3)	0.1(2)	0.3(2)	2.3(2)
C39	2.1(4)	2.6(3)	2.8(3)	0.1(3)	0.7(3)	-0.2(2)	2.5(2)
C40	3.5(4)	1.9(3)	3.3(3)	0.5(3)	1.1(3)	-0.1(3)	2.9(2)
C41	2.3(3)	1.6(2)	1.4(2)	0.1(2)	0.8(2)	0.2(2)	1.7(1)
C42	0.8(3)	2.6(3)	1.3(2)	0.1(2)	-0.3(2)	0.4(2)	1.6(1)

The form of the anisotropic temperature factor is:
exp[-0.25(h2a2B(1,1) + k2b2B(2,2) + l2c2B(3,3) + 2hkabB(1,2) + 2hlacB(1,3) + 2klbcB(2,3))] where a,b, and c are reciprocal lattice constants.

$(Me_5C_5)_2Yb(\mu\text{-}Br)Ti(Me_5C_5)_2$

Table of Positional Parameters and Their Estimated Standard Deviations

Atom	x	y	z	B(A2)
YB	0.24297(1)	0.38981(1)	0.32590(1)	1.971(5)
BR	0.25823(1)	0.56377(1)	0.41163(1)	2.81(2)
TI	0.26012(7)	0.73864(7)	0.40638(6)	1.61(2)
C1	0.0892(4)	0.3998(5)	0.2426(4)	2.8(2)
C2	0.1127(4)	0.3076(5)	0.2423(5)	3.6(2)
C3	0.1147(4)	0.2740(5)	0.3249(5)	3.5(2)
C4	0.0926(4)	0.3467(5)	0.3737(4)	2.8(2)
C5	0.0762(4)	0.4244(5)	0.3231(4)	2.5(1)
C6	0.0744(5)	0.4570(7)	0.1669(5)	5.5(2)
C7	0.1225(6)	0.2519(7)	0.1668(6)	7.0(3)
C8	0.1245(5)	0.1770(6)	0.3518(8)	7.3(3)
C9	0.0889(5)	0.3457(8)	0.4659(5)	5.5(2)
C10	0.0382(5)	0.5114(6)	0.3508(6)	4.5(2)
C11	0.4116(4)	0.4024(4)	0.3297(4)	2.3(1)
C12	0.3841(4)	0.3495(5)	0.2559(4)	2.5(1)
C13	0.3540(4)	0.2660(5)	0.2839(4)	2.4(1)
C14	0.3611(4)	0.2651(5)	0.3699(4)	2.6(2)
C15	0.3956(4)	0.3496(5)	0.3971(4)	2.2(1)
C16	0.4563(4)	0.4909(5)	0.3291(5)	3.1(2)
C17	0.3881(5)	0.3791(6)	0.1690(4)	3.7(2)
C18	0.3339(5)	0.1847(6)	0.2289(5)	4.5(2)
C19	0.3438(5)	0.1864(5)	0.4239(5)	4.0(2)
C20	0.4162(5)	0.3765(6)	0.4853(5)	3.8(2)
C21	0.3334(4)	0.7586(4)	0.2874(4)	1.8(1)
C22	0.2606(4)	0.7070(4)	0.2639(4)	1.8(1)
C23	0.1894(4)	0.7612(4)	0.2752(4)	2.0(1)
C24	0.2183(4)	0.8496(4)	0.3008(4)	2.1(1)
C25	0.3078(4)	0.8464(4)	0.3096(4)	2.0(1)
C26	0.4235(4)	0.7297(5)	0.2814(4)	2.9(2)
C27	0.2590(4)	0.6162(5)	0.2216(4)	2.7(1)
C28	0.0990(4)	0.7359(5)	0.2543(4)	3.2(2)
C29	0.1637(5)	0.9307(5)	0.3029(4)	3.2(2)
C30	0.3668(5)	0.9253(5)	0.3232(4)	3.1(2)
C31	0.1859(4)	0.8057(4)	0.5104(4)	2.2(1)
C32	0.2584(4)	0.8600(4)	0.5021(4)	2.1(1)
C33	0.3301(4)	0.8055(5)	0.5255(4)	2.3(1)
C34	0.3014(4)	0.7192(5)	0.5506(4)	2.3(1)
C35	0.2126(4)	0.7196(4)	0.5411(4)	2.0(1)
C36	0.0959(4)	0.8386(6)	0.4999(4)	3.4(2)
C37	0.2590(5)	0.9618(5)	0.4946(4)	3.2(2)
C38	0.4201(5)	0.8370(6)	0.5354(5)	3.7(2)
C39	0.3554(5)	0.6441(5)	0.5874(4)	3.3(2)
C40	0.1554(5)	0.6458(5)	0.5660(4)	3.3(2)

Starred atoms were included with isotropic thermal parameters.
The thermal parameter given for anisotropically refined atoms is the isotropic equivalent thermal parameter defined as:
(4/3) * [a2*B(1,1) + b2*B(2,2) + c2*B(3,3) + ab(cos gamma)*B(1,2) + ac(cos beta)*B(1,3) + bc(cos alpha)*B(2,3)]
where a,b,c are real cell parameters, and B(i,j) are anisotropic betas.

Table of Anisotropic Thermal Parameters - B's

Name	B(1,1)	B(2,2)	B(3,3)	B(1,2)	B(1,3)	B(2,3)	Beqv
YB	1.61(1)	1.81(1)	2.49(1)	-0.04(1)	0.162(9)	-0.65(1)	1.971(5)
BR	4.36(3)	1.80(3)	2.31(3)	0.02(3)	0.52(3)	-0.22(2)	2.81(2)
TI	1.83(5)	1.45(5)	1.56(5)	0.07(4)	0.23(4)	-0.10(4)	1.61(2)
C1	1.8(3)	3.5(3)	3.0(3)	-0.7(3)	-0.3(2)	-0.2(3)	2.8(2)
C2	1.7(3)	4.9(4)	4.3(4)	-0.8(3)	0.2(3)	-2.5(3)	3.6(2)
C3	1.3(3)	1.8(3)	7.4(5)	-0.2(3)	-0.0(3)	0.1(3)	3.5(2)
C4	1.5(3)	3.8(3)	3.2(3)	-0.4(3)	0.2(2)	0.5(3)	2.8(2)
C5	1.5(3)	2.7(3)	3.1(3)	0.1(2)	-0.1(2)	-0.1(3)	2.5(1)
C6	3.7(4)	9.3(6)	3.3(4)	-2.8(4)	-1.2(3)	2.0(4)	5.5(2)
C7	3.5(4)	10.2(6)	7.1(5)	-0.6(4)	0.2(4)	-6.2(4)	7.0(3)
C8	2.8(4)	3.0(4)	16.0(9)	-0.7(3)	-0.3(5)	1.5(5)	7.3(3)
C9	3.7(4)	9.3(6)	3.5(4)	-1.1(4)	0.1(3)	1.3(4)	5.5(2)
C10	3.1(4)	3.5(4)	7.0(5)	0.2(3)	0.3(3)	-1.3(4)	4.5(2)
C11	1.3(2)	1.9(3)	3.6(3)	0.1(2)	0.1(2)	-0.2(3)	2.3(1)
C12	1.5(3)	3.2(3)	2.7(3)	0.9(3)	0.3(2)	-0.3(3)	2.5(1)
C13	2.1(3)	2.1(3)	2.9(3)	0.3(2)	-0.1(2)	-0.7(3)	2.4(1)
C14	2.0(3)	1.8(3)	4.1(3)	0.2(2)	0.2(3)	0.6(3)	2.6(2)
C15	2.0(3)	2.2(3)	2.3(3)	0.2(2)	-0.0(2)	-0.1(2)	2.2(1)
C16	2.2(3)	2.7(3)	4.5(4)	0.1(3)	-0.1(3)	0.1(3)	3.1(2)
C17	2.7(3)	5.7(4)	2.6(3)	1.3(3)	0.5(3)	0.5(3)	3.7(2)
C18	3.3(4)	3.8(4)	6.3(5)	0.4(3)	-0.3(3)	-2.0(3)	4.5(2)
C19	3.4(3)	2.9(4)	5.7(4)	-0.3(3)	0.5(3)	0.4(3)	4.0(2)
C20	3.9(4)	4.3(4)	3.0(3)	0.4(3)	-0.4(3)	-0.0(3)	3.8(2)
C21	1.6(3)	1.9(3)	2.2(3)	0.3(2)	0.8(2)	0.3(2)	1.8(1)
C22	2.4(3)	1.9(3)	1.2(2)	0.2(2)	0.3(2)	0.1(2)	1.8(1)
C23	1.9(3)	2.4(3)	1.7(3)	-0.2(2)	0.1(2)	0.7(2)	2.0(1)
C24	2.9(3)	1.7(3)	1.7(3)	0.7(2)	0.1(2)	0.3(2)	2.1(1)
C25	2.7(3)	1.8(3)	1.6(3)	-0.7(2)	0.3(2)	0.4(2)	2.0(1)
C26	2.6(3)	2.6(3)	3.7(3)	-0.0(3)	1.2(3)	0.4(3)	2.9(2)
C27	3.7(3)	2.6(3)	2.0(3)	-0.5(3)	0.4(2)	-0.1(3)	2.7(1)
C28	2.5(3)	4.1(4)	2.8(3)	-0.4(3)	-0.3(3)	0.9(3)	3.2(2)
C29	4.0(3)	2.7(3)	2.9(3)	1.0(3)	0.8(3)	0.3(3)	3.2(2)
C30	3.9(3)	2.3(3)	3.3(3)	-0.3(3)	0.9(3)	0.3(3)	3.1(2)
C31	2.7(3)	2.3(3)	1.5(3)	0.4(2)	0.2(2)	-0.5(2)	2.2(1)
C32	3.3(3)	1.3(3)	1.6(3)	-0.0(2)	-0.0(2)	-0.2(2)	2.1(1)
C33	2.9(3)	2.2(3)	1.6(3)	-0.2(3)	0.0(2)	-0.6(2)	2.3(1)
C34	2.8(3)	2.7(3)	1.3(3)	-0.1(3)	-0.1(2)	-0.1(2)	2.3(1)
C35	2.8(3)	1.8(3)	1.5(3)	0.0(3)	0.6(2)	-0.7(2)	2.0(1)
C36	3.0(3)	4.3(4)	2.9(3)	1.2(3)	0.5(3)	-0.4(3)	3.4(2)
C37	4.4(4)	2.2(3)	2.9(3)	0.1(3)	0.4(3)	-0.7(3)	3.2(2)
C38	3.4(3)	3.7(4)	3.9(4)	-0.7(3)	-0.8(3)	-0.7(3)	3.7(2)
C39	3.9(3)	3.0(3)	2.9(3)	0.7(3)	-0.8(3)	0.2(3)	3.3(2)
C40	4.5(4)	2.6(3)	3.1(3)	-0.6(3)	1.3(3)	-0.0(3)	3.3(2)

The form of the anisotropic temperature factor is:
exp[-0.25(h2a2B(1,1) + k2b2B(2,2) + l2c2B(3,3) + 2hkabB(1,2) + 2hlacB(1,3) + 2klbcB(2,3))] where a,b, and c are reciprocal lattice constants.

$(Me_5C_5)_2Yb(\mu\text{-}Me)Ti(Me_5C_5)_2$

Table of Positional Parameters and Their Estimated Standard Deviations

Atom	x	y	z	B(A2)
YB	0.04683(2)	0.16748(2)	0.25740(1)	2.250(4)
TI	0.37718(8)	0.50408(8)	0.23794(5)	1.70(2)
C1	0.2261(5)	0.3564(5)	0.2385(3)	3.2(1)
C11	0.2385(5)	0.0318(5)	0.2564(3)	2.5(1)
C12	0.1471(5)	-0.0070(5)	0.1810(4)	3.0(1)
C13	0.0400(5)	-0.0680(5)	0.2038(4)	3.3(1)
C14	0.0642(5)	-0.0645(5)	0.2923(4)	3.1(1)
C15	0.1863(5)	-0.0010(5)	0.3252(3)	2.7(1)
C16	0.3723(5)	0.0838(5)	0.2608(4)	3.4(1)
C17	0.1644(7)	0.0060(6)	0.0936(4)	4.6(2)
C18	-0.0719(7)	-0.1399(6)	0.1414(5)	5.3(2)
C19	-0.0151(6)	-0.1309(6)	0.3431(5)	4.8(2)
C20	0.2520(6)	0.0189(6)	0.4172(4)	3.9(1)
C21	-0.0967(5)	0.3526(5)	0.2516(3)	2.7(1)
C22	-0.1657(5)	0.2571(5)	0.1911(3)	2.6(1)
C23	-0.2036(5)	0.1584(5)	0.2336(4)	3.2(1)
C24	-0.1549(5)	0.1940(6)	0.3218(4)	3.4(1)
C25	-0.0885(5)	0.3113(5)	0.3314(4)	3.0(1)
C26	-0.0540(5)	0.4797(5)	0.2333(4)	4.0(1)
C27	-0.1959(6)	0.2613(7)	0.0962(4)	4.6(2)
C28	-0.2940(6)	0.0467(7)	0.1949(5)	5.8(2)
C29	-0.1834(7)	0.1233(7)	0.3926(4)	5.6(2)
C30	-0.0335(6)	0.3858(7)	0.4147(4)	5.1(2)
C31	0.2713(5)	0.4752(5)	0.0915(3)	2.5(1)
C32	0.3903(5)	0.4332(5)	0.0977(3)	2.7(1)
C33	0.4848(5)	0.5335(5)	0.1246(3)	2.6(1)
C34	0.4234(5)	0.6390(5)	0.1362(3)	2.5(1)
C35	0.2930(5)	0.6024(5)	0.1187(3)	2.5(1)
C36	0.1463(6)	0.4056(7)	0.0501(4)	4.3(2)
C37	0.4123(7)	0.3045(6)	0.0728(4)	4.5(2)
C38	0.6207(5)	0.5291(6)	0.1267(4)	3.8(1)
C39	0.4831(7)	0.7692(6)	0.1480(4)	4.3(2)
C40	0.1924(6)	0.6846(6)	0.1213(4)	4.0(1)
C41	0.4145(5)	0.4738(5)	0.3845(3)	2.5(1)
C42	0.5312(5)	0.4760(5)	0.3593(3)	2.6(1)
C43	0.5641(5)	0.5955(5)	0.3402(3)	2.6(1)
C44	0.4672(5)	0.6667(5)	0.3585(3)	2.5(1)
C45	0.3739(5)	0.5918(5)	0.3764(3)	2.4(1)
C46	0.3572(6)	0.3734(6)	0.4259(4)	4.1(1)
C47	0.6181(6)	0.3736(6)	0.3621(4)	4.7(2)
C48	0.6922(6)	0.6464(7)	0.3294(4)	4.7(2)
C49	0.4704(7)	0.8030(5)	0.3510(4)	4.0(2)
C50	0.2591(6)	0.6350(6)	0.3978(4)	4.2(2)
HB	0.182(6)	0.358(6)	0.285(4)	6(2)*
HA	0.254(5)	0.305(5)	0.252(3)	4(1)*
HC	0.176(5)	0.330(5)	0.204(4)	4(1)*

Starred atoms were included with isotropic thermal parameters.
The thermal parameter given for anisotropically refined atoms is the isotropic equivalent thermal parameter defined as:
(4/3) * [a2*B(1,1) + b2*B(2,2) + c2*B(3,3) + ab(cos gamma)*B(1,2) + ac(cos beta)*B(1,3) + bc(cos alpha)*B(2,3)]
where a,b,c are real cell parameters, and B(i,j) are anisotropic betas.

Table of Anisotropic Thermal Parameters - B's

Name	B(1,1)	B(2,2)	B(3,3)	B(1,2)	B(1,3)	B(2,3)	Beqv
Y8	2.239(8)	2.149(8)	2.498(8)	0.315(7)	0.866(7)	0.098(7)	2.250(4)
TI	1.81(3)	2.07(3)	1.23(3)	0.59(3)	0.22(3)	0.03(3)	1.70(2)
C1	3.4(3)	4.1(3)	1.6(2)	-0.1(2)	-0.2(2)	0.4(2)	3.2(1)
C11	2.8(2)	1.7(2)	3.3(2)	0.7(2)	1.1(2)	0.3(2)	2.5(1)
C12	4.1(2)	2.2(2)	2.8(2)	1.2(2)	0.9(2)	-0.0(2)	3.0(1)
C13	3.1(2)	2.1(2)	4.3(3)	0.4(2)	0.3(2)	-0.5(2)	3.3(1)
C14	3.0(2)	2.1(2)	4.5(3)	0.1(2)	1.7(2)	0.4(2)	3.1(1)
C15	3.1(2)	2.1(2)	3.0(2)	0.8(2)	0.7(2)	0.5(2)	2.7(1)
C16	3.4(2)	2.5(2)	5.0(3)	0.9(2)	1.9(2)	0.7(2)	3.4(1)
C17	7.3(4)	3.8(3)	3.3(3)	2.0(3)	1.6(3)	0.1(2)	4.6(2)
C18	4.0(3)	3.8(3)	7.1(4)	1.0(2)	-0.3(3)	-1.8(3)	5.3(2)
C19	4.5(3)	3.4(3)	7.5(3)	0.9(2)	3.2(2)	1.5(3)	4.8(2)
C20	5.2(3)	3.1(2)	3.5(3)	0.9(2)	1.2(2)	0.8(2)	3.9(1)
C21	2.1(2)	2.6(2)	3.5(2)	0.4(2)	1.3(2)	-0.1(2)	2.7(1)
C22	2.0(2)	3.5(2)	2.3(2)	0.8(2)	0.6(2)	0.2(2)	2.6(1)
C23	2.5(2)	2.2(2)	4.5(3)	-0.1(2)	1.0(2)	-0.8(2)	3.2(1)
C24	3.4(2)	4.4(3)	3.3(2)	1.6(2)	2.1(2)	1.0(2)	3.4(1)
C25	2.4(2)	3.6(2)	3.0(2)	0.6(2)	0.9(2)	-0.5(2)	3.0(1)
C26	3.0(2)	2.7(2)	7.0(3)	0.7(2)	2.2(2)	0.6(2)	4.0(1)
C27	4.3(3)	6.7(4)	2.9(3)	2.0(3)	0.7(2)	-0.2(3)	4.6(2)
C28	2.8(3)	4.9(3)	9.3(4)	-0.5(3)	2.1(3)	-2.2(3)	5.8(2)
C29	6.6(3)	6.3(3)	6.2(3)	2.6(3)	4.4(2)	3.0(3)	5.6(2)
C30	3.5(3)	7.7(4)	3.9(3)	0.8(3)	0.9(2)	-1.7(3)	5.1(2)
C31	2.9(2)	3.1(2)	1.6(2)	0.1(2)	0.5(2)	0.5(2)	2.5(1)
C32	4.2(2)	2.3(2)	1.8(2)	0.7(2)	1.2(2)	0.2(2)	2.7(1)
C33	3.2(2)	3.2(2)	1.8(2)	0.7(2)	1.2(2)	0.8(2)	2.6(1)
C34	3.4(2)	2.4(2)	1.8(2)	0.1(2)	0.8(2)	0.5(2)	2.5(1)
C35	3.2(2)	2.6(2)	2.0(2)	1.1(2)	0.6(2)	0.6(2)	2.5(1)
C36	4.6(3)	5.5(3)	2.1(2)	-0.6(3)	-0.2(2)	0.3(2)	4.3(2)
C37	7.8(3)	3.1(3)	3.7(2)	1.7(2)	3.0(2)	0.3(2)	4.5(2)
C38	3.0(2)	5.6(3)	3.6(2)	1.1(2)	1.5(2)	1.2(2)	3.8(1)
C39	6.6(3)	3.1(3)	3.4(3)	0.1(3)	1.6(2)	0.8(2)	4.3(2)
C40	4.8(3)	4.6(3)	3.5(2)	2.5(2)	1.6(2)	1.5(2)	4.0(1)
C41	2.7(2)	2.8(2)	1.5(2)	-0.6(2)	0.1(2)	-0.1(2)	2.5(1)
C42	2.4(2)	3.1(2)	2.0(2)	0.7(2)	-0.1(2)	-0.1(2)	2.6(1)
C43	2.1(2)	3.5(2)	1.9(2)	-0.4(2)	0.1(2)	-0.1(2)	2.6(1)
C44	3.1(2)	2.4(2)	1.8(2)	-0.0(2)	0.3(2)	-0.2(2)	2.5(1)
C45	2.1(2)	3.1(2)	1.8(2)	-0.1(2)	0.3(2)	-0.7(2)	2.4(1)
C46	5.0(3)	4.0(3)	2.4(2)	-1.3(3)	-0.0(2)	0.6(2)	4.1(1)
C47	4.0(3)	5.2(3)	4.3(3)	2.2(2)	-0.8(3)	0.0(3)	4.7(2)
C48	2.8(2)	7.7(4)	3.1(3)	-1.1(3)	0.7(2)	-0.5(3)	4.7(2)
C49	5.8(3)	2.6(2)	3.2(3)	-0.4(2)	0.6(2)	-0.4(2)	4.0(2)
C50	3.6(3)	5.4(3)	3.6(3)	0.6(2)	1.1(2)	-1.2(2)	4.2(2)

The form of the anisotropic temperature factor is:
exp[-0.25(h2a2B(1,1) + k2b2B(2,2) + l2c2B(3,3) + 2hkabB(1,2) + 2hlacB(1,3) + 2klbcB(2,3))] where a,b, and c are reciprocal lattice constants.

LAWRENCE BERKELEY LABORATORY
UNIVERSITY OF CALIFORNIA
INFORMATION RESOURCES DEPARTMENT
BERKELEY, CALIFORNIA 94720